ADVANCED OPTICAL MATERIALS
www.advopticalmat.de

Engineered Optical Fibers for Deep-Tissue Applications

Yuzhen Li, Siyang Zheng, Wenzhao Li, Kai Chen, Tianting Zhong, Chi Man Woo, Weiran Pang, Chuqi Yuan, Xiaozhou Xiao, Xianguang Yang, Long Jin, Xiang Qian, Qiyao Tan, Changyuan Yu,* Liwei Liu,* Junle Qu,* and Puxiang Lai**

High-precision optical diagnostics and therapy in deep tissues are hindered by light scattering and absorption. Engineered optical fibers, serving as minimally invasive optical fibers, provide a powerful platform to bypass these barriers. This review systematically deconstructs the design of these advanced fibers from the unified perspectives of materials science and structural engineering. First, key material systems are analyzed—from traditional silica to emerging polymers and hydrogels—evaluating how their intrinsic properties dictate the fiber's optical performance, mechanical compliance, and biocompatibility. Then, critical structural paradigms are examined, including propagation modes, refractive index profiles, and core geometries, elucidating how these designs control features such as signal fidelity, resolution, and functional integration. The review further considers how the fiber's potential is amplified by auxiliary front-end physical modulation and back-end computational reconstruction techniques. Building on this foundational framework, the application of these engineered fibers is comprehensively surveyed in state-of-the-art biomedical diagnostics, such as endoscopic imaging and biosensing, and in targeted therapeutics, including optogenetics, phototherapies, and drug delivery. Ultimately, by systematically linking engineering principles to biomedical functions, this review establishes a foundational framework for designing next-generation, clinically focused fiber-optic systems, concluding with a critical assessment of prevailing challenges to illuminate future research directions in this burgeoning field .

1. Introduction

Real-time observation and precise intervention deep within living organisms at cellular and even subcellular resolutions represent a major frontier in modern biomedical science and engineering.[1,2] Optical methods, owing to their high resolution, high sensitivity, and non-invasiveness, render a key enabling technology for achieving this goal. However, the intrinsic optical properties of biological tissues pose a fundamental challenge as the penetration depth increases. The complex microscopic structures within tissue lead to strong photon scattering, while endogenous chromophores such as hemoglobin and water cause significant light absorption.[3–5] These two effects collectively result in the rapid attenuation and broadening of the light beam during propagation, severely limiting the effective optical penetration depth and spatial resolution.[6–10] To address this challenge, researchers have developed various strategies. The first involves optimizing the light source, for instance, by utilizing the near-infrared (NIR-I/II) as a biological optical window where

Y. Li, S. Zheng, W. Li, K. Chen, T. Zhong, C. M. Woo, W. Pang, C. Yuan, X. Xiao, Q. Tan, P. Lai
Department of Biomedical Engineering
The Hong Kong Polytechnic University
Hong Kong, SAR 999077, China
E-mail: 22042297r@connect.polyu.hk; puxiang.lai@polyu.eu.hk

Y. Li, S. Zheng, W. Li, K. Chen, T. Zhong, C. M. Woo, W. Pang, C. Yuan, X. Xiao, C. Yu, P. Lai
Shenzhen Research Institute
The Hong Kong Polytechnic University
Shenzhen 518057, China
E-mail: changyuan.yu@polyu.edu.hk

The ORCID identification number(s) for the author(s) of this article can be found under https://doi.org/10.1002/adom.202502861

DOI: 10.1002/adom.202502861

X. Yang
Guangdong Provincial Key Laboratory of Nanophotonic Manipulation
Institute of Nanophotonics
College of Physics & Optoelectronic Engineering
Jinan University
Guangzhou 511443, China

L. Jin
MOE Key Laboratory of Laser Life Science
Guangdong Key Laboratory Laser Life Science
School of Optoelectronic Science and Engineering
South China Normal University
Guangzhou 510006, China

X. Qian
Tsinghua-Shenzhen International Graduate School
Tsinghua University
Shenzhen 518055, China

C. Yu
Department of Electrical and Electronics Engineering
The Hong Kong Polytechnic University
Hong Kong, SAR 999077, China

absorption and scattering are relatively low, thereby enhancing penetration depth.[11,12] Furthermore, optimizations are pursued from two main aspects: signal generation and light beam propagation. On the one hand, advanced microscopy techniques, such as confocal and multiphoton microscopy, improve the signal-to-noise ratio by effectively rejecting scattered noise through spatial filtering or nonlinear localized excitation. On the other hand, more cutting-edge technologies like adaptive optics (AO)[13] and wavefront shaping (WFS)[14,15] attempt to counteract the effects of tissue scattering by actively compensating for scattering-induced wavefront distortions. The goal of these techniques is to achieve efficient energy delivery and diffraction-limited focusing deep within the tissue.[16,17] Nevertheless, despite their significant success in specific scenarios, these techniques still encounter a general limitation: they fundamentally rely on combating tissue scattering from the outside. Once the penetration depth goes beyond the optical diffusion limit (empirically ≈1 mm beneath skin), the effective signal diminishes exponentially. Moreover, cutting-edge methods like wavefront shaping are highly sensitive to dynamic changes in the tissue, which restricts their widespread application in vivo.[18–20] Therefore, to break through this depth barrier, there remains an urgent need for a new technological paradigm capable of effectively guiding photons to bypass the tissue scattering barrier.

To directly confront the aforementioned challenges, optical fiber offers a distinctly different strategy. Its core principle is not to contend or battle with scattering externally but to serve as a minimally invasive, physical optical fiber that bypasses the opaque biological medium to deliver photons.[21–23] This functionality is based on the principle of total internal reflection: in a coaxial structure composed of a high-refractive-index core and a low-refractive-index cladding, light rays striking the core-cladding interface at an angle greater than the critical angle undergo total reflection, thereby being confined within the core and propagating along the fiber axis.[24–28] In biomedical applications, optical fibers are inserted directly into tissue, serving both as precise conduits for delivering light from an external source to a deep target and as efficient channels for collecting photons generated within the tissue and transmitting them out of the body for analysis.[29,30] While effective in specific scenarios, standard optical fibers still face numerous challenges when applied in complex biological environments. Beyond the optical performance required for ideal light transmission, biomedical applications impose far more stringent demands, including biocompatibility, mechanical compliance, and functionalization capabilities.[31–33] To meet these needs, which far exceed those of the traditional telecommunications field, optical fibers must undergo systematic engineering and enhancement. This process has directly driven their evolution from passive transmission components into highly instrumentalized and complex platforms. Through the precise design of their intrinsic properties and extrinsic functions, engineered optical fibers to date possess sophisticated capabilities for serving both precise diagnostics (high-resolution imaging and real-time sensing) and targeted therapeutics (specific modulation and localized energy delivery).[34–36]

The goal of this review is to elucidate how systematic engineering of optical fibers—precisely tailoring their physical, chemical, and biological properties—can meet the diverse and highly challenging demands of deep-tissue applications. This is primarily achieved through the following strategies. First, Material Engineering, which not only involves optimizing traditional inorganic materials for broader spectral transmission and higher power tolerance but also encompasses the development of bio-friendly polymeric materials for superior flexibility and mechanical compliance. It also extends to the design of biodegradable polymers and hydrogel-based fibers, aimed at applications that obviate the need for post-implantation removal or achieve a high degree of modulus matching with soft tissues. Second, Structural Engineering, which enables fine control over light propagation at the micro- and nanoscale. Advances in this area include gradient-index (GRIN) fibers for high-resolution endoscopy, multi-core fiber arrays for multi-point parallel stimulation or sensing, and microstructured and photonic crystal fibers that achieve unique light confinement and enhance light-matter interactions. Furthermore, the potential of these physical-layer engineering designs is often amplified when combined with advanced auxiliary technologies, such as computational imaging and machine learning. In summary, these engineering strategies yield highly customized fiber-optic tools, enabling advanced functionalities and precision in deep-tissue diagnostics and therapeutics.

Although there are reviews that have provided detailed accounts of specific optical techniques or certain classes of fiber-optic devices, this article aims to systematically establish the intrinsic link between the fundamental design principles of optical fibers and their cutting-edge deep-tissue biomedical applications from a unified material science and engineering perspective. It places a strong emphasis on elucidating how a diverse array of engineering strategies determines and ultimately realizes specific biomedical functions. To this end, the article will first review the fundamental challenges of deep-tissue optics and the waveguiding principles of optical fibers. Building on this foundation, as illustrated in **Figure 1**, we will delve into the core engineering strategies for fiber functionalization, focusing on their material compositions and structural paradigms, as well as the key synergistic auxiliary technologies. Subsequently, this review will systematically showcase how these meticulously designed engineered fibers address practical biomedical problems in state-of-the-art diagnostics (covering high-resolution endoscopy and multifunctional biosensing) and therapeutic interventions

C. Yu, P. Lai
Jinjiang Technology and Innovation Research Institute
The Hong Kong Polytechnic University
Jinjiang 518117, China
C. Yu, P. Lai
Photonics Research Institute
The Hong Kong Polytechnic University
Hong Kong, SAR 999077, China
L. Liu, J. Qu
Key Laboratory of Optoelectronic Devices and Systems of Guangdong Province and Ministry of Education
College of Physics and Optoelectronic Engineering
Shenzhen University
Shenzhen 518060, China
E-mail: liulw@szu.edu.cn; jlqu@szu.edu.cn
Q. Tan
Research Institute for Sports Science and Technology
The Hong Kong Polytechnic University
Hong Kong, SAR 999077, China

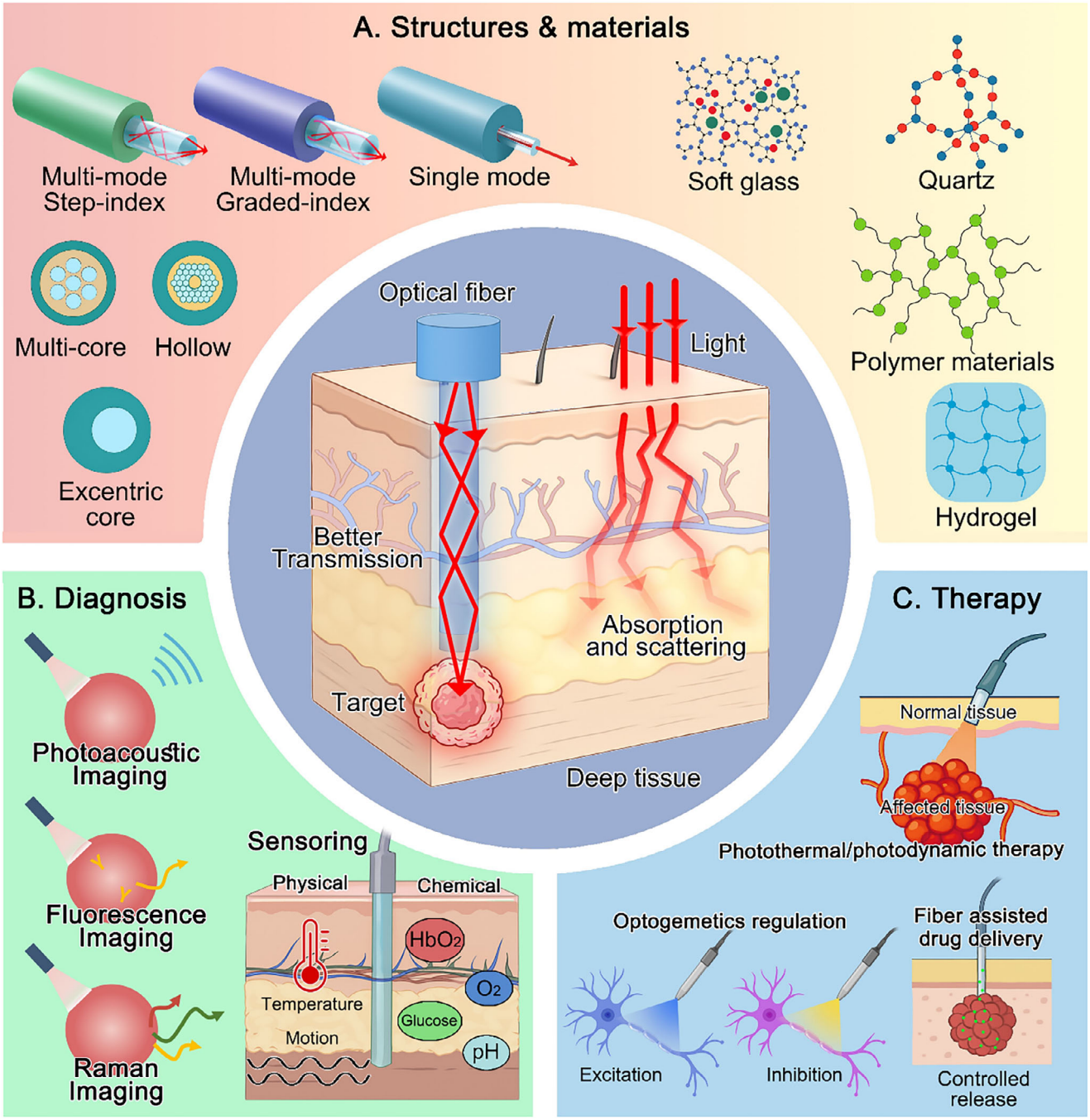

Figure 1. Engineering optical fibers for deep tissue applications. a) Structures and materials: Structurally, optical fibers derive single-mode and multi-mode propagation modes, as well as various core configurations, which regulate the transmission behavior of photons. Materials such as soft glass, quartz, and polymer materials fundamentally determine the intrinsic optical, mechanical, and biological properties of optical fibers. b) Optical fibers enable diagnostic techniques, including imaging and sensing, such as photoacoustic imaging, fluorescence imaging, and Raman imaging, along with sensing capabilities for monitoring physical (temperature) and chemical (glucose, pH) parameters in tissues. c) Optical fibers are also used in a range of deep tissue treatments and regulation, including photothermal and photodynamic therapies, facilitating targeted therapy for deep tissue, along with optogenetic regulation and drug delivery for precise treatment.

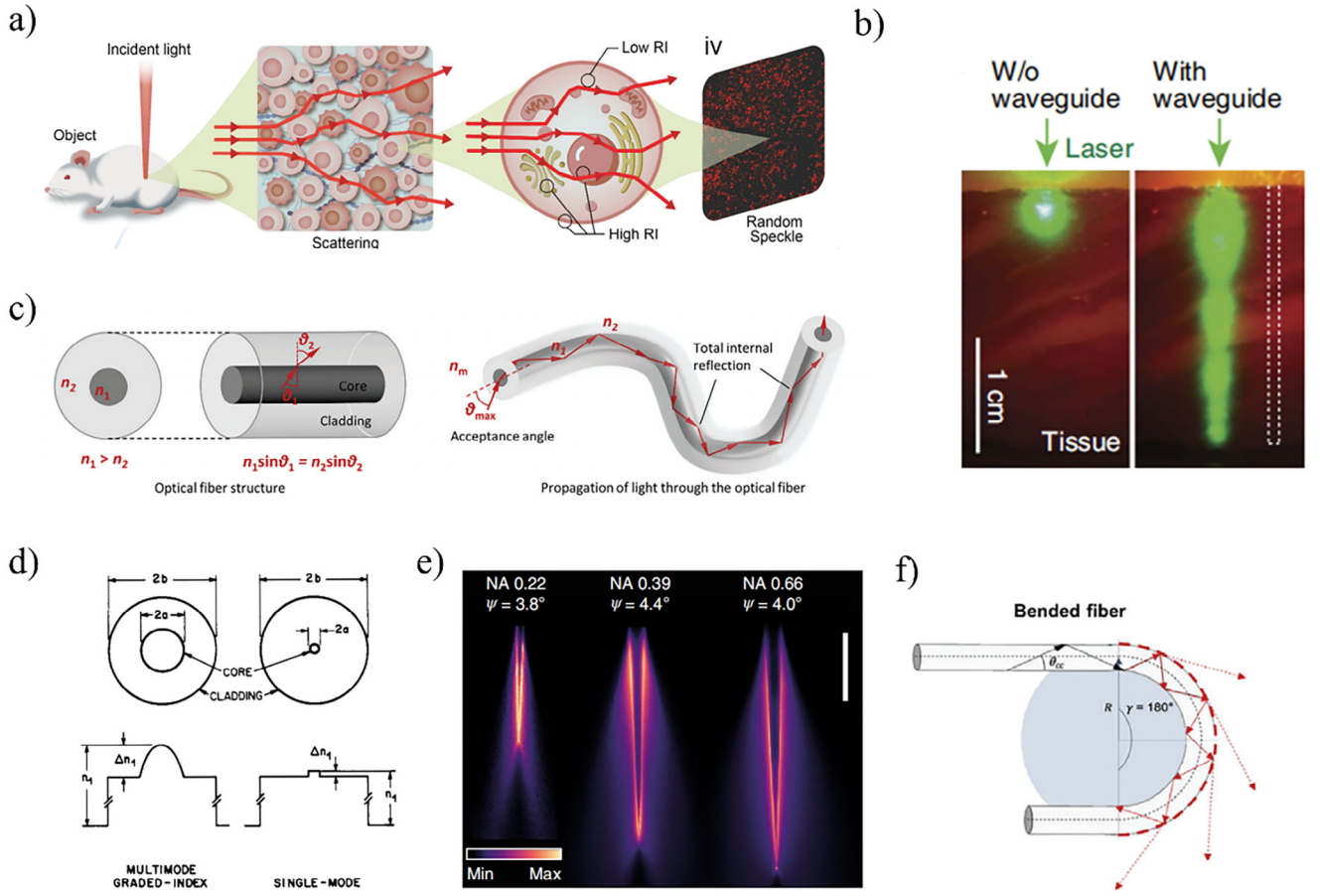

Figure 2. Light propagation in tissue and guidance in optical fibers. a) Refractive index mismatches within biological tissue cause strong light scattering, limiting penetration depth and creating random speckle patterns. Reproduced with permission.[40] Copyright 2024, SPIE. b) Left: Direct laser illumination fails to penetrate thick tissue. Right: An implanted optical fiber effectively delivers light to deep regions. Scale bar: 10 mm. Reproduced with permission.[42] Copyright 2016, Springer Nature. c) An optical fiber consists of a high-index core and a low-index cladding. Light is guided within the core via total internal reflection (TIR) at the core-cladding interface. Reproduced with permission.[43] Copyright 2024, Wiley-VCH. d) A single-mode fiber (SMF) has a small core supporting a single light mode, whereas a multimode fiber (MMF) has a larger core supporting multiple modes. Reproduced with permission.[44] Copyright 1980, IEEE. e) A larger numerical aperture (NA) provides a wider acceptance angle, enabling a larger field of view and more efficient light collection. Reproduced with permission.[45] Copyright 2019, Springer Nature. f) Significant fiber bending (macro-bending) disrupts TIR, causing light to leak from the core and creating lateral emission (dashed arrows). Reproduced with permission.[43] Copyright 2024, Wiley-VCH.

(covering optogenetics, targeted phototherapy, and tissue engineering). This paper will conclude with an outlook on the frontier interdisciplinary directions in the field and a thorough discussion of the key challenges and future opportunities in translating these technologies from laboratory research to clinical practice.

2. Optical Fundamentals of Fibers

2.1. Challenges in Deep-Tissue Optics

With the advancement of life science research moving towards in vivo, in situ, and deep tissue studies, the high-resolution, long-term, real-time observation of biological tissue microenvironments, cellular behaviors, and molecular events has become a core requirement for understanding disease mechanisms and developing precise therapies. Optical technologies, with their advantages of high resolution, high sensitivity, and non-invasiveness, theoretically are ideal tools for achieving this goal.[37,38] However, when light penetrates tissue from the outside, its propagation is greatly challenged by the complex optical properties of the tissue itself, which represents a fundamental barrier in deep tissue optics research. This barrier primarily arises from two major physical processes: light scattering and light absorption.[39]

Light scattering is the primary factor limiting the penetration depth and image quality of optical methods in tissues. The physical origin of scattering lies in the refractive index heterogeneity of biological tissues at the microscopic scale. Tissues are not optically homogeneous, but rather consist of components of varying refractive indices (**Figure 2a**).[40] For example, the refractive index of extracellular fluid is approximately $n \approx 1.35$, while the refractive index of the cytoplasm is slightly higher, ranging from $n \approx 1.36–1.38$. The refractive indices of dense structures within the cell, such as the nucleus ($n \approx 1.39$), mitochondria ($n \approx 1.42$), and lipid droplets ($n \approx 1.44$), are significantly higher than the surrounding environment.[41] As photons propagate through

tissue, their path is repeatedly deflected by numerous microstructures with varying refractive indices. This refraction, governed by Snell's law, occurs at interfaces such as those between the cell membrane and cytoplasm or the nucleus and cytoplasm. The dense arrangement of these structures, with sizes ranging from hundreds of nanometers to tens of micrometers, results in numerous scattering events. As a result, the key physical quantities carrying spatial information, such as the beam's intensity distribution, initial collinearity, polarization state, and coherence, are rapidly disrupted, causing the photon flow to transition into a diffuse state (Figure 2a). This effect directly leads to two severe consequences: first, the beam cannot maintain a sharp focus deep within the tissue; second, the signal light emitted from the target area is similarly disrupted on its return path to the outside. The ultimate result is that the image resolution and contrast deteriorate sharply as the tissue thickness or depth increases.[39]

Light absorption is another key factor causing the attenuation of light energy within tissues. The physical essence of absorption is the capture of photon energy at specific wavelengths by chromophore molecules within the tissue, which excites them to undergo electronic transitions or vibrations, converting the light energy into other forms of energy and thus resulting in energy loss.[46] There are many types of endogenous absorbers within tissues, each with different absorption spectra. In the ultraviolet and visible (≈400–600 nm) light ranges, hemoglobin (Hb) in blood and melanin in the skin are the two dominant absorbing substances. Notably, hemoglobin has a very high absorption coefficient at ≈415 nm in its Sorte band, which means that visible light cannot penetrate more than a millimeter of blood-containing tissue.[47] In the NIR range, the absorption effects of water and lipids become more significant. The absorption peaks of water molecules are primarily located around 970, 1200, and 1450 nm. These absorption peaks help define the biological optical windows (first window: 650–950 nm; second window: 1000–1350 nm), where both absorption and scattering effects reach their relative minima, significantly enhancing light penetration capability.[48] However, even within the optimal window, absorption remains significant and, together with scattering, follows the Beer-Lambert law, leading to exponential attenuation of photon flux as the depth increases, which severely limits the signal-to-noise ratio (SNR) achievable in deep tissue.

In summary, scattering disrupts the spatial information of light, while absorption further weakens its energy delivery. The combined effects of these two phenomena make traditional free-space optical methods inadequate for deep-tissue applications.

2.2. Optical Fibers and Their Guiding Mechanism

Faced with the fundamental challenges of deep-tissue optics, specifically the disruption of spatial information due to light scattering and energy attenuation due to absorption, traditional free-space optical methods fall short. In this context, fiber optic technology offers a fundamentally different paradigm.[42] Instead of attempting to counteract or compensate for tissue scattering, optical fibers act as a minimally invasive physical channel, directly bypassing most of the scattering media along the optical path and efficiently transporting high-quality light patterns and/or energy to the deep target regions. At the same time, fibers can also serve as efficient local signal collectors, capturing photons before they are scattered and absorbed by the tissue and guiding them to external detectors. This operational mode fundamentally reduces energy loss and signal distortion in free-space optical paths, establishing an indispensable physical foundation for achieving high-resolution imaging, high-sensitivity sensing, and high-precision interventions in deep tissue.[49]

To achieve effective confinement and guidance of light, typical optical fibers are physically designed as micron-scale cylindrical optical fibers composed of a high refractive index core and a low refractive index cladding.[50] The core serves as the primary channel for light energy transmission, and the refractive index of the cladding is precisely controlled to be slightly lower than that of the core, which is key to achieving light confinement. This structure allows the fiber to transport light energy precisely to deep tissues, overcoming the signal attenuation problems caused by tissue scattering and absorption in traditional free-space transmission mode. In contrast, without fiber guidance, light in deep tissues would be severely deflected and attenuated due to multiple scattering (μs) and absorption (μa) within biological tissues, leading to randomized photon paths, drastically reduced penetration depth, and a significant decrease in SNR, making high-resolution imaging or precise treatment localization nearly impossible.[45]

The guiding ability of this core-cladding structure is fundamentally based on the phenomenon of total internal reflection. Typically, when a light beam encounters the interface between two different media, part of the light is reflected according to the law of reflection, while the rest enters the new medium, bending its direction in accordance with Snell's law:

$$n_1 \sin\theta_1 = n_2 \sin\theta_2 \quad (1)$$

where n_1 and n_2 are the refractive indices of the incident and refracting media, and θ_1 and θ_2 are the incident and refracted angles, respectively (Figure 2c). When light travels from a high refractive index medium to a lower refractive index medium, and the incident angle exceeds a specific critical angle, the refracted phenomenon disappears, and light is 100% reflected back into the original medium. In optical fibers, as long as the light strikes the core-cladding interface at an angle greater than the critical angle, total internal reflection occurs repeatedly, keeping the light firmly trapped in the core, enabling low-loss long-distance transmission.

In summary, optical fibers, with their core-cladding structure and the principle of total internal reflection, form efficient photon optical fibers. However, when used for deep-tissue treatment and diagnosis, their complexity far exceeds a simple physical model. From a functional standpoint, a biomedical optical fiber needs to serve as both a photon channel and a medical device interacting with the tissue. The efficacy of a photon channel is defined by its precision in coupling, confining, and guiding photons. This performance is dictated by the channel's geometric and optical properties, including its core size, numerical aperture, and mode characteristics. These properties, in turn, determine crucial metrics such as imaging resolution and signal fidelity.[51] As a medical device, its performance is determined by its behavior during long-distance transmission within tissue and complex biological environments. This performance is defined by key transmission, mechanical, and biological characteristics, including

attenuation, bandwidth, flexibility, and biocompatibility. These properties directly influence the SNR of biological signals, the minimally invasive nature of implantation, and long-term operational stability.[52] On a fundamental level, optimizing these parameters can be achieved through material engineering (e.g., doping or modifying glass and polymer components), structural engineering (e.g., via the design of microstructured or multi-core fibers), and the application of auxiliary techniques at both ends of the device.[53–55] A systematic examination and evaluation of these core parameters is essential to guide design trade-offs and device selection for specific applications. The following sections will discuss these in detail.

3. Key Parameters

In biomedical applications aimed at deep tissue, the design and selection of optical fibers represent a multi-variable optimization engineering process. To precisely achieve specific functions, a comprehensive consideration of a series of key parameters is necessary. These parameters primarily cover four dimensions: geometric, optical, transmission, and mechanical/biological performance. Among these, geometric and optical parameters are fundamental in determining the guiding properties of the optical fiber, while transmission parameters quantify the macroscopic efficiency of photon transport. Mechanical and biological performance define the fiber's applicability and reliability in complex biological environments. Therefore, careful selection and optimization of these parameters are prerequisites for realizing specific biomedical functions and ultimately determine the success or failure of the fiber in diagnostic and therapeutic applications.

3.1. Geometric Parameters

Geometric parameters form the basis for optical fiber structural design and directly define its physical dimensions and shape. In complex and dynamic biological environments, such as deep tissue imaging, the rational configuration of geometric parameters directly influences coupling efficiency, propagation stability, and compatibility with biological tissue. These parameters mainly include core diameter,[43] cladding diameter, fiber length, cladding structure, and NA,[44] all of which together determine the core performance of optical fibers in terms of optical field coupling, spot control, penetration depth, and imaging resolution.

The core diameter determines the fiber's mode characteristics and light flux (Figure 2d). For high-resolution imaging, such as OCT and confocal microscopy, single-mode fibers are typically used, with core diameters strictly controlled within the range of 8–10 μm to ensure that only the fundamental mode (such as LP_{01}) propagates in the fiber. This design avoids signal distortion caused by multimode interference, thus ensuring high spatial coherence and structural clarity in deep-tissue imaging.[56] In contrast, applications requiring high optical power transmission or signal collection efficiency, such as photoacoustic imaging and deep fluorescence detection, typically employ multimode fibers with core diameters of ≥50 μm. Larger core diameters improve light coupling efficiency and return light flux, which is crucial for enhancing weak signal detection, especially in cases where deep-tissue signals are severely attenuated.[57]

Cladding diameter, along with the overall fiber size, affects the fiber's insertion stability and mechanical reliability within tissues. For applications involving deep-tissue implantation (e.g., brain, liver) or puncture into lesion areas, fibers must be sufficiently thin to minimize tissue damage, yet maintain enough structural strength to avoid bending or breaking during implantation or operation.[58]

The NA represents the fiber's ability to collect and emit light at various angles and is a key factor affecting coupling efficiency, focus size, and imaging depth. A high NA helps efficiently collect scattered or emitted light from biological tissue, making it suitable for deep tissue imaging where signal attenuation is significant (Figure 2e). On the other hand, a low NA is beneficial for collimated illumination and long working distance of focusing.[45]

To address challenges such as tissue heterogeneity and limited optical path space, researchers have developed various specialized fiber structures. For example, tapered fibers[45] regulate light intensity distribution through a gradient in core diameter, achieving deep focusing or mode conversion. Double-cladding fibers[59] support both high-quality excitation light transmission and large flux signal collection, widely used in fluorescence microscopy or multimodal imaging.[60] Multi-core fibers or fiber bundles[61] allow spatial parallelism or angular multiplexing, enabling multi-point simultaneous excitation or large field-of-view signal integration, significantly improving imaging efficiency and sensitivity.

3.2. Optical Parameters

Optical parameters describe the intrinsic physical properties of the interaction between fiber materials and light waves, which directly affect the choice of imaging techniques, signal fidelity, and the final imaging quality. Typical optical parameters include working wavelength, dispersion characteristics, transmission loss, supported mode types, and coherence.[62]

The choice of working wavelength is the primary consideration for adapting to specific imaging techniques. Since the optical properties (scattering and absorption) of biological tissues differ significantly across wavelengths,[63] a balance must be struck between imaging depth and signal attenuation. For example, in photoacoustic imaging, researchers often use the near-infrared II window (NIR-II, 1000–1700 nm), combined with semiconductor polymer nanoparticles that exhibit strong absorption within this window, enabling deep-tissue imaging at the centimeter scale. Kenry et al.[64] developed TII-TEG polymer nanoparticles (TSPNs) that, when excited by 1064 nm laser light, produce high-contrast photoacoustic signals at depths of up to 5.3 cm, with a SNR of 82.

Dispersion characteristics, particularly group velocity dispersion (GVD), are crucial for coherent imaging systems that rely on broad-spectrum light sources. For instance, optical coherence tomography (OCT)[65] uses a broad-spectrum low-coherence light source; significant dispersion in the fiber would lead to temporal broadening of different wavelength components during propagation, thereby degrading the clarity of interference signals and directly reducing the system's axial resolution. Therefore, high-resolution imaging applications must use single-mode fibers with ultra-low dispersion or dispersion compensation designs[66]

to maintain consistency in optical path differences, thus preserving tissue microstructure information to the highest degree.

Mode types and coherence determine the propagation behavior of light within tissue and the applicability of imaging techniques. Single-mode fibers, which support only a single mode, offer high coherence and collimated beam output, making them ideal for imaging techniques that require interference or phase information, such as in OCT and coherent Raman scattering. In contrast, multimode fibers support multiple propagation modes, providing higher light flux and light collection efficiency, making them more suitable for large-area illumination or weak signal collection scenarios. For example, Du et al. developed a hybrid multimode-multicore fiber (M^3CF), which can achieve a spatial resolution of 2 µm within a 230 µm field of view in a static state and maintain stable light transmission through 61 independent cores (corelets) when bent. This fiber was successfully applied in long-term optogenetic stimulation and monitoring of neurons in freely moving animals.[67] However, the inherent modal dispersion and lower coherence of multimode fibers require wavefront shaping[68] or machine learning algorithms for correction when used in applications that demand precise light field control.

3.3. Transmission Parameters

Transmission parameters quantify the macroscopic performance of light signals after long-distance propagation in optical fibers and are core indicators for assessing their efficiency and fidelity as photon channels. Deep-tissue applications typically involve longer optical paths and weaker signals, thus requiring higher transmission stability and resistance to interference. In this context, transmission parameters mainly encompass loss coefficient, transmission bandwidth, and nonlinear optical effects.[69–71]

The loss coefficient, or attenuation, is a key metric for evaluating the energy transmission efficiency of optical fibers. This parameter is particularly critical in deep-tissue imaging, where light must penetrate multiple tissue layers to reach a target and then return to a detector after being reflected or emitted. Therefore, excellent energy retention capabilities are required. High attenuation leads to significant signal dissipation during transmission, especially in techniques where echo signals are weak and can easily be overwhelmed by background noise, such as in fluorescence imaging or Raman spectroscopy.[72] Therefore, an ideal optical fiber should have extremely low loss characteristics (<0.2 dB/m) to ensure efficient delivery of excitation light to the target region while maintaining the integrity of the returning signal. For example, Koike et al. reported a CYTOP-based graded-index polymer optical fiber with an attenuation as low as 10 dB km^{-1} (≈0.01 dB/m) at wavelengths of 670–680 nm, far better than traditional PMMA fiber's 200 dB km^{-1}. It has been verified to support high-speed transmission at 40 Gbps over 100 meters.[73] This ultra-low loss characteristic demonstrates great potential in biomedical applications, such as deep-tissue weak signal detection.

Transmission bandwidth is a critical indicator for determining whether an optical fiber can support broadband light sources and high-speed signal modulation. In deep- tissue imaging, many cutting-edge techniques rely on wide-spectrum light sources and rapid pulse responses, such as broadband OCT, femtosecond laser photoacoustic imaging, and multispectral fluorescence imaging.[74] Therefore, the optical fiber must have sufficiently high bandwidth capacity to avoid excessive delay or distortion of different frequency or wavelength components during propagation, thus maintaining the integrity of the signal in both the time and frequency domains. Insufficient bandwidth can lead to signal distortion, blurred images, or cross-talk between multispectral channels, and in severe cases, it can even prevent normal imaging.

In high-power laser excitation scenarios, a range of nonlinear optical effects,[74] such as self-focusing, stimulated Raman scattering (SRS), and four-wave mixing (FWM), may occur within the fiber. These effects can cause beam distortion, spectral broadening, and energy fluctuations, which in turn affect the authenticity and stability of the imaging signal. Additionally, nonlinear effects induced by high power may create local hotspots within the fiber, increasing the risk of thermal damage to the tissue, which must be avoided in in vivo imaging applications. Therefore, when designing deep-tissue imaging systems, laser power density must be strictly controlled, and fibers with high nonlinear thresholds, such as low-nonlinearity silica fibers or doped modified fibers, should be chosen. Beam shaping and filtering strategies are also essential to mitigate potential risks.[75]

3.4. Mechanical and Biological Performance

In addition to optical and transmission performance, the success of optical fiber implantation and its long-term stability in living tissue also depend on its mechanical and biological properties. These parameters collectively determine the size of implantation trauma, the device's tolerance to physiological dynamic environments, and the host's long-term biological response. They are key factors in determining whether optical fiber can be successfully utilized in vivo. This section primarily discusses core indicators such as fiber flexibility, tensile strength, and biocompatibility.

Mechanical flexibility, defined by low bending stiffness, is essential for optical fibers to accommodate the dynamic changes in living tissue and ensure stable signal transmission (Figure 2f). Tissues are subject to continuous micro-movements from processes such as respiration, blood flow, and muscle contraction, making fiber flexibility a critical requirement.[76] Traditional quartz fibers are relatively rigid, and when the bending radius is less than a few centimeters, they are prone to brittle fracture or micro-cracks, leading to optical path interruptions. In contrast, flexible optical fibers made from elastic polymer matrices exhibit excellent mechanical performance, even under millimeter-scale bending radii, without mechanical failure. For example, Jiang et al. developed flexible soft polymer optical fibers (SPOF) that maintain an additional loss of less than 0.6 dB cm^{-1} at a 70° bending angle. These fibers were successfully implanted into 2 cm deep in pig tissue using a 21G needle, demonstrating their reliability and safety in complex dynamic environments.[77]

Biocompatibility and surface engineering are fundamental to ensuring good interaction between the fiber and host tissue, enabling long-term, stable application. Ideal biocompatibility minimizes immune rejection and inflammatory responses. Fibrous encapsulation after implantation maintains a stable optical coupling interface between the fiber and tissue. A key strategy is

using biodegradable or biologically inert materials. For example, Shan et al. reported a biodegradable fiber based on citric acid, which showed no significant protein deposition after being implanted in the peritoneal cavity of SD rats. The fiber maintained a low loss of 0.4 dB cm^{-1}.[78] In addition, advanced surface coating technologies not only enhance biocompatibility but also integrate additional functionalities. Park et al. used silver nanowire-PDMS composites as coating layers for multifunctional fiber probes, successfully achieving long-term electro-optical monitoring in the spinal cord of freely moving mice without significant inflammatory reactions.[58] This highlights the important role of functional coatings in improving the safety and functionality of long-term implants.

Overall, the series of key parameters discussed in this section collectively form the core objectives of optical fibers designed for specific applications. To precisely control these performance metrics in response to the complex challenges of deep tissue, foundational design based on materials engineering and structural engineering is essential. The fiber's constituent materials impart its intrinsic optical, mechanical, and biological properties, while the engineered design of its structure and geometry provides higher-dimensional control, ultimately determining how light is confined and guided within the fiber. Therefore, the next sections will focus on these two engineering approaches in fiber design, beginning in section 4 with an exploration of diverse material systems, followed by a detailed discussion of innovative structural paradigms in section 5.

4. Material Composition

The performance and functionality of optical fibers in biomedical applications are fundamentally determined by their core materials. The intrinsic properties of these materials not only directly define the optical characteristics of the fibers—such as transmission loss, working wavelength, and dispersion—but also determine their mechanical properties (flexibility, Young's modulus) and biological behavior (biocompatibility, degradability).[79] Therefore, to balance different performance dimensions, it is crucial to carefully design and select optical fiber materials for different deep-tissue applications. This section will systematically review key materials currently used in biomedical optical fibers: from quartz (SiO_2), the gold standard for industrial and research applications, to polymers that provide great mechanical flexibility, soft glasses that open new windows in the mid-infrared spectrum, and hydrogels designed to achieve ideal tissue matching. While no single perfect material exists, this section aims to provide clear material science guidance for the design of functionalized optical fibers aimed at specific diagnostic and therapeutic needs by deeply analyzing the unique advantages and inherent limitations of various materials.

4.1. Quartz

Quartz optical fibers, composed primarily of high-purity silicon dioxide (SiO_2), are the most technically mature and widely used optical fibers in biomedical applications. Their core advantage lies in their exceptional optical performance: over a broad spectral range of 240–2500 nm, quartz optical fibers can maintain ultra-low transmission loss of <0.2 dB km^{-1},[76] enabling stable and efficient transmission of high-power lasers from visible to near-infrared wavelengths. For example, near the water absorption peak at 1470 nm, quartz optical fibers can achieve precise penetration of 0.4 mm into soft tissues, such as blood vessels, making them ideal for efficient laser coagulation and tissue welding.[80]

In terms of biocompatibility, surface-passivated quartz exhibits high biological inertness. Experiments have shown that even when its outer surface temperature rises to around 74 °C, no significant tissue inflammatory response is triggered, demonstrating excellent thermal stability and the potential for repeated high-temperature sterilization.[80] However, quartz also has notable drawbacks. Its high Young's modulus of 72 GPa causes a significant mechanical mismatch with soft tissues (typically in the kPa to MPa range), leading to poor mechanical compliance and susceptibility to brittle fracture under minor bending. Furthermore, its high fusion technology requirements and cost limit its application in certain scenarios. As a result, quartz optical fibers are better suited for short-duration deep-tissue imaging and therapy that require high beam quality, transmission power, and positional accuracy. For long-term implantation, flexible cladding or composite structures are typically used to alleviate mechanical mismatch issues.

With its unique advantages, quartz optical fibers have played an indispensable role in several cutting-edge deep-tissue optical technologies. In multiphoton imaging, quartz fibers are ideal carriers for transmitting high-energy femtosecond laser pulses. Their low dispersion and high damage threshold ensure temporal and energy stability during transmission. Andresen et al.[81] demonstrated the use of quartz fibers to transmit 1100 nm femtosecond laser pulses without damage to a depth of 700 µm beneath the lymph nodes of mice, successfully achieving two-photon excitation of DsRed2 fluorescence protein. This approach maintained lateral resolution at 564 nm and reduced the fluorescence bleaching rate fourfold compared to traditional 760 nm excitation, proving quartz fibers' crucial role in high-resolution, low-light-toxicity deep-tissue imaging. In optogenetics, the thin diameter and controllable output beam of quartz fibers are ideal for precise neural stimulation needs in neuroscience. Petrovic et al.[82] developed a tapered quartz fiber with a core diameter of 200 µm, which reduced the output beam diameter to 656 µm by polishing the tip at a 15° taper. This fine beam control allows for precise stimulation of specific neuronal clusters in the motor cortex of mice, while the integrated dual electrodes (spacing of 500 µm) enable synchronous recording of local field potentials. This tapered tip design also significantly reduces tissue damage during implantation, validating the enormous potential of quartz fibers in precise neuronal control. In optical fiber-based photoacoustic endoscopy, the thermal stability and ease of end-face engineering of quartz fibers make them ideal platforms for integrating ultrasound sensors, enabling both excitation light transmission and ultrasound signal reception. To address its rigidity issues, Nazempour et al.[83] proposed a solution to fabricate quartz-polymer composite fibers through thermal drawing (TDP) processes to effectively reduce bending stiffness and enhance long-term implantation stability in soft tissues (**Figure 3a**). Based on this, Xiao et al.[84] integrated a quartz optical fiber into an 8 mm-diameter acoustic-resolution photoacoustic endoscopy (AR-PAE)

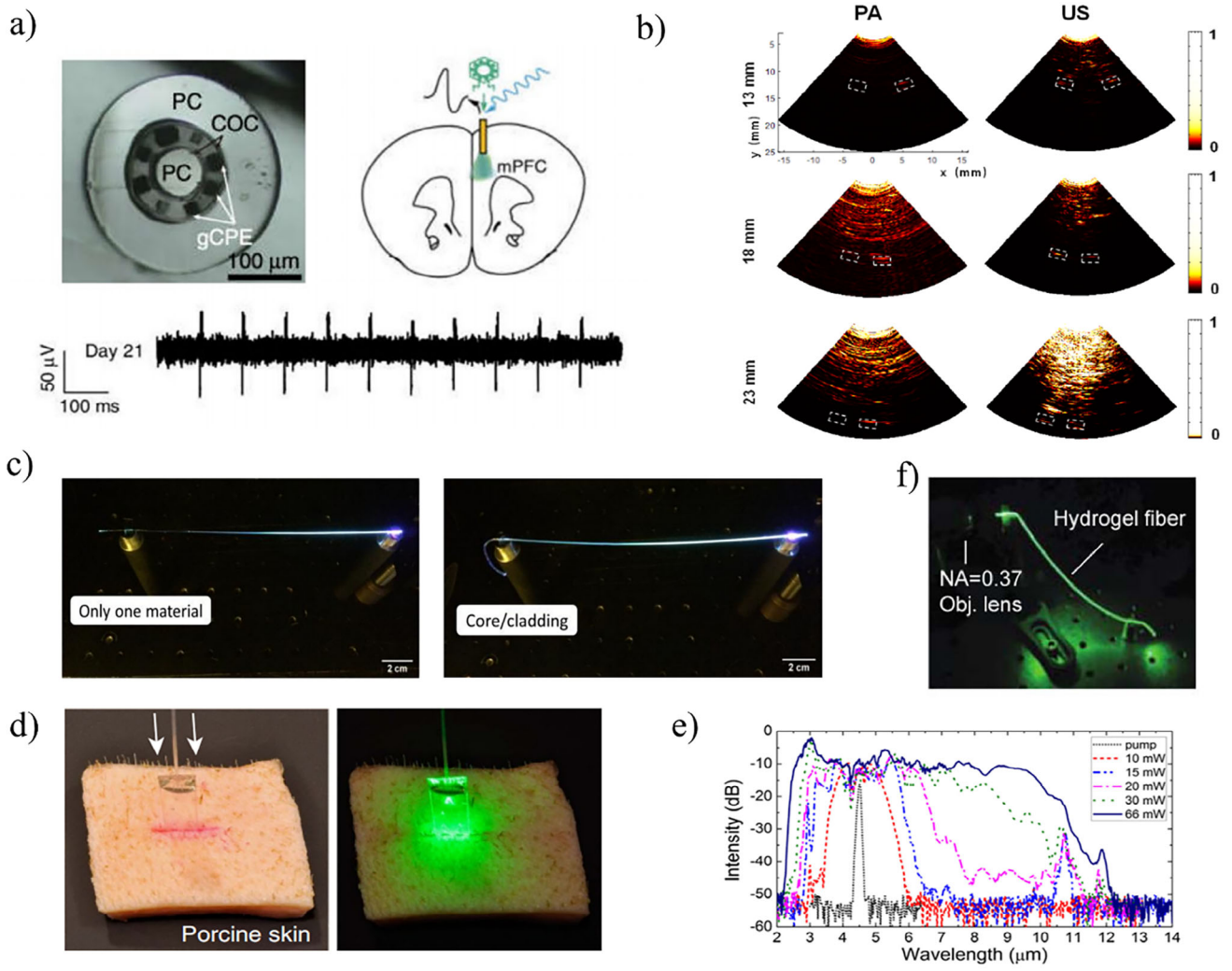

Figure 3. a) A multi-functional composite fiber probe was implanted into the mouse prefrontal cortex for optogenetic stimulation, viral injection, and electrophysiological signal recording. Reproduced with permission.[83] Copyright 2021, Springer Nature. b) Photoacoustic (PA) and ultrasound (US) imaging of channels located at different depths (9, 14, and 19 mm) beneath chicken breast tissue were performed using a multimode fiber probe. Reproduced with permission.[84] Copyright 2022, Optica. c) The transmission of a 405 nm light beam was demonstrated in a single soft glass fiber and in an optical fiber with a core/cladding structure, respectively. Reproduced with permission.[85] Copyright 2020, dissertation. d) A green laser was transmitted through a polymer optical fiber inserted into porcine skin tissue, which had been pre-stained with Rose Bengal dye. Reproduced with permission.[42] Copyright 2016, Springer Nature. e) Broadband mid-infrared supercontinuum generation was achieved from two soft glass fibers with different compositions (Ge15Sb15Se70/Ge20Sb80), pumped by a 4.485 µm femtosecond pulse. Reproduced with permission.[86] Copyright 2021, Springer Nature. f) The transmission of a 532 nm laser in a hydrogel optical fiber was demonstrated, along with the light transmission after the hydrogel fiber was connected to a multimode quartz optical fiber. Reproduced with permission.[87] Copyright 2016, Wiley-VCH.

probe, which was able to transmit 800 nm pulsed laser and efficiently collect 10 MHz ultrasound signals, achieving 1.4 cm imaging depth and 0.77 mm lateral resolution in the rabbit rectum (Figure 3b). Quartz fiber's excellent thermal stability ensures long-term stable operation even at a 20 Hz laser repetition rate, highlighting its unique advantages in miniaturization, multi-functional integration, and harsh in-vivo environments.

4.2. Polymer Materials

Polymer optical fibers (POFs), made from organic polymer-based materials, have become key components in modern biomedical and wearable technologies due to their excellent flexibility, low cost, and electromagnetic compatibility. While they sacrifice some optical performance compared to rigid quartz fibers, they offer superior mechanical flexibility, lower production costs, and more versatile fabrication methods. These characteristics make POFs ideal for biomedical applications requiring high mechanical compatibility (Figure 3d).

In deep-tissue optics, POFs exhibit unique advantages. First, their mechanical properties are closer to soft tissues, with Young's moduli typically in the range of MPa to GPa, much lower than the 50–100 GPa of quartz fibers. This significant difference reduces mechanical damage to tissues during implantation.[58] Furthermore, POFs can be manufactured into complex shapes

via thermal drawing or 3D printing, allowing them to adapt to the intricate paths within deep tissues. For example, PLA-based POFs have been used to penetrate 5–8 cm of pig muscle tissue to activate photochemical reactions. In another study, Nizamoglu et al. utilized bioabsorbable polymers such as poly (lactic acid) (PLA) and poly (lactic-co-glycolic acid) (PLGA) to create optical fibers. These optical fibers, designed for deep-tissue photomedicine, are not only biocompatible and biodegradable but also offer significant advantages over traditional optical fibers. Additionally, POFs have larger core diameters (250–400 µm) and higher numerical apertures (NA = 0.4–0.6), improving light coupling efficiency and keeping light attenuation in biological tissue between 0.1–0.5 dB cm^{-1}.[88,89] Notably, degradable POFs, such as PLGA copolymers, gradually degrade after imaging, eliminating the need for surgical removal.

However, the use of POFs in deep tissue imaging presents some challenges. The most notable is their higher light attenuation coefficient (0.1–1 dB cm^{-1}) compared to quartz fibers (≈0.2 dB km^{-1}), which limits their effective transmission distance within tissues (only 5–10 cm in pig muscle).[84] Although studies have introduced novel materials, such as D,L-dithiothreitol (DTT) – modified polyethylene glycol diacrylate (PEGDA-DTT), which reduce light loss to 0.1–0.4 dB cm^{-1},[89] optimization of light source power or the use of multi-stage relay systems is still needed to compensate for attenuation. Additionally, POFs may suffer from refractive index changes and optical loss due to water absorption in humid environments. Despite these limitations, POFs made from thermoplastic materials like PLA and its copolymers provide significant flexibility and biocompatibility in dynamic tissue environments, though their degradation products' potential impact on optical performance remains a concern.[90]

In summary, while POFs offer superior mechanical flexibility and biocompatibility compared to quartz fibers, their higher light loss presents major challenges for long-distance, high-precision sensing applications. Continuous innovation in materials science and fiber manufacturing technology is crucial for overcoming these limitations and fully unlocking the potential of POFs in medical imaging and therapy.

4.3. Soft Glass

Soft glass optical fibers are specialized fibers made from non-silica-based glass materials such as phosphate, tellurite, borate, and germanate. These materials are characterized by low melting points, high refractive indices, and excellent optical properties. Compared to traditional quartz fibers, the core advantage of soft glass fibers lies in their significantly expanded transmission window, particularly in the mid-infrared (2–5 µm) and longer wavelengths. This feature makes them ideal for directly detecting the molecular fingerprint region. Additionally, they offer higher nonlinear optical coefficients and stronger rare-earth ion doping capabilities (Figure 3e).

The unique advantages of soft glass fibers have led to their vast application potential in several cutting-edge fields. Their wide transmission window (covering 2–16 µm wavelength) enables the generation of ultra-broadband supercontinuum (SC) outputs that span the entire molecular fingerprint region (3–13 µm), opening new pathways for deep tissue imaging and biological molecule detection. For example, Wang et al. utilized tellurite-based soft glass fibers to achieve supercontinuum output in the 2–16 µm range, providing the key technical foundation for label-free imaging of lipid deposits and atherosclerotic plaques in deep tissues.[86] Additionally, soft glass fibers' high nonlinear coefficients (As_2Se_3 with $n2 \approx 1.1 \times 10^{-18} m2/W$) excel in nonlinear effects such as spectral broadening and self-phase modulation (SPM), significantly enhancing spatial and spectral resolution in imaging.

The broad bandwidth transmission capability of soft glass fibers is critical for multimodal imaging. By transmitting light signals of multiple wavelengths through a single fiber, it is possible to integrate OCT, fluorescence imaging, and other modes, providing more comprehensive and detailed information on tissue structure and function. Klimczak et al. utilized this broad bandwidth characteristic to generate supercontinuum spectra from 1.0 to 2.4 µm, covering several biological molecular absorption peaks, thus laying the foundation for multimodal biological imaging.[91] Additionally, certain soft glasses, such as phosphate glasses, exhibit good biocompatibility and degradability, making them ideal for developing implantable optical fiber sensors, with broad applications in long-term in vivo monitoring for tumor diagnosis, vascular imaging, and other biomedical scenarios.

Despite its excellent optical performance, soft glass fibers also have some inherent drawbacks.[92–94] First, their mechanical strength and impact resistance are much weaker than those of traditional quartz fibers, and they are prone to micro-cracking under bending or external force, affecting their long-term reliability. Second, soft glass fibers have poor thermal stability, and high-temperature environments can lead to performance degradation or structural deformation. Moreover, their chemical stability is insufficient, making them vulnerable to damage in acidic, alkaline, or corrosive media. Therefore, while soft glass fibers offer significant potential in label-free molecular imaging and sensing with their unique mid-infrared transmission capabilities, their widespread application still needs to overcome inherent limitations in mechanical strength, thermal stability, and chemical resistance.

4.4. Hydrogels

Hydrogel optical fibers are flexible light optical fibers constructed from high-water-content polymer networks (Figure 3f). Their core advantages lie in their excellent biocompatibility, tissue-like softness, high water content, and superior mechanical stretchability. These characteristics enable seamless integration with biological tissues at both physical and chemical levels, showcasing enormous potential in in vivo optical sensing, biological signal transmission, and light-controlled drug release in cutting-edge biomedical fields.[95,96]

For seamless integration with biological tissues, matching mechanical properties is crucial. For example, Guo et al. developed a hydrogel optical fiber based on sodium alginate and polyacrylamide, with a Young's modulus (≈80 kPa) that closely matches brain tissue (3–10 kPa). This mechanical compatibility significantly reduces immune responses and damage to the blood-brain barrier after implantation, creating favorable conditions for long

-term, high-fidelity in vivo optical monitoring and intervention.[87] Due to their inherent hydrophilicity and stability in aqueous environments, hydrogel optical fibers are well-suited for real-time monitoring of bodily fluids (sweat, blood). Compared to traditional rigid, hydrophobic fibers, their fundamental property is the ability to integrate tightly with living organisms while maintaining optical transmission capabilities. This unique biophotonic interface makes them highly valuable in implantable sensors, tissue engineering scaffolds, and smart prosthetics. Particularly in neural modulation applications, hydrogel fibers can efficiently transmit NIR, which is highly penetrating in biological tissues, providing an ideal tool for precise deep neuron stimulation.[97]

Although hydrogel optical fibers are regarded as a promising next-generation biomaterial for optical fiber technology due to their unique biological adaptability, their inherent disadvantages should not be overlooked. First, their mechanical strength is much lower than traditional optical fibers, and they are prone to permanent deformation or even breakage under repeated stretching or bending.[98] Second, their high water content makes their performance highly sensitive to environmental temperature and humidity, with water evaporation leading to structural shrinkage and optical performance degradation, thus shortening their lifespan.[58] Additionally, their higher optical loss limits their ability to transmit signals over long distances. Therefore, hydrogel optical fibers still face multiple challenges regarding mechanical robustness, environmental stability, and optical performance.

5. Structural Paradigms

Based on the intrinsic properties of materials, the structural paradigm of optical fibers further affects the transmission behavior of light signals within the optical fiber. By precisely controlling key parameters such as core size, refractive index distribution, and geometry, the propagation modes, intermodal dispersion, polarization-maintaining ability, and spatial multiplexing potential of the fiber can be directly influenced. Therefore, careful structural design can transform general optical fibers into functionalized optical fibers tailored for specific biomedical applications, such as high-resolution imaging, high-fidelity sensing, and multi-point parallel detection.[99–101] This section will systematically discuss how different structural designs confer unique performance advantages and applications, focusing on three core dimensions: propagation modes, refractive index profiles, and core configurations.

5.1. Propagation Modes

The number of propagation modes supported by an optical fiber is its most fundamental structural parameter and directly determines the trade-off between signal fidelity and light collection efficiency. Based on the number of modes they support, optical fibers can be classified into two main categories: SMF and MMF (**Figure 4a**). These categories are suited for different application scenarios, with SMF emphasizing signal quality and MMF focusing on light flux.[102–104]

SMF have very small core diameters (typically 8–10 μm) and support only a single propagation mode at a specific wavelength, thereby fundamentally eliminating intermodal dispersion and ensuring extremely high spatial and temporal coherence. Their output beams are stable and well-collimated, making them ideal for long-distance, high-bandwidth, and high-resolution imaging applications.[105–107]

In the biomedical field, SMFs are widely used in OCT, fiber interferometry, and Raman probe systems. For example, in intravascular OCT applications, a probe integrated with SMF (with an outer diameter of 2.67 mm) can transmit a 1310 nm central wavelength light source, achieving non-invasive measurement of the 0.4 mm compressed thickness of pig renal arteries, with axial and lateral resolutions of 11 and 25 μm, respectively.[108] In Raman spectroscopy, SMF's high coherence ensures precise excitation of lasers and accurate analysis of Raman scattering signals, making it possible to chemically analyze tumor markers in deep tissues. In fiber interferometers, the coherent light transmitted by SMF can monitor nanometer-scale tissue displacements or pressure, such as in real-time monitoring of intracranial pressure.[108]

However, the use of SMF also faces several challenges. First, its small core size leads to lower light source coupling efficiency and stringent alignment requirements. The coupling efficiency between standard SMFs and laser sources is typically below 60%, requiring sub-micron-level alignment platforms to ensure stable transmission.[110] Second, its small numerical aperture (typically 0.1–0.22) limits the ability to collect scattered light. For example, in brain tissue imaging, its light collection efficiency is only 1/5 that of MMF.[57] Furthermore, in scenarios requiring high flexibility (such as endoscopy), the bending loss of SMF is significant. When the bending radius is less than 5 mm, light loss can increase by over 30%, making it difficult to adapt to dynamic, bending environments like the gastrointestinal tract.[108]

MMF, with larger core diameters (typically ≥50 μm), support hundreds or even more propagation modes, resulting in high light source coupling efficiency and light collection capacity.[110,111] For example, MMF with a 62.5 μm core diameter can achieve coupling efficiency of over 85% with LED light sources, much higher than that of SMF.[111] This makes MMF particularly advantageous for signal collection in applications where light signals are weak. MMFs play a key role in photoacoustic imaging (PAI), Diffuse Optical Tomography (DOT), and fiber photometry (Figure 4b,c). In PAI, MMF efficiently transmits high-energy pulsed lasers and collects the photoacoustic signals generated by tissues. Xiao et al.[109] integrated quartz MMF into an 8 mm diameter probe, transmitting 800 nm pulsed light, achieving photoacoustic imaging of rabbit rectum to a depth of 1.4 cm, with lateral resolution of 0.77 mm. In brain functional imaging, MMFs are used in DOT systems to efficiently transmit light in the 650–900 nm range and collect scattered light to monitor brain oxygen saturation (sO_2), achieving spatial resolution of 5 mm.[117] In fiber photometry, MMFs transmit 475 nm excitation light and collect fluorescence from calcium indicators (GCaMP), monitoring neuronal activity in freely moving mice with a high signal-to-noise ratio of 30 dB.[117]

Despite their excellent light collection capabilities, MMFs also have significant inherent limitations. Their primary drawback is severe intermodal dispersion: light of different modes propagates along different paths, causing pulse broadening that reduces temporal resolution and bandwidth. For instance, in a 1 m

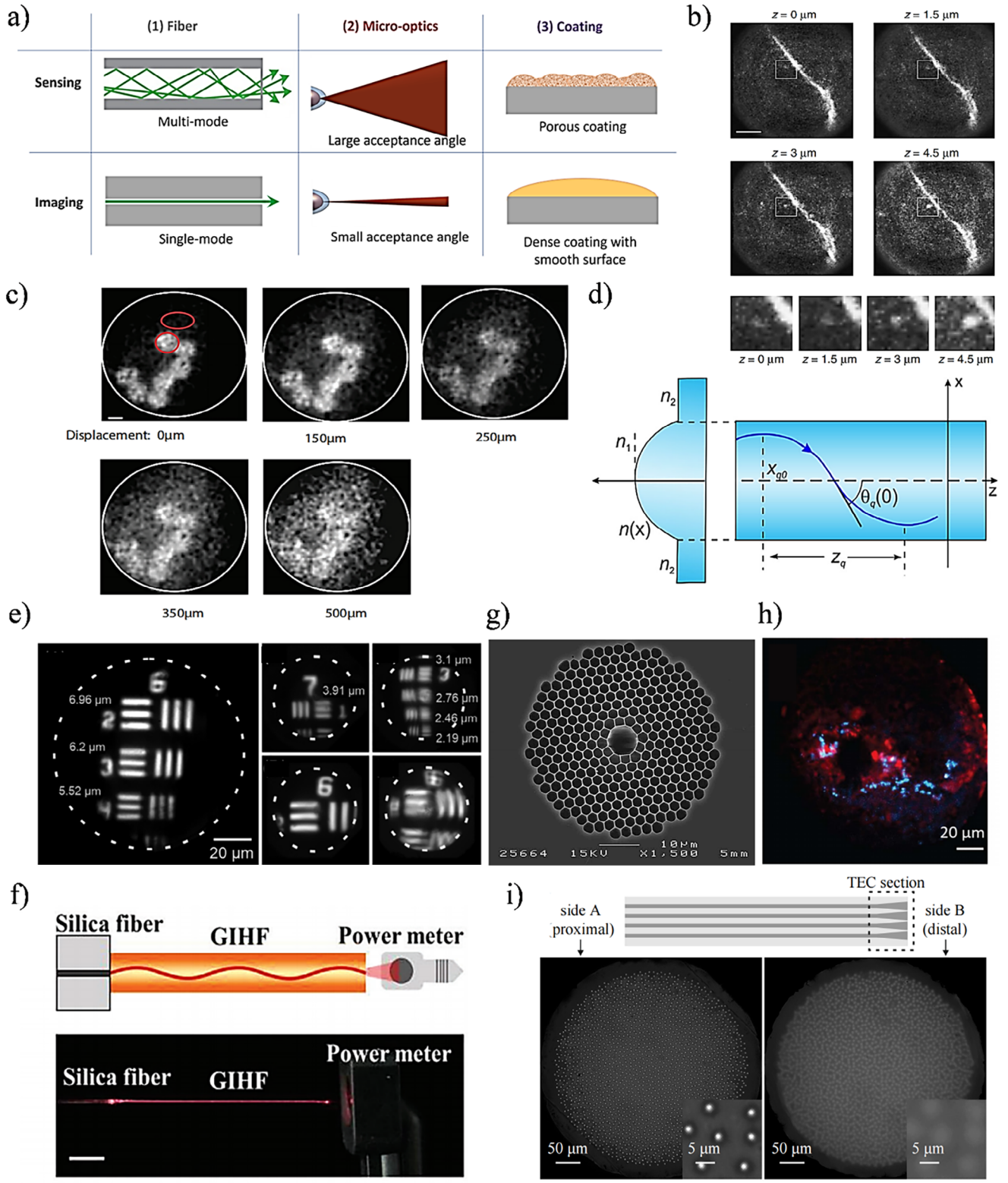

Figure 4. a) This illustrates the different applications of single-mode and multi-mode fibers in imaging and sensing, where single-mode fibers are suitable for high-resolution imaging, and multi-mode fibers enhance fluorescence signal collection. Reproduced with permission.[109] Copyright 2024, Optica. b) Multi-mode fiber imaging clearly reveals the 3D structure of dendritic spines. Scale bar: 10 μm. Reproduced with permission.[110] Copyright 2018, Springer Nature. c) Multi-mode fiber imaging was conducted by adjusting the fiber position to assess the maximum bending tolerance. Reproduced with permission.[111] Copyright 2018, Optica. d) Graded-index fibers improve light signal propagation through a gradual change in refractive index, enhancing imaging performance. Reproduced with permission.[112] Copyright 2022, Wiley-VCH. e) Graded-index fiber imaging demonstrates the impact of varying

long MMF, the mode delay difference can reach 5 ns, which is sufficient to blur fine vascular structures in high-resolution photoacoustic imaging.[109] Additionally, speckle patterns are generated due to multimode interference, and they are extremely sensitive to environmental disturbances such as vibration and temperature changes. For example, it has been reported that a 1 °C temperature fluctuation can cause a 15% change in photoacoustic signal intensity, severely affecting the stability and reproducibility of imaging.[109] Therefore, the core challenge for MMFs in precision applications is how to mitigate or compensate for intermodal dispersion and environmental sensitivity while leveraging their high light throughput.

Coherent fiber bundles (CFBs), consisting of thousands of individual fiber cores, provide a unique parallel imaging platform that enables "scan-less" endoscopy. However, their translation to deep tissue imaging is met with several constraints, including the "honeycomb" artifact from inter-core cladding and the large footprint (>500 µm) required for a sufficient field of view. Critically, CFBs are highly sensitive to bending-induced phase decorrelation, which scrambles the phase relationship between cores. This pronounced sensitivity makes CFBs particularly ill-suited for coherent imaging modalities like holography or phase-contrast imaging, which are essential for many advanced applications. Consequently, the vast majority of CFB-based endomicroscopy research has concentrated on fluorescence imaging. As an incoherent process, fluorescence relies on transmitting light intensity from each core—a task for which CFBs are fundamentally designed and which remains robust against the phase shifts induced by bending. This focus is further driven by the critical role of fluorescence in providing molecular specificity for diagnostics and functional imaging, despite the remaining challenges of pixelation and limited optical sectioning.[118]

Despite these limitations, recent innovations are pushing the boundaries of CFB performance in fluorescence imaging. One approach focuses on enhancing the optical design at the probe tip. For example, a study by Pablo et al.[119] developed a high-contrast endoscope by integrating an ultrafast laser-fabricated fused silica end-cap into a polymer CFB (PMMA CFB) with a 1.36 mm FOV. This system, designed for selective plane illumination microscopy (SPIM), provided optical sectioning to effectively suppress background fluorescence, enabling real-time (5–7 fps) visualization of alveolar tissue autofluorescence in an ex vivo human lung model without exogenous fluorophores. This demonstrates how micro-optical hardware can significantly improve 2D image contrast and reduce artifacts.

Further advancing beyond 2D, another innovative strategy shifts the paradigm from optical design to computational reconstruction. This method utilizes a diffuser at the distal tip of the CFB to encode a 3D scene into a single 2D speckle pattern, which is then decoded by a neural network. For instance, a recent study by Lich et al.[120] demonstrated a "diffuser-fiber-endoscope" capable of single-shot 3D non-coherent fluorescence imaging through a probe tip with a diameter of just 700 µm. The neural network reconstructs the 3D volume in under 20 ms, enabling video-rate imaging at up to 50 fps with an axial resolution of 125 µm. Critically, because this approach relies on intensity patterns, it is robust against bending-induced phase shifts. This combination of a passive optical encoder and a powerful computational decoder opens new avenues for real-time, 3D functional imaging, such as in vivo deep-brain calcium imaging, in dynamic environments.

5.2. Refractive Index Profile

The refractive index profile of an optical fiber, or the distribution of the refractive index between the core and cladding, is a critical design element that controls the propagation paths of light within multimode optical fibers and governs intermodal dispersion. Based on whether the refractive index profile is step-index or graded-index, optical fibers can be classified into Step-Index Fibers (SIF) and Graded-Index Fibers (GIF). These two types of fibers differ significantly in their ability to suppress pulse broadening.[121,122]

Step-index fibers have a uniform and higher refractive index in the core compared to the cladding, creating a sharp step-like change at the core-cladding interface. This refractive index distribution confines light within the core via total internal reflection, and light propagates along a zig-zag path through the core.[123–125] In deep tissue imaging, step-index fibers are particularly effective due to their high light coupling efficiency and excellent light scattering collection ability. In photoacoustic imaging, Saini et al.[126] used a 3 cm long chalcogenide step-index fiber (core material $AsSe_2$, cladding As_2S_5) to generate a supercontinuum spectrum spanning 1.6–3.7 µm via 2.6 µm femtosecond laser pumping. This spectrum effectively penetrated deep tissues to excite specific photoacoustic signals, achieving functional imaging of a mouse tumor model at a depth of 1.2 cm with a spatial resolution of about 30 µm. Similarly, in DOT, Gordon et al.[127] employed a multi-core fiber bundle made of 6000 step-index fibers (core diameter 2.9 µm) to construct an endoscope. Its high-light coupling efficiency greatly improved the system's ability to collect scattered light from tissues, enhancing the signal-to-noise ratio by 40%, which was critical for blood oxygen metabolism imaging in breast cancer patients at a depth of 2 cm. Notably, in applications requiring high signal fidelity, such as real-time monitoring of dynamic physiological processes, single-mode step-index fibers are ideal. Their small core size supports single-mode propagation, effectively eliminating intermodal dispersion and preserving the integrity of the light signal. For example, Yazdi et al.[128] used a single-mode step-index fiber in a combined Diffuse Optical Spectroscopy (DOSI) and Diffuse Correlation Spectroscopy (DCS) system to monitor tumor hemodynamics in breast cancer patients

core diameter and numerical aperture (NA) on image resolution. Reproduced with permission.[112] Copyright 2022, Wiley-VCH. f) The structure and transmittance measurement method of graded-index hydrogel fibers (GIHF) are shown, illustrating the fiber's light transmission capability. Reproduced with permission.[113] Copyright 2023, Wiley-VCH. g) Hollow-core photonic bandgap fibers (HC-PBGF) with an 8 µm core and seven-cell defects effectively guide light signals. Reproduced with permission.[114] Copyright 2015, Frontiers Media S.A. h) Hollow-core fibers are applied in human brain section imaging, demonstrating three-photon and third-harmonic generation imaging. Reproduced with permission.[115] Copyright 2024, IEEE. i) The cross-sectional structure of multi-core fibers displays the arrangement of different fiber cores and their imaging applications. Reproduced with permission.[116] Copyright 2024, Springer Nature.

with a time resolution of 0.5 s, capturing instantaneous physiological changes in tissues.

While step-index fibers offer significant advantages in deep-tissue imaging, they also have some limitations. The primary issue is intermodal dispersion. Because light enters the fiber at different angles (corresponding to different modes), the path lengths within the core vary, resulting in different arrival times at the output. This time delay causes significant pulse broadening, reducing temporal resolution and system bandwidth. Additionally, step-index fibers exhibit relatively high bending loss. When the fiber is bent, some modes may have an incident angle smaller than the critical angle for total internal reflection, causing light leakage from the core into the cladding, leading to energy loss. In applications that require fiber bending, such as endoscopic imaging, bending loss reduces the light intensity reaching the tissue, thereby lowering the image's signal-to-noise ratio.[127] Furthermore, the numerical aperture (NA) of step-index fibers is determined solely by the refractive indices of the core and cladding, limiting their flexibility. This restricts their ability to collect light from different incident angles. In applications like diffuse optical tomography, where light needs to be collected from multiple scattering angles, the inability to match the NA of the fiber with the scattering light field can affect the accuracy of physiological parameter measurements.[128]

Graded-index fibers (GIF) optimize light propagation paths by designing a continuous, gradually changing refractive index distribution from the center of the core to its edge, typically in a parabolic shape (Figure 4d).[123,124,129,130] The higher refractive index at the center of the core slows down light, while the lower refractive index at the edges speeds it up. This design causes light of different modes to propagate along nearly sinusoidal paths, with higher-order modes (longer paths) traveling faster in lower refractive index regions, compensating for path length differences. As a result, the propagation times of different modes converge, significantly suppressing intermodal dispersion. This characteristic gives graded-index fibers a unique advantage in deep tissue imaging applications requiring high temporal and spatial resolution.

In deep-tissue imaging, graded-index fibers are ideal light transmission mediums due to their excellent temporal stability and spatial uniformity. Pochechuev et al.[112] implanted a GRIN fiber (core diameter 230 µm, NA 0.22) into the retrosplenial cortex of a mouse, achieving cellular-level resolution imaging of the mouse's brain at a depth of 8.1 mm (Figure 4e,f). Thanks to the low dispersion properties of GRIN fibers, the system successfully captured calcium signal dynamics of neurons with a time resolution of 30 fps and a fluorescence signal contrast of 0.4. To overcome the rigidity of traditional quartz fibers, Zhuo et al.[113] developed a graded-index hydrogel optical fiber (GIHF). This fiber showed an extremely low bending loss of only 0.24 dB/90° and achieved photoacoustic signal transmission to a depth of 2 cm in simulated brain tissue. Its excellent control of modal dispersion improved the lateral resolution of tumor microenvironment imaging to 5 µm. Additionally, GRIN fibers themselves can act as objective lenses, making them ideal for constructing ultra-thin endoscopes. Sivankutty et al.[131] demonstrated the use of a 125 µm diameter, 4 cm long GRIN multimode fiber to build an ultra-thin two-photon endoscope, achieving a lateral resolution of 1.55 µm and an axial resolution of 18.1 µm for imaging 200 nm fluorescent beads, showing great potential in deep neural network 3D imaging in mouse brains.

Despite their excellent performance, graded-index fibers face some challenges. Their performance heavily depends on precise control of the refractive index gradient, as any slight inhomogeneity can destroy their low dispersion properties, thus impairing imaging quality. For example, fabricating GIHF requires precision in controlling the gradient distribution of the refractive index from 1.38 to 1.34 using projection-assisted 3D printing technology.[132] Graded-index fibers are also more sensitive to material uniformity and mechanical stability. Thermal expansion or external mechanical stress can alter the internal refractive index distribution, leading to fluctuations in optical performance.

5.3. Core Geometry

Innovation in optical fiber core configurations has broken through the limitations of traditional circular solid-core designs, endowing optical fibers with entirely new functional dimensions beyond simple light signal transmission. Special structures, such as Hollow-Core Fibers (HCF) and Multi-Core Fibers (MCF), have been developed to address the inherent limitations of conventional fibers in advanced applications like polarization control[114,115] and multi-channel parallel processing.[133,134]

As the most mature and widely used optical transmission medium, circular solid-core fibers offer high-quality, low-loss light signal transmission due to their symmetrical structure and uniform refractive index distribution. They perform excellently in efficiently guiding laser or broadband light into deep biological tissues and effectively collecting internal reflected and scattered light. These fibers are indispensable elements in deep tissue imaging technologies such as endoscopy, PAI, and near-infrared spectroscopy.[135,136] However, the simple circular symmetry of these fibers also brings limitations. Standard circular core fibers do not possess birefringence characteristics, meaning they cannot maintain the polarization state of light. This makes them unsuitable for detection scenarios requiring precise polarization control, such as enhancing imaging contrast via polarization modulation or identifying specific tissue structures (collagen fiber orientation) based on polarization differences. Additionally, in complex and dynamic physiological environments (heartbeats, blood vessel curvature), the bending of the fiber can disrupt mode orthogonality, leading to mode coupling and energy loss, which distorts the signal and reduces the quality and accuracy of imaging.

To address these limitations, researchers have developed fibers with alternative core configurations, such as hollow-core fibers (HCF) (Figure 4g), to enable additional functionalities. These fibers guide light through a hollow core, and their unique geometry typically introduces strong birefringence effects, which effectively suppress coupling and crosstalk between different polarization modes, ensuring high fidelity in maintaining polarization states during transmission, also known as polarization-maintaining (PM) properties.[137–139] This feature greatly enhances the reliability of polarization-sensitive detection. For example, Labat et al.[140] designed a hollow-core double-clad fiber coupler that reduces mode coupling through structural optimization, achieving stable polarization transmission in

nonlinear endoscopes and significantly improving the contrast of two-photon imaging. In polarization spectroscopy applications, hollow-core fibers can precisely capture slight changes in tissue polarization states, effectively differentiating between healthy and diseased tissue, such as early tumor screening by monitoring polarization changes caused by extracellular matrix remodeling (Figure 4h). Septier et al.[115] used hollow-core fibers' polarization-maintaining properties in a multimodal endoscope to successfully distinguish different orientations of collagen fibers in mouse skin. Moreover, Zhang et al.[141] used mid-infrared lasers generated by hollow-core fibers in polarization-sensitive photoacoustic imaging to detect the myelin arrangement direction in mouse brain tissue. The primary challenge of hollow-core fibers is coupling efficiency and alignment precision. Due to their different light-guiding modes compared to standard solid-core fibers, hollow-core fibers require extremely precise alignment when coupled with light sources or detectors. Lyu et al.[142] confirmed that even small deviations can lead to severe mode mismatch and power loss, directly impacting the final image's signal-to-noise ratio.

Multi-core fibers (MCF) integrate multiple independent cores within a single optical fiber cross-section, enabling spatially parallel information transmission and collection, significantly expanding the application potential of optical fibers in the biomedical field.[143–146] Their most prominent advantage is the ability to perform real-time, multi-parameter physiological monitoring. Each core can be designed to transmit different signals or sense various parameters (e.g., temperature, pH, oxygen saturation), making MCFs an ideal platform for building multimodal integrated detection systems. In tumor microenvironment monitoring, a multi-core fiber can simultaneously collect local temperature, hypoxia levels, and pH values, providing comprehensive data for evaluating the metabolic state of tumors. Wang et al.[147] combined multi-core fibers with deep learning algorithms, collecting spontaneous fluorescence signals from different cores to achieve high-resolution boundary identification of glioblastomas. Zolnacz et al.[116] developed a thermally expanded core multi-core fiber, which increased the core diameter to improve light collection efficiency and enhanced image contrast by 2.6 times in lensless imaging.

However, the main obstacle in the widespread application of multi-core fibers is the crosstalk among cores. Due to the small spacing between the neighboring cores, light signals from one core may leak or couple into adjacent cores, causing interference between channels, which reduces the signal-to-noise ratio and measurement accuracy. It is worth noting that some designs aimed at optimizing other performance aspects can exacerbate crosstalk. For instance, research by Zolnacz et al. demonstrated that efforts to improve light collection efficiency through thermal core expansion resulted in a significant increase in inter-core crosstalk, with the value worsening from better than −30 dB to −16 dB.[116] Therefore, the key challenge in multi-core fiber design is how to effectively suppress crosstalk while improving performance, which requires careful design consideration.

6. Auxiliary Techniques for Optical Fibers

Although optical fibers efficiently deliver light to deep tissues, a passive fiber alone is insufficient to form a complete, high-performance biomedical photonics system. Its ultimate performance is constrained by two fundamental limitations: the inherent boundaries of physical transmission and challenges related to signal fidelity.[148] Physically, the fiber's NA and material dispersion define the theoretical limits of spatial and temporal resolution. As a passive optical fiber, optical fibers lack the ability to actively control light wave parameters such as wavelength.[33,149] Regarding information, the transmission and collection of light through fibers and tissue inevitably introduce wavefront distortions and noise, resulting in data that do not directly reflect the true tissue structure and function.[150,151] Therefore, to overcome these bottlenecks, a range of auxiliary technologies must be introduced at the physical front-end and computational back-end of the fiber system to optimize both photon flow and information flow collaboratively.

6.1. Front-End Physical Modulation

Physical front-end control technologies focus on actively modifying the physical properties of light before its interaction with biological tissues.[152–154] This strategy is primarily implemented through two pathways: controlling photon properties and converting energy forms. Nonlinear optical effects are used to alter the wavelength of light to precisely match the optical window of biological tissues or the spectral characteristics of specific molecules.[155–157] Alternatively, the light energy delivered by the fiber can be efficiently converted into sound (photoacoustic effect) or heat (photothermal effect), enabling new imaging modes or targeted therapy.[15,158,159]

6.1.1. Wavelength Conversion

Wavelength conversion technology is one of the key strategies for improving tissue optical imaging depth and resolution. The core idea is to use nonlinear optical effects to convert light at the initial wavelength into new wavelengths that are more suitable for biological applications, such as tissue penetration, target excitation, or signal detection.[160–162] There are two main approaches to this technology.

The first is to convert longer wavelengths of light (near-infrared light) that are easier to transmit in fibers into shorter wavelengths that can efficiently excite specific targets. For example, Li et al.[163] used the Cherenkov Radiation effect of nonlinear fibers to blue-shift 1.03 µm near-infrared femtosecond laser light to the 0.6–0.8 µm range, effectively exciting the blue fluorescent probe DAPI, allowing imaging of the mouse skin hair follicle cell nuclei. Similarly, Charan et al.[117] used the soliton self-frequency shift effect within the fiber to first convert a 1550 nm laser into a 1880 nm soliton, then generate a 940 nm laser through second-harmonic generation, which could efficiently excite green fluorescent markers (fluorescein) for brain vascular imaging in mice. In this study, the nonlinear fiber simultaneously transmitted multiple wavelengths of light (0.6–0.8 µm, 1.03 µm, and 1.2–1.4 µm), guiding the excitation light to the hair follicle deep within the tissue and synchronously collecting multiple fluorescent signals, achieving multi-color imaging of different structures within the hair follicle with both improved depth and resolution compared to traditional methods.

The second approach reverses the process, converting short-wavelength fluorescence signals generated deep within tissues into near-infrared light for more efficient transmission through the fiber. Kobat et al.[164] demonstrated this by finding that while two fluorescent molecules had different excitation wavelengths, the 700 nm fluorescence signal produced by Alexa680 had much lower absorption in blood compared to the 518 nm fluorescence signal from FITC, making it more suitable for efficient collection via fibers.

6.1.2. Energy Conversion

Energy conversion technology uses optical fibers to precisely deliver light energy to a target area and convert it into other energy forms. The photoacoustic (PA) effect—the conversion of light energy into sound waves—is a powerful tool for achieving high-resolution imaging in deep tissues.[15,165] For example, Xu et al.[166] developed a photoacoustic tomography (PACT) system based on a negative focus fiber laser ultrasonic transducer. The system used fiber to transmit laser light and converted the light energy into sound using the photoacoustic effect, achieving non-invasive imaging of mouse brains at depths greater than 7 mm with a spatial resolution of about 130 μm. In another photoacoustic application, Zhao et al.[167] integrated multimode fibers with optical fiber ultrasound sensors into a 20G medical needle (outer diameter 0.9 mm), creating a thin photoacoustic endoscopic microscope probe. Using wavefront shaping technology, the probe focused excitation light through the fiber to deep tissues, achieving sub-cellular resolution imaging of mouse red blood cells, demonstrating potential for guiding minimally invasive surgery (**Figure 5a**).

Another key application is the photothermal effect, where light energy is converted into heat energy, commonly used for targeted therapy and controlled drug release. For example, Yang et al.[168] designed a fiber needle array (OFNA) by inserting multimode fibers into small needles to deliver near-infrared light directly to subcutaneous tumors. The light energy was converted into heat for photothermal therapy (Figure 5b). Compared to traditional direct laser irradiation, this method significantly reduced thermal damage to the skin and allowed real-time monitoring of the activation state of gold nanocaps in the tumor through the central imaging fiber bundle. Similarly, Zhang et al.[27] proposed an optical fiber drug delivery system that used fiber to transmit 980 nm laser light, with rare-earth ions in the fiber core acting as a photothermal converter. The generated heat triggered the release of doxorubicin (Dox) from thermosensitive hydrogels wrapped around the fiber's surface, achieving a combined photothermal-chemotherapy treatment, while built-in sensors monitored temperature and drug release in real-time.

6.2. Back-End Signal Processing and Reconstruction

Complementing the hardware control of the physical front-end, the computational and algorithmic back-end focuses on the information processing layer. It treats the optical fiber as an integral part of the entire computational system, aiming to fundamentally address the challenges of signal fidelity faced during optical signal transmission through fibers and biological tissues. The core data processing chain can be summarized in three synchronized steps: first, using wavefront shaping techniques to encode the light field, compensating or reversing the joint distortions introduced by the fiber and biological tissue;[15,165] second, using image reconstruction algorithms to decode the indirect data collected by the detectors and restore meaningful images or sensor information;[161,162] and finally, leveraging machine learning and other data-driven methods to optimize the results, achieving precise light field control in deep tissues, thus enabling efficient targeted therapy, high-resolution imaging, or high-precision sensing.[160]

6.2.1. Wavefront Shaping and Computational Imaging

Wavefront shaping is an active computational imaging strategy. The core idea is to precisely control the phase, amplitude, or polarization of the incident light field before the light signal transmission, using devices like spatial light modulators (SLM), to actively compensate for wavefront distortions caused by biological tissues or multimode fibers. This pre-compensation encoding aims to transform random scattering processes into a determined and reversible transmission process.

This technology effectively combats dynamic disturbances, achieving stable deep focusing or imaging. For example, Wen et al.[169] developed the stable endoscope technology, which uses spatial frequency beacon tracking and full-vector modulation to maintain sub-diffraction-limit resolution of 250 nm even under fiber bending and twisting conditions, successfully achieving in vivo imaging of the mouse gastrointestinal tract (Figure 5c).

Furthermore, by precisely measuring and inverting the system's transmission matrix (TM), researchers can achieve precise control over the light field, even breaking through traditional imaging mode limitations. For instance, Cheng et al.[173] applied a combination of natural gradient ascent strategies and an improved non-convex optimization algorithm (RAF 2-1) to not only project high-quality patterns through 15 meters of unstable multimode fiber but also improve the image quality of an acoustic-resolution photoacoustic microscope (AR-PAM) to optical-resolution (OR-PAM) levels, enhancing lateral resolution from 54.0 to 5.1 μm.

To address the challenges of strong scattering and dynamic changes in deep tissues, Cheng et al.[161,174] developed high-gain, high-speed wavefront shaping (HGHS-WFS) technology. This technology, by introducing concepts like stimulated emission light amplification, improved energy gain to nearly perfect unity (≈1000 times that of traditional AOPC technology) and enhanced response speed to the microsecond level (≈10 μs). With these breakthroughs, the technology successfully penetrated strongly scattering dynamic media such as 4 mm thick chicken breast slices and live mouse ears, achieving effective optical focusing and paving the way for clinical applications of wavefront shaping in optogenetics, minimally invasive surgery, and photodynamic therapy.

Beyond the aforementioned strategies based on computation and active feedback, another rapidly emerging direction is the direct integration of advanced micro-optical elements, such as diffractive optical elements (DOEs) and meta-optics, into fiber

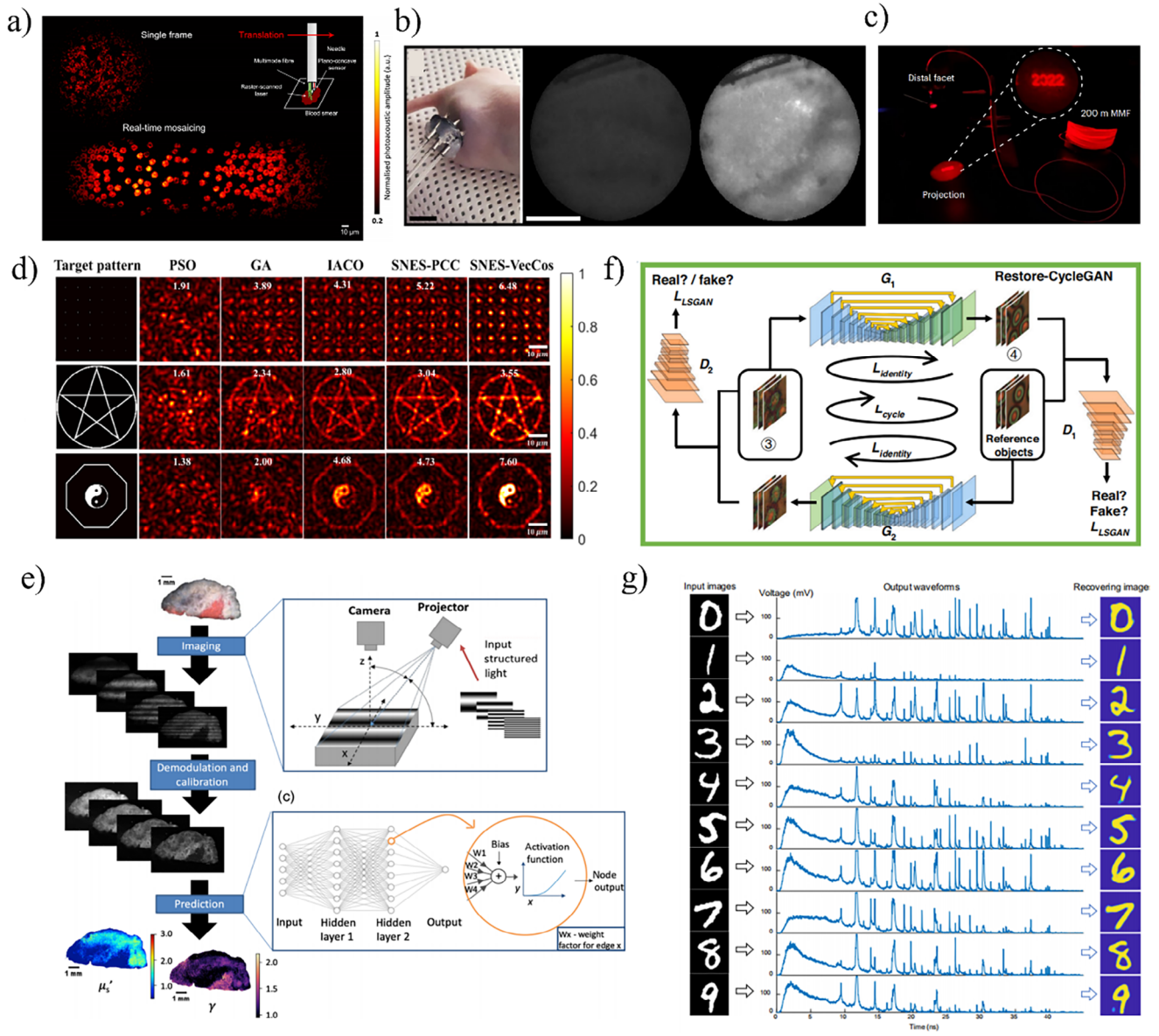

Figure 5. a) Mosaic imaging of a mouse blood smear sample was performed over a 100 μm × 250 μm area, with each frame covering a 100 μm diameter area and 1 μm scanning steps, enhanced by wavefront shaping for better resolution. Reproduced with permission.[167] Copyright 2022, Optica. b) Real-time PTT monitoring was conducted in vivo on a mouse tumor, with images captured by the fiber bundle showing enhanced signals from gold nanoparticle activation at the tumor site. Scale bars: 10 mm and 100 μm. Reproduced with permission.[168] Copyright 2017, Optica. c) High-contrast projection through a 200 μm MMF demonstrated improved resolution and contrast in deep tissue imaging using spatial-frequency tracking and adaptive beacon light-field encoding. Reproduced with permission.[169] Copyright 2023, Springer Nature. d) Pattern projections through a 15 m unstable MMF using various optimization methods improved image contrast and resolution, with the corresponding contrast value. Scale bar: 10 μm. Reproduced with permission.[170] Copyright 2022, Optica. e) A CycleGAN network was used to recover image details by translating between images and reference objects, generating high-quality reconstructed images. Reproduced with permission.[28] Copyright 2023, Springer Nature. f) Digit images from a test database were converted into waveforms and reconstructed, showcasing the fast detection capability enabled by deep learning. Reproduced with permission.[171] Copyright 2022, Springer Nature. g) A sub-diffuse spatial frequency domain imaging method with sinusoidal light patterns was used to measure tissue optical properties, with data processed by a neural network to enhance tissue characterization. Reproduced with permission.[172] Copyright 2021, SPIE.

-optic endoscopic platforms, thereby enabling precise light field modulation at the hardware level.[175,176] This approach promises to replace or supplement complex computational correction algorithms. For example, to address the scattering issue in multimode fibers (MMFs), Yu et al.[177] demonstrated a pioneering approach by integrating a miniaturized diffractive neural network (DN^2s) onto the MMF's distal facet. This component, fabricated via 3D two-photon nanolithography, has a footprint of just 150 × 150 μm^2. It functions as an all-optical image processor, enabling single-shot, real-time image transportation through the MMF without the need for traditional wavefront shaping or computational reconstruction, and achieved a minimum

reconstructed feature size of ≈4.90 µm. This design, which effectively "embeds" computational functionality onto the fiber tip, opens new pathways for compact photonic systems. Meanwhile, in more traditional scanning endoscopes, DOEs also play a key role in enhancing system performance. As demonstrated by Ekaterina et al.,[59] in an ultra-compact fiber scanning platform for multimodal nonlinear imaging, researchers integrated a linear diffractive grating into its 2.4 mm diameter endoscopic objective. This diffractive grating covered the foci across the entire field of view, enabling diffraction-limited performance and allowing the system to image tissue with sub-micron spatial resolution at one frame per second. These studies indicate that whether used as all-optical computing units or as corrective elements for high-performance imaging, integrated diffractive optics technology is a key direction for endoscopic miniaturization and functionalization.

A key challenge in this area, however, has been that traditional meta-optics suffer from strong aberrations, especially chromatic aberrations, which complicate full-color imaging. Recent work has directly addressed these limitations. For instance, Johannes et al.[178] demonstrated an inverse-designed meta-optic (MOFIE) for use with a 1 mm coherent fiber bundle. By optimizing the meta-optic at a system level, they achieved real-time, full-color operation in the visible spectrum with a large field of view (22.5°) and a long depth of field (>30 mm) without computational reconstruction. This approach also reduced the rigid tip length by 33% compared to traditional GRIN lens endoscopes. Beyond full-color imaging, meta-optics are also pushing the boundaries of resolution in miniaturized formats. Liu et al.[179] proposed a "meta-objective" using cascaded metalenses (400 µm and 180 µm diameters) integrated with a fiber bundle. This design achieved a sub-micrometer lateral resolution of 775 nm by correcting monochromatic aberrations over a 125 µm field of view, enabling the clear observation of single cell contours in biological tissue, which was not possible with conventional GRIN lenses.

6.2.2. Image Reconstruction Algorithms

Image reconstruction is a core step in optical information processing, responsible for translating raw data collected at the front end into clear, accurate images.[170,180] Traditional iterative reconstruction algorithms, such as Expectation-Maximization (EM) and Newton's method, form the foundation in this field. Similarly, the Newton-Raphson method is commonly used in DOT for image reconstruction, where optical parameters such as absorption and scattering coefficients are iteratively updated to minimize the error between measured and predicted values, thus precisely inverting the optical properties of tissues.

Although these algorithms can reduce errors and improve image quality by leveraging prior knowledge or physical models, their high computational complexity and long iterative cycles constitute significant bottlenecks for real-time imaging applications. Whether it is the massive forward computation based on the Radiative Transfer Equation (RTE) or the additional iterations required to ensure convergence when handling high-noise data, these processes severely limit their clinical potential. For example, in time-resolved DOT, the time required for reconstruction based on the diffusion equation can be up to 120 times longer than the moment method.

In contrast, emerging unsupervised learning methods offer a solution. Hu et al.[28] demonstrated that by combining high-sampling-rate GALOF fibers with the Restore-CycleGAN network, single-image reconstruction time could be reduced to 1.6 seconds while maintaining high fidelity even under dynamic conditions, such as fiber bending by 60°, greatly enhancing the system's real-time capability and robustness (Figure 5e).

6.2.3. Machine Learning Methods

As the intelligent core of the computational back-end, machine learning, particularly deep learning, provides revolutionary optimization techniques for processing optical data in deep tissues.[174,181–183] Unlike traditional algorithms that rely on fixed mathematical models, deep neural networks can autonomously learn complex prior knowledge from vast amounts of data, performing highly nonlinear mapping and enhancement tasks. By constructing deep models based on architectures like Convolutional Neural Networks (CNN), Recurrent Neural Networks (RNN), or Transformers (Figure 5f), these algorithms can effectively extract multi-level, multi-modal features from images.[184–186]

In image denoising, deep learning can precisely distinguish signal from noise, preserving fine details of images while removing noise. For example, Dong et al.[187] used Generative Adversarial Networks (GANs) to denoise OCT images. By introducing speckle modulation strategies, their method outperformed traditional techniques in contrast-to-noise ratio (CNR) and peak signal-to-noise ratio (PSNR).

In super-resolution and high-speed imaging, deep learning shows potential to break through the physical limitations of hardware. Liu et al.[171] proposed a high-speed full-fiber imaging method based on U-Net, utilizing modal dispersion of multimode fibers to encode two-dimensional spatial information into one-dimensional time waveforms, which were then reconstructed by neural networks. This method achieved a frame rate of 15.4 Mfps and a spatial resolution of 15 µm.

This efficient data processing capability is also crucial in distributed sensing. By applying Convolutional Neural Networks (CNNs) to extract features from the Brillouin gain spectrum, Venketeswaran et al.[188] demonstrated a processing speed 3500 times faster than traditional nonlinear regression. This approach concurrently ensured high-precision temperature sensing, achieving an error of just 1.172°C at the end of a 41 km fiber and thus enabling long-term environmental monitoring in deep tissues.

In conclusion, functionalized optical fiber platforms rely on a series of engineering foundations. These begin with material selection and modification, which fundamentally determine the optical, mechanical, and biological properties of the fiber. On this foundation, precise structural paradigm designs—from propagation modes, refractive index profiles, to core configurations—enable fine control over the transmission behavior of photons within the optical fiber. However, the intrinsic physical properties of the fiber alone are insufficient to address the complex challenges in deep tissue applications. Therefore, a range of auxiliary techniques, including front-end physical control and back-end

computational imaging, must be introduced to break through the inherent performance boundaries of the fiber and decode high-fidelity biological information from raw signals. The organic integration of these three engineering dimensions transforms the fiber from a passive optical fiber into a functional system capable of actively interacting with biological systems. Its interactive modes can be summarized into two basic types: as a high-fidelity sensor for reading deep tissue information, and as a high-precision actuator for delivering specific materials and energy to targeted locations. The subsequent sections will delve into the specific practices of these engineered optical fibers in two core application fields: biomedical diagnosis and precision therapy, systematically demonstrating how they address key challenges in clinical and research contexts.

7. Optical Fiber-Based Diagnostics

Among the myriad biomedical demands, diagnostics—the acquisition of precise information regarding physiological or pathological states from deep within a living body—stands as one of the most direct and pivotal application areas. However, the strong scattering properties of biological tissues make it difficult for existing high-resolution optical diagnostic techniques to be directly applied to deep regions of living organisms. Engineered optical fibers, with their flexibility, light-guiding capability, slender form factor, and minimally invasive nature, provide an ideal physical platform for achieving this goal. Engineered optical fibers provide an ideal physical vehicle to achieve this goal. Their slender geometry and excellent flexibility enable them to be inserted deep into tissue in a minimally invasive manner, directly accessing targets that are inaccessible to conventional *free-space* optical techniques. Via the fiber, interrogation light can be efficiently delivered to the region of interest, while returning photons carrying biological information can be effectively collected and transmitted out of the body. This capability for efficient light delivery and retrieval forms the foundation for deep-tissue diagnostics with a high signal-to-noise ratio. Based on the nature of the information being acquired, fiber-optic diagnostic technologies are typically classified into two primary categories. The first is Biomedical Imaging, where the primary objective is to acquire structural and morphological images of tissues or cells to resolve their spatial relationships with high resolution. The second category is biomedical sensing, which aims to perform real-time, quantitative measurements of physical parameters (such as temperature and pressure) or the concentration of chemical/biological molecules at specific locations. In essence, imaging focuses on resolving structure and morphology, whereas sensing is centered on quantifying specific parameters. The remainder of this section will adhere to this classification. We will first introduce the specific applications of engineered optical fibers in various deep-tissue imaging technologies, and subsequently discuss their role as high-performance sensors for biomedical measurements.

7.1. Deep-Tissue Imaging

The core principle of this approach lies in using optical fibers as miniature conduits to deliver light into deep regions of biological tissues and to collect the returning signals for image reconstruction. Optical fibers cannot only efficiently focus light into deep tissue to form localized illumination spots but also effectively collect the generated signals from the same or nearby locations. However, strategies for achieving deep-tissue imaging vary widely. Different optical fiber platforms—such as single-mode fibers, multimode fibers, and fiber bundles—and distinct imaging paradigms—such as mechanical scanning, computational scanning, and parallel acquisition—result in markedly different imaging characteristics.

This section focuses on four representative imaging modalities, each exploiting a specific optical response of biological tissues to generate signals: backscattering caused by refractive index mismatches, fluorescence from endogenous or exogenous molecules, photoacoustic effects induced by thermoelastic expansion following optical absorption, and inelastic Raman scattering arising from molecular vibrations. For each modality, we will examine its imaging methodology in detail, including the employed fiber platform and imaging paradigm, performance trade-offs (particularly between field of view and resolution), acquisition and reconstruction speed (i.e., whether it approaches real-time imaging and is suitable for dynamic in vivo applications), as well as key limitations such as scanning stability and sensitivity to biological motion.

7.1.1. Conventional Optical Imaging

The core advantage of fiber-optic bright-field imaging lies in its ability to perform in situ, real-time morphological observation deep within the body in a minimally invasive and relatively straightforward technical manner. However, a fundamental trade-off exists within mainstream technologies. Conventional coherent fiber bundles (CFBs), while capable of stably transmitting incoherent white-light images, essentially act as two-dimensional (2D) image relays and lack depth-resolving capability, leading to the loss of critical 3D structural information. Conversely, a single multimode fiber (MMF), despite offering a thinner diameter and higher modal density for potential high-resolution imaging, is extremely sensitive to bending and deformation. This causes severe scrambling of image information during transmission, rendering it impractical for clinical environments that require flexible operation.[189,190]

To overcome the bending sensitivity of MMFs, researchers have developed various dynamic compensation strategies. For instance, Farahi et al.[191] proposed a scheme based on a "virtual coherent beacon source". The technique integrates a permanent virtual point source at the fiber's distal end via holographic methods to sense the fiber's bending state. The system rapidly matches the specific speckle pattern generated by this beacon with a prestored database to instantaneously determine the precise fiber conformation. Once identified, the system reconstructs a stable, diffraction-limited focus at the distal end through digital phase conjugation, enabling scanning-based bright-field imaging under dynamic conditions.

In a further advancement, Wen et al.[169] introduced the Spatio-Temporal frequency tracking Adaptive Beacon Light-field Encoding (STABLE) endoscope. This technique not only addresses bending sensitivity but also achieves super-resolution imaging. It ingeniously integrates a white-light endoscope (WLE)

providing a wide 120° field of view (FOV) with a super-resolution STABLE probe, enabling cross-scale imaging from centimeter-scale navigation to nanometer-scale analysis. Clinicians can first use the WLE for macroscopic localization, then switch to the STABLE probe for precise subcellular observation with its impressive 250 nm sub-diffraction-limited resolution. Due to the high resilience of the STABLE system to probe motion and deformation, it can maintain stability under dynamic clinical conditions, offering a promising pathway toward in vivo optical biopsies comparable to ex vivo pathology.

7.1.2. Optical Coherent Tomography

OCT is a non-invasive optical imaging technique based on the core principle of low-coherence interferometry. It operates by directing a beam of near-infrared light into biological tissue and detecting the faint light signals that are reflected or backscattered from interfaces at various depths. This information is then used to construct cross-sectional images of the internal tissue structure with micron-scale resolution. Conventional OCT systems have often relied on bulky, free-space optical platforms, which has limited their application in clinical settings, particularly in the field of endoscopic diagnosis and therapy. In response, fiber-optic-based OCT technology has emerged. Its central innovation is the use of flexible optical fibers to connect key functional modules of the system—such as light splitting, scanning, and detection—which are ultimately integrated into a miniaturized fiber-optic probe. This design not only dramatically reduces the system's footprint but also endows the probe with excellent flexibility, making it compatible with various endoscopes. Consequently, the reach of OCT has been extended from the body surface to deep-seated luminal organs and parenchymal tissues, such as blood vessels, the gastrointestinal tract, and the respiratory tract, opening up new avenues for in-vivo diagnostics.

Within this technological framework, the miniaturization of the fiber-optic probe is a primary prerequisite for achieving minimally invasive or even non-invasive detection. The outer diameter of the probe becomes a critical bottleneck, especially in extremely confined application scenarios like intravascular lumens. To this end, researchers have continuously explored the limits of miniaturization. For example, Abid et al.[192] employed hydrofluoric acid etching to successfully reduce the outer diameter of a fiber-optic probe to 70 µm, with only a ≈1 dB decreases in sensitivity, offering a size-optimized solution for high-precision imaging of the fundus and gastrointestinal tract. The probe was validated using a spectral-domain OCT system with a central wavelength of 840 nm and a bandwidth of 50 nm, achieving a baseline sensitivity of 85 dB. At a working distance of 400 µm, the probe provided a maximum signal-to-noise ratio (SNR) of ≈64 dB. B-scan imaging performed with a 1 µm lateral scanning step revealed highly reflective regions in the porcine retina, although individual layered structures could not be clearly resolved. Moreover, this mechanical scanning paradigm poses significant challenges. The stability of piezoelectric or mechanical scanning mechanisms is crucial, as nonlinearity, vibration, and hysteresis effects can directly cause image distortion. In lumen imaging, rotational scanning stability—commonly referred to as non-uniform rotational distortion (NURD) remains a well-known and persistent issue. Concurrently, the mechanical strength and optical stability of the probe are equally crucial. Wu et al.[193] integrated a spherical lens and a 45° total internal reflection surface within a needle, reducing the astigmatism ratio to 1.016. This design achieved excellent focusing performance of 18.7–19.0 µm while maintaining a low insertion loss (0.25 dB) and high mechanical robustness, providing a reliable technical solution for applications such as subcutaneous tissue puncture (**Figure 6c,d**).

The trade-off in imaging performance is equally critical, as high resolution typically comes at the cost of a shallower depth of field (DOF)—a fundamental limitation that defines this core performance balance. To overcome this limitation, Qiu et al.[198] designed a novel filter based on the modal interference principle of a gradient-index liquid-crystal-filled fiber (GRIN-LCF), which extended the depth of focus by a factor of 2.6 while maintaining a high resolution of 4.6 µm. This design is intended to directly mitigate the aforementioned trade-off. In terms of acquisition speed, OCT offers extremely fast A-scan rates, enabling two-dimensional (B-scan) imaging at video frame rates. However, 3D imaging still requires sequential acquisition (e.g., through rotational pullback), making it highly susceptible to biological motion such as heartbeat and respiration, which can introduce motion artifacts. Furthermore, the inherently strong scattering properties of biological tissues severely limit both the effective imaging depth and the signal-to-noise ratio (SNR). In practical endoscopic applications, a certain fluid working distance—typically water or saline—must be maintained between the probe and the tissue surface. This additional transmission medium further attenuates the signal, exacerbating the SNR degradation problem. To address the issue of signal attenuation in long-range imaging, Lee et al.[195] utilized a high-refractive-index epoxy lens and a common-path optical design to enhance the SNR by 25 dB in a 1.5 mm water environment, providing a technical safeguard for applications requiring stable long-distance imaging, such as in ophthalmology and intravascular procedures (Figure 6e).

Building upon the enhancements in structural imaging performance, the superior compatibility of the fiber-optic platform has also spurred the development of multimodal and functional integration. By merging OCT with other sensing or imaging technologies, physiological and pathological information about the tissue can be acquired from multiple dimensions. For instance, Chen et al.[194] combined OCT with pH sensing technology to enable simultaneous measurement of tissue structure and acidity, providing dual criteria for determining tumor margins during surgery (Figure 6a). The probe employs a three-section structure consisting of a double-clad fiber, a no-core fiber, GRIN fiber. It achieves a lateral resolution of ≈10.6 µm and a working distance of about 506 µm. In pH sensing, the probe demonstrates a measurement accuracy of 0.01 pH units. Buenconsejo et al.[199] went a step further by integrating three modalities—narrow-band RGB, autofluorescence imaging (AFI), and OCT—into a single catheter, successfully achieving multi-scale and multi-dimensional screening of the tongue mucosa. The system utilizes a sub-millimeter-diameter double-clad fiber rotary–pullback imaging catheter, achieving a spatial resolution of 25 µm in both the rotational and pullback directions.

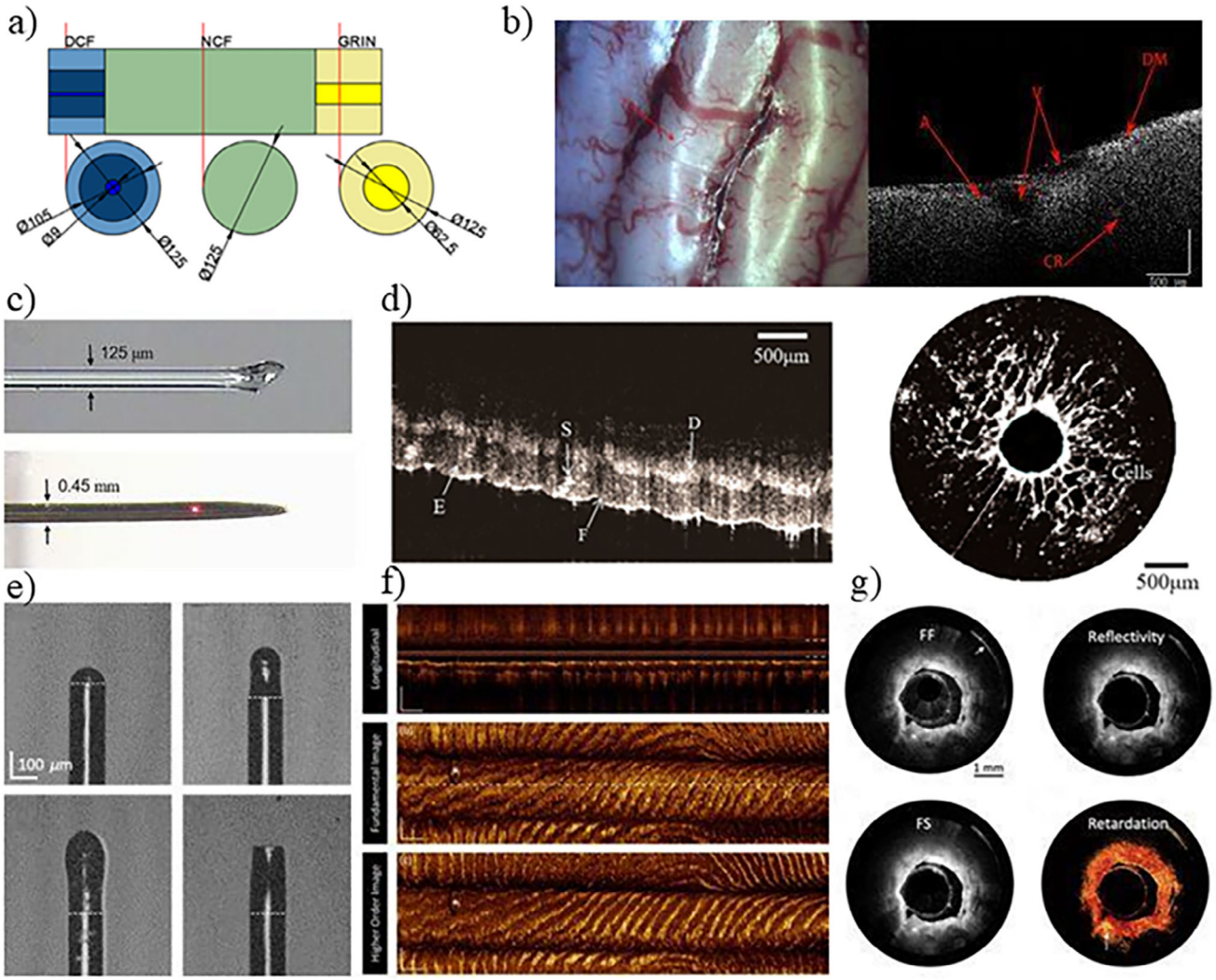

Figure 6. Applications of fiber-optic devices in coherence tomography imaging. a) Schematic of the all-fiber probe. DCF, double-clad fiber; NCF, no-core fiber. Reproduced with permission.[194] Copyright 2021, Wiley-VCH. b) Porcine brain imaging. Left: Photograph of the sample. Right: Corresponding OCT image showing anatomical structures (A: arachnoid, CR: cortex region, DM: dura mater, V: vasculature). Reproduced with permission.[194] Copyright 2021, Wiley-VCH. c) Probe characterization: (top) Fiber ball lens microscopy image. (down) Assembled 26-gauge needle tip showing focused laser spot (red) exiting the side opening. Reproduced with permission.[193] Copyright 2022, Elsevier. d) OCT imaging of biological tissues using a fiber probe. Left: Human finger skin showing epidermis (E), dermis (D), fingerprint (F), and sweat duct (S). Right: Grape tissue microstructure from circumferential scan. Reproduced with permission.[193] Copyright 2022, Elsevier. e) En-face OCT images of fiber probe with lens with 240 μm expansion rod. Reproduced with permission.[195] Copyright 2019, SPIE. f) OCT and multipath contrast of a human fingertip. Scale bars are 1 mm. A longitudinal slice (up) is taken from the dashed line in the panel. (down) Demonstrate en-face views of the sample. Reproduced with permission.[196] Copyright 2023, Optica. g) OCT images of atherosclerotic plaque. FF image, FS image, normal reflectivity image, and map of sample-field retardation. Scale bar: 1 mm. Reproduced with permission.[197] Copyright 2022, Springer Nature.

Furthermore, the intrinsic physical properties of the fiber itself can be harnessed for functional imaging. Li et al.,[197] for example, introduced a 12-meter-long polarization-maintaining fiber and leveraged its birefringence effect to visualize cholesterol crystals in ex vivo coronary arteries without the need for active modulation. Its two polarization modes generate separate OCT images, with a spatial separation of 2.7 mm between the images obtained from the two polarization detection channels, offering a novel (Figure 6f,g), passive polarization-sensitive solution for assessing the mechanical stability of atherosclerotic plaques.

7.1.3. Fluorescence Imaging

Fluorescence imaging operates by exciting fluorophores within a sample, causing them to absorb photons of a specific wavelength and subsequently emit photons at a longer wavelength; an image is then formed by detecting these emitted photons. Owing to its high sensitivity and molecular specificity, this technique offers an indispensable advantage for observing cellular activities and molecular changes. Unlike OCT, fiber-based fluorescence imaging employs a variety of distinct imaging paradigms, which can be broadly categorized into two main types: parallel image

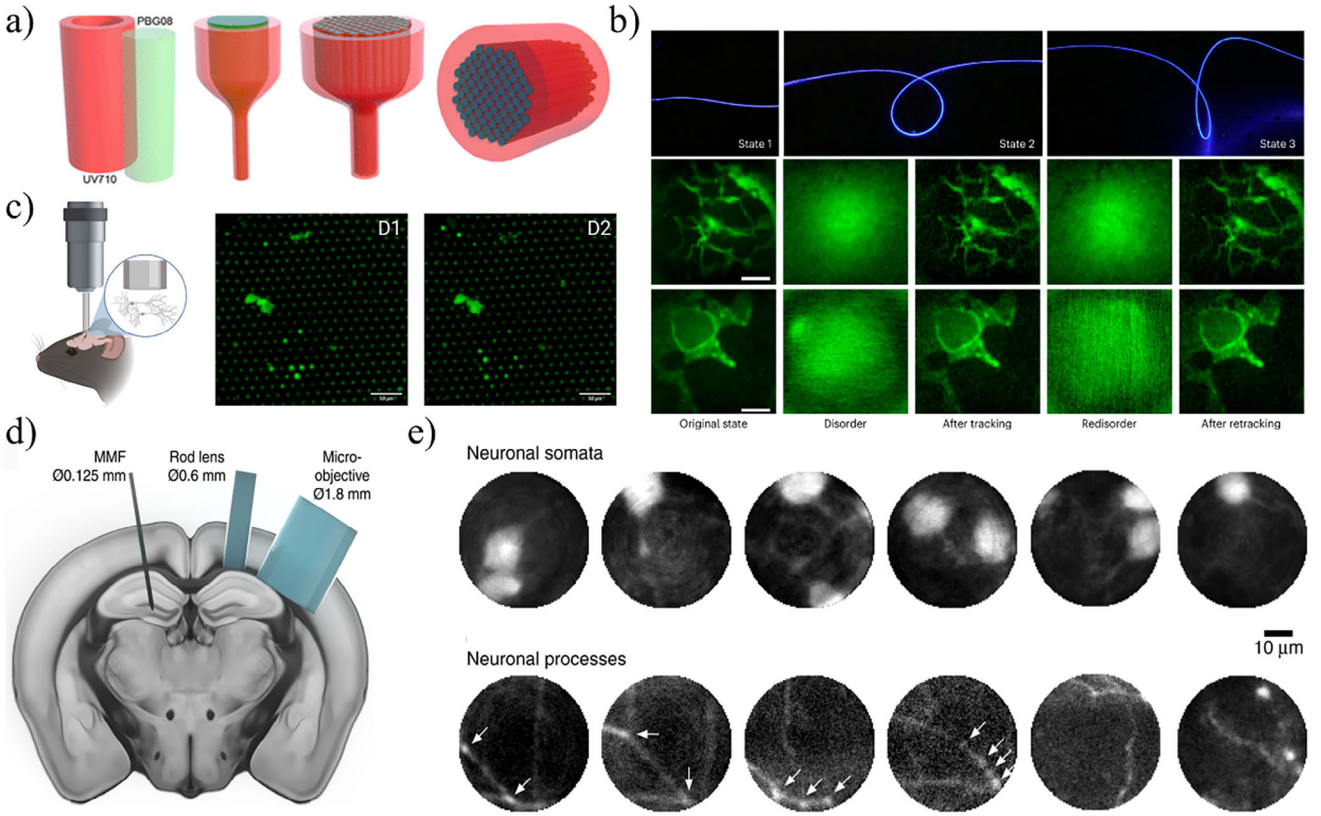

Figure 7. Applications of fiber-optic devices in fluorescence imaging. a) A schematic illustration of the stack-and-draw method for fabricating a fiber-optic bundle. The process includes the initial preparation of rods and capillaries, drawing of a single-pixel preform, assembly and subsequent drawing of the multi-pixel preform, and the final cutting and polishing of the optical bundle. Reproduced with permission.[200] Copyright 2023, ACS. b) Demonstration of robustness against fiber disturbances for a single multimode fiber, a dynamic compensation multimode fiber (MMF) imaging system. (Top row) Shows the different fiber states of the MMF at different times, resulting from bending or movement. (Middle and bottom rows) Show the imaging results for atherosclerotic and lung pathology slides, respectively, under the corresponding fiber states. Crucially, despite the significant changes in the fiber state (top row), the system successfully tracks these changes and recovers clear microscopic images, demonstrating its imaging stability in environments with dynamic perturbations. (Scale bars, 25 µm). Reproduced with permission.[169] Copyright 2023, Springer Nature. c) In vivo imaging of Fos activity patterns in the mouse RS using FIB and a 10 × Plan-Neofluar objective lens. Corresponding images of the same RS area after home cage exploration (D1) and novel box exploration (D2). Reproduced with permission.[200] Copyright 2023, ACS. d) Assessment of invasiveness. Scale-preserved comparison of common endoscopic probes and MMF. Reproduced with permission.[57] Copyright 2018, Springer Nature. e) Demonstration of an MMF-based imaging system for in vivo applications. The image shows neuronal somata and the detailed processes of inhibitory neurons, observed after direct insertion of the multi-mode fiber probe into the mouse brain. Arrows are used to indicate specific features like branching points and synaptic boutons. Reproduced with permission.[57] Copyright 2018, Springer Nature.

relaying via fiber bundles and computational imaging through a single multimode fiber (MMF). These two strategies differ fundamentally in terms of resolution, speed, and stability.

The first strategy involves the use of multi-core fiber bundles (MCF), where each core acts as a pixel, directly relaying the image from the distal end to the proximal detector in a parallel acquisition manner. The advantage of this approach is its extremely fast acquisition speed, enabling real-time video-rate imaging. This makes it highly suitable for capturing rapid biological dynamics. For instance, Bijoch et al.[200] successfully recorded calcium signals from cortical neurons in mice using a high-numerical-aperture (NA = 1.15) fiber bundle. The fiber bundle consists of 825 multimode cores arranged in a hexagonal lattice, with a total diameter of 914 µm. Utilizing a 910 nm femtosecond laser, it achieves an imaging resolution of 14 µm. However, the spatial resolution of this method is limited by the core size and spacing (only able to resolve structures ≥20 µm), and the outer diameter of several hundred micrometers remains considerably invasive (**Figure** 7a,c).

The second category involves computational imaging through a single multimode fiber (MMF). As described previously in section 5.1, the MMF acts as a scattering medium, scrambling image information into speckle patterns due to modal dispersion. Imaging relies on computational methods (e.g., holographic wavefront shaping) to generate a diffraction-limited focus at the distal end; this focus is then scanned by modulating the proximal input wavefront. The advantages of this approach include extremely high, diffraction-limited resolution and minimal invasiveness. Turtaev et al.[57] employed holographic wavefront shaping to precisely pre-compensate for light propagation through a single multimode fiber (50 µm core diameter), thereby generating a diffraction-limited focal spot at the fiber's distal end. This technique not only improved the resolution to 1.18 µm, enabling dynamic imaging of fine structures like neuronal dendrites, but

also demonstrated immense potential for ultra-minimally invasive neuroscience research due to its minimal insertion damage (<50 μm) (Figure 7d,e). However, the drawbacks of this strategy include slow acquisition speeds, which are typically far below video rates, making it difficult to capture rapid biological dynamics. Furthermore, its stability is extremely poor—a critical vulnerability of MMF imaging. The system is exceptionally sensitive to any physical perturbations of the fiber, such as bending or temperature changes, which lead to image decorrelation. The computational reconstruction required also adds to the system's complexity. An effective strategy to partially address image distortion caused by fiber perturbations involves pre-characterizing the fiber's transmission matrix (TM) or its equivalent under various perturbation states. During imaging, this allows for the rapid detection and tracking of the fiber's current state from the proximal end. In this vein, Wen et al.[169] developed an endoscopic technique named STABLE (Spatial-frequency tracking adaptive beacon light-field-encoded), presenting a highly resilient solution. By employing a spatial-frequency beacon tracking mechanism operating at up to 1 kHz, they achieved millisecond-scale tracking and compensation for dynamic fiber perturbations. This approach ensures stable image acquisition even when the long-distance MMF undergoes bending and other operational manipulations. Combined with full-vector modulation and fluorescence emission difference (FED) techniques, it achieves a sub-diffraction resolution of 250 nm, and its cross-scale imaging capabilities were validated in a live mouse model (Figure 7b).

7.1.4. Photoacoustic Imaging

Photoacoustic imaging (PAI) is an emerging hybrid imaging modality based on the fundamental principle of the photoacoustic effect. When a short-pulsed laser illuminates biological tissue, light-absorbing molecules within the tissue (such as hemoglobin) absorb the optical energy, leading to a transient temperature increase. This, in turn, induces thermoelastic expansion, which propagates outward in the form of ultrasound waves. By detecting these ultrasound waves, the distribution of light absorbers within the tissue can be reconstructed to form a high-contrast image. This technique ingeniously merges the high chemical contrast of optical imaging with the deep tissue penetration capability of ultrasound imaging. In PAI systems, optical fibers not only serve as flexible and minimally invasive light delivery paths to guide excitation light into deep tissue but can also be engineered into high-sensitivity optical ultrasound sensors, thereby enabling all-optical and highly integrated detection systems.

One strategy is the mechanically scanned photoacoustic endoscope, with typical applications such as intravascular photoacoustic imaging (IVPA).Wang et al.[201] integrated the optical fiber for light delivery and the π-FBG sensor into a miniature probe, images are constructed through mechanical rotation and pullback. This all-optical design enables an extremely small size (1.3 mm) and high lateral resolution (18.6 μm) (**Figure 8a**). It has been validated in rabbit iliac arteries and porcine coronary arteries, demonstrating its significant clinical potential for finely delineating vascular structural details. Beyond intravascular imaging, intraluminal imaging in the gastrointestinal tract is another important application direction for mechanically scanned probes. For example, Chang et al.[202] developed a molecularly targeted photoacoustic endoscopy system specifically for in vivo assessment of the invasion depth of gastrointestinal tumors. This system employs a 4.2 mm diameter side-viewing probe, with its core scanning mechanism utilizing a piezoelectric (PZT) bender to control an optical fiber, enabling rapid lateral beam scanning. Combined with rotation and pullback motions, it constructs 3D images. This system achieved an axial resolution of 119 μm over an imaging depth of 3.1 mm. However, its acquisition speed is limited by the mechanical scanning rate, making 3D imaging non-real-time and susceptible to motion artifacts such as those caused by heartbeat (Figure 8d,e). Similar to OCT endoscopes, it relies on the mechanical stability of the scanning. Furthermore, although the probes used in the aforementioned work are extremely slender, the final probe size integrating optical and scanning components is on the millimeter scale. While this is sufficient for insertion into the instrument channel of a standard endoscope, this size remains relatively large for applications pursuing extremely low invasiveness or exploring narrower lumens.

The second strategy is based on optically scanned photoacoustic endoscopy, which offers a higher signal-to-noise ratio (SNR) and faster scanning speeds. For instance, Liang et al.[9] developed a miniaturized, optical-resolution photoacoustic endoscope using a laser ultrasound sensor, specifically designed for high-resolution hemodynamic response imaging. The core advantage of this sensor lies in its amplification of the acoustic response by measuring optical phase changes induced by acoustic waves, thereby achieving an extremely high detection sensitivity of below 1.5 mPa $Hz^{-1}/^{2}$ over a broad bandwidth of 5–25 MHz. Additionally, the dual-frequency laser heterodyne phase detection technique employed by this system enables effective resistance to thermal drift and vibrational disturbances (Figure 8b). The research team successfully used this endoscope for in vivo imaging of the rat rectum and observed changes in oxygen saturation during acute inflammation, which are difficult to observe with other imaging modalities. Within optical strategies, achieving high-resolution forward-viewing imaging is another key challenge, as traditional MEMS scanning mirrors or rotary joints struggle to balance small diameter and forward-viewing requirements. To address this issue, Li et al.[203] developed a miniature PAE probe with a diameter of only 2.4 mm. The sophistication of this design lies in its elimination of the need for an integrated scanner within the probe. Instead, it combines an imaging fiber bundle, a GRIN objective lens, and a fiber-optic tip-based Fabry–Perot ultrasound sensor. Through the integration of the GRIN lens, the probe achieves a wide field of view (>3.5 mm) significantly larger than the probe diameter while maintaining high resolution (7.7–10.4 μm), demonstrating its application potential in gastrointestinal endoscopy and cystoscopy. However, the inherent pixelated structure of the imaging fiber bundle introduces honeycomb artifacts and fundamentally limits the spatial resolution to the core-to-core spacing of the fibers. This necessitates the use of higher-density fiber fabrication or advanced image reconstruction algorithms to overcome. Second, there is still room for improvement in the performance and integration level of the optical components integrated at the probe tip. Future improvements will focus on optimizing the integration process of

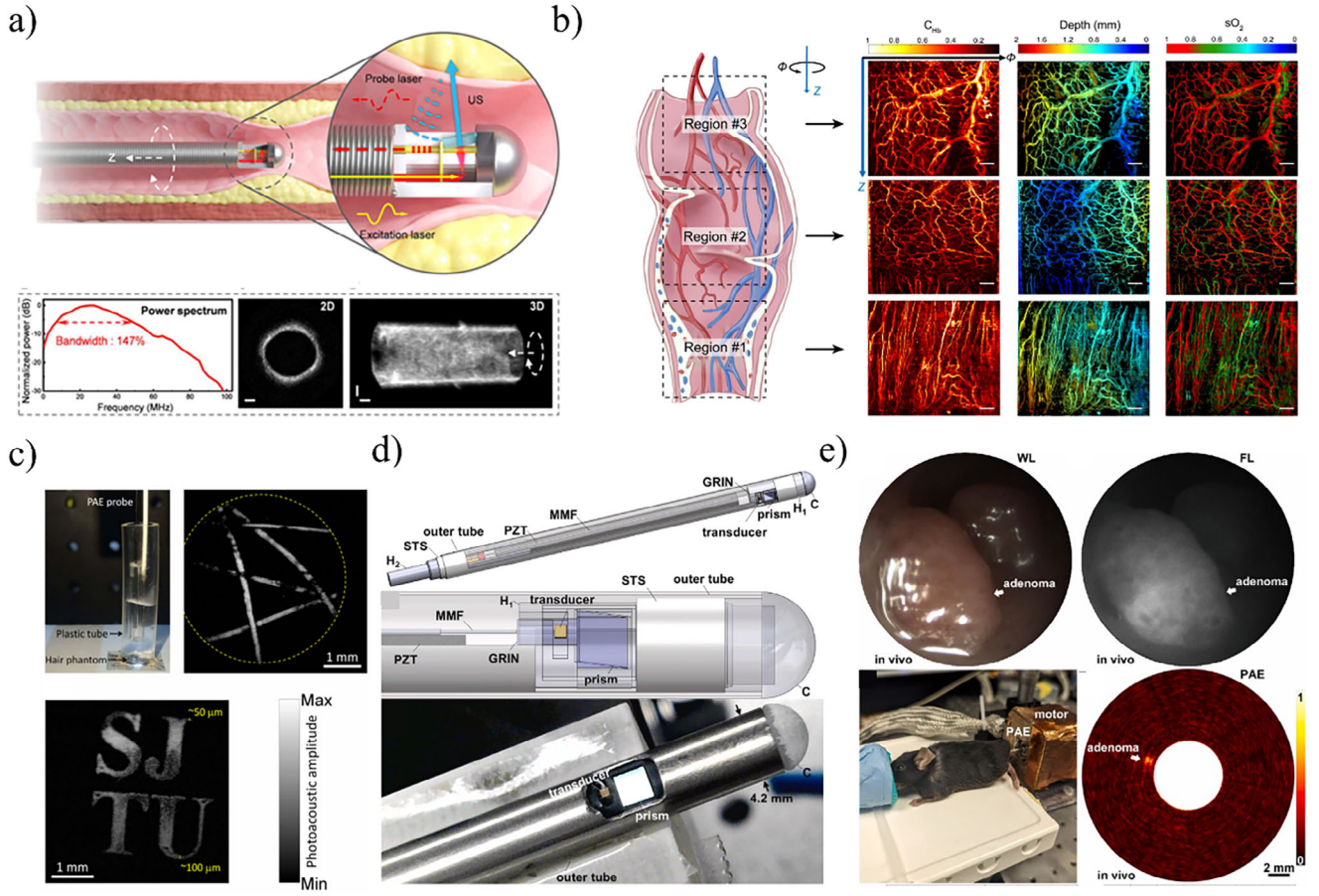

Figure 8. Applications of fiber-optic devices in photoacoustic imaging. a) All-optical intravascular ultrasound (AO-IVUS) imaging of vessel walls. (up) System schematic and catheter ultrasound response spectrum. (down) Cross-sectional 2D and 3D rotational pullback images of arterial wall (scale bars: 1 mm). Reproduced with permission.[201] Copyright 2023, AAAS. b) In vivo photoacoustic endoscopy of a rat rectum. This image simultaneously quantifies the spatial distributions of hemoglobin concentration (CHb), oxygen saturation (sO2), and anatomical depth, providing a multi-parametric functional assessment. The data are presented across three distinct regions of interest. (Scale bar: 1 mm). Reproduced with permission.[9] Copyright 2022, Springer Nature. c) Demonstration of a forward-viewing photoacoustic endoscopy (PAE) probe and its imaging capabilities. The probe enables high-resolution imaging with a wide field of view (FOV), as evidenced by its ability to resolve fine structures like human hairs and clearly distinguish patterned targets such as the letters "SJTU". The wide FOV, indicated by the dashed circle, exceeds the physical dimensions of the miniature probe itself. Reproduced with permission.[203] Copyright 2019, IEEE. d) Design and packaging of a photoacoustic endoscopy (PAE) prototype. The imaging instrument features an overall rigid length of 65 mm and a compact outer diameter of 4.2 mm. The detailed structure includes a support tube shell (STS), internal holders (H1, H2), and a protective cap at the distal tip, which is covered by a transparent thin film (not shown in the photo). Reproduced with permission.[202] Copyright 2025, Elsevier. e) In vivo multimodal imaging of a mouse colon adenoma using a photoacoustic endoscopy (PAE) prototype. Following localization by white light endoscopy, the adenoma was identified with a NIR fluorescence probe, showing a tumor-to-background (T/B) ratio of 2.22. The PAE image subsequently acquired from the same region revealed an even higher T/B ratio of 2.83, demonstrating the enhanced contrast and detection capability of the PAE technology for in vivo tumor imaging. Reproduced with permission.[202] Copyright 2025, Elsevier.

these optical components and significantly increasing data acquisition and processing speeds to achieve real-time 3D photoacoustic imaging truly suitable for endoscopic examinations (Figure 8c).

7.1.5. Raman Imaging

Raman spectroscopy is a label-free analytical technique based on the principle of detecting the frequency shift of photons that occurs after a laser interacts with molecular vibrations, thereby acquiring a sample's unique chemical fingerprint. However, the fundamental challenge of Raman imaging lies in its extremely weak signal. This weak-signal challenge is further exacerbated in fiber-optic endoscopic applications. It is extremely difficult to efficiently couple the weak Raman scattered light back into the fiber core. More critically, as the excitation laser propagates through the fiber, it generates a strong background Raman signal from the fiber itself. This background noise often completely overwhelms the authentic characteristic signal originating from the biological tissue. Consequently, compared to in vivo endoscopic applications, where managing this background interference is highly challenging, Raman imaging (particularly spontaneous Raman) is more commonly employed in in vitro microscopy systems. In an in vitro setting, the system can utilize high NA objectives for efficient signal collection and is free from the background

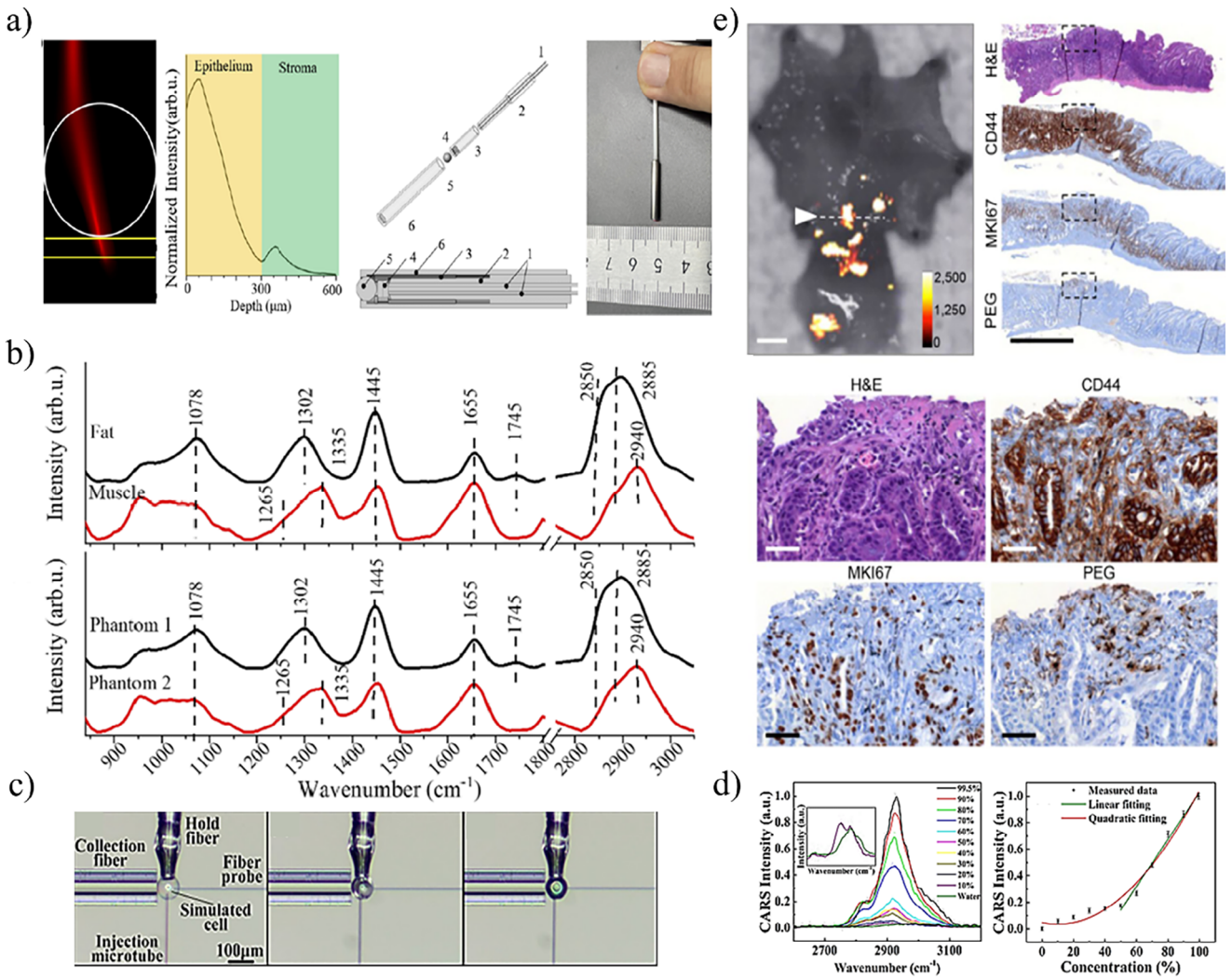

Figure 9. Applications of fiber-optic devices in Raman imaging. a) Raman photon detection with a two-beveled-fiber polarized (TBFP) probe. The excitation laser propagates through the fiber, polarizer, and ball lens into the epithelial tissue. The probe's depth-dependent Raman collection efficiency was characterized, and its design was verified via SolidWorks modeling and physical prototyping. Reproduced with permission.[204] Copyright 2023, Optica. b) Raman spectra of pork fat and muscle tissues (top) and their corresponding tissue phantoms (down). Reproduced with permission.[204] Copyright 2023, Optica. c) Optical fiber probe interaction with a simulated cell: (left) physical contact with the cell, (middle) liquid injection process, and (right) final liquid-filled state. Reproduced with permission.[206] Copyright 2022, Springer Nature. d) CARS spectroscopy of acetone-water mixtures. Main: Concentration-dependent spectral evolution. Inset: 10% v/v acetone spectrum. Right: Linear intensity growth at 2921 cm^{-1} with increasing acetone fraction. Reproduced with permission.[206] Copyright 2022, Springer Nature. e) Detection of gastric dysplasia in H. felis/MNU-treated GAS-KO mice using SERRS-Raman imaging and immunohistochemistry. Left: In vivo SERRS-positive lesion mapping at pyloric antrum (2 mm scale). Right: Corresponding IHC showing dysplastic regions (CD44/MKI67 expression) at low (1 mm) and high (50 μm) magnification. Reproduced with permission.[205] Copyright 2019, ACS.

interference generated by a long delivery fiber.[1–3] This has led fiber-optic Raman technology to be, to a large extent, an optical biopsy-like point-measurement technique. Imaging is generally achieved via extremely slow point-by-point scanning or signal enhancement. For example, Wang et al.[204] developed a dual-beveled fiber-optic polarization-gated Raman probe (TBFP). With an outer diameter of only 3.2 mm, the probe employs sophisticated polarization gating and optical design to effectively filter out background signals from non-target regions, ensuring that 91.2% of the collected signal originates from the critical epithelial layer. However, the single-point acquisition time is ≈3 s (**Figure 9**a,b). While this is fast for a single spectrum, it is unacceptable for imaginga low-resolution 100 × 100 pixel image would require over 8 hours. Consequently, this method is absolutely incapable of capturing biological dynamics; even static in vivo imaging would be severely affected by motion artifacts.

To enhance the signal, researchers have explored various strategies. The first strategy involves chemical enhancement. For example, Harmsen et al.[205] utilized the surface-enhanced resonance Raman scattering (SERRS) effect by intravenously injecting specially designed gold-core nanoparticles, which then accumulate in the tumor regions of mice. This allows the signal to be

successfully captured by a miniature fiber-optic probe integrated into an endoscope channel, achieving a high detection sensitivity of 93.1% for sub-millimeter lesions, enabling faster imaging to become possible (Figure 9e). Although this method significantly improves the detection limit, the reliance on external nanoparticles and their potential long-term biosafety issues represent critical bottlenecks that must be resolved before clinical translation.

The second strategy involves physical enhancement or optimized design. For example, Wang et al.[206] designed an adiabatic tapered fiber-optic probe with a tip diameter of only a few hundred nanometers. This design generates a strong electromagnetic field enhancement effect at the tapered tip, enabling the direct excitation and collection of Raman signals from specific chemical bonds (such as C-H bonds) within a single cell without any labels, thereby achieving subcellular resolution (Figure 9c,d). However, it suffers from a near-zero field of view (FOV) and significant system complexity, which restricts its clinical utility. Fiber-optic Raman technology offers superior chemical specificity, but its imaging capabilities are fundamentally constrained by weak signals and slow acquisition speeds. At present, it holds greater clinical viability as a point-scanning optical biopsy tool rather than as a true imaging modality (such as OCT or fluorescence).

7.2. Biomedical Sensing

In addition to serving as flexible light-guiding components in imaging systems, optical fibers can also function directly as sensing elements for the detection of biomedical parameters. The core principle of fiber-optic sensing technology is to convert a physical measurand (pressure, temperature) or a biochemical quantity (pH, molecular concentration, antigen-antibody binding) into a precisely demodulated optical signal, such as a change in wavelength, intensity, phase, or polarization state. Owing to their intrinsic advantages, including miniature size, high sensitivity, good biocompatibility, and immunity to electromagnetic interference (EMI), fiber-optic sensors demonstrate immense potential in the field of real-time in vivo monitoring. They provide a critical technological means for the dynamic diagnosis of diseases, the monitoring of therapeutic processes, and the implementation of precision drug delivery.

7.2.1. Physical Sensing

The core principle of fiber-optic physical sensing is to convert changes in external physical parameters (such as strain, pressure, and temperature) into precisely measurable characteristics of an optical signal (such as intensity, phase, or wavelength). In the biomedical field, a direct application of this principle involves using the deformation of flexible optical fibers to monitor human body motion. For instance, Andreas et al.[207] reported a stretchable, purely elastomeric optical fiber where deformations, caused by large-scale movements like the bending of a joint, induce a predictable loss in its light-guiding performance, thereby enabling the monitoring of such motions (**Figure 10a**).

However, this mechanism, which relies solely on deformation-induced loss in a pure optical fiber, lacks sufficient sensitivity for the minute deformations caused by respiration, heartbeat, or vocalization. To overcome this challenge, researchers have shifted toward the design of functionalized optical fibers, which involves intentionally doping a flexible fiber matrix with functional materials to amplify the optical response to weak deformations. For example, Guo et al.[208] successfully achieved real-time monitoring of subtle physiological signals, such as speaking and deep breathing, by doping a PDMS fiber with dye molecules and leveraging their light-absorbing properties (Figure 10b). In another study, Wang et al.[212] incorporated graphene into a PDMS fiber; due to graphene's exceptionally high sensitivity to strain, the strain response of the functionalized fiber was enhanced fourfold (its optical loss coefficient also increased from 0.63 to 2.58 dB cm^{-1}). This strategy of improving fundamental performance through functionalized design offers a new direction for the development of highly sensitive sensors for wearable health monitoring devices. While this strategy of enhancing fundamental performance through functional design is promising, it simultaneously introduces significant technical challenges. For instance, the incorporation of functional materials, such as graphene or dyes, can improve target sensitivity but may also significantly increase the fiber's intrinsic optical loss, thereby limiting the effective sensing length. Moreover, signal cross-sensitivity presents a critical hurdle. Many functional materials, notably graphene, exhibit high sensitivity to both strain and temperature, rendering the decoupling of these convolved signals essential for achieving precise measurements. Finally, long-term material stability, encompassing issues like dye photobleaching and material-substrate compatibility, along with the need for robust and repeatable manufacturing processes, such as ensuring uniform doping, remains a critical barrier to practical integration in wearable health monitoring devices. Consequently, future research will likely focus on developing novel functional composite materials that achieve ultra-high sensitivity and high-specificity responses to target physical quantities (e.g., pressure or strain) without incurring high baseline optical loss, as well as on exploring novel sensing structures PLGA designed for robust multimodal signal decoupling.

7.2.2. Chemical and Biomolecular Sensing

Fiber-optic chemical and biosensing operates by modifying a fiber structure—typically the core or cladding surface—with sensitive materials that interact with specific target molecules, thereby converting molecular binding events into detectable optical signals. Based on the integration method and sensing mechanism of these sensitive materials, two primary technical approaches have been developed.

The first approach is matrix functionalization, which involves covalently integrating sensitive molecules into the fiber matrix (such as a hydrogel). For instance, Yetisen et al.[210] integrated phenylboronic acid (PBA) derivatives into a hydrogel optical fiber. They utilized the conformational change of PBA upon binding with glucose to alter the light-guiding properties of the fiber, thus achieving label-free, real-time monitoring of glucose and providing a new tool for diabetes management (Figure 10c). However, this matrix-based approach often faces significant challenges with response time, as analytes must diffuse deep into the

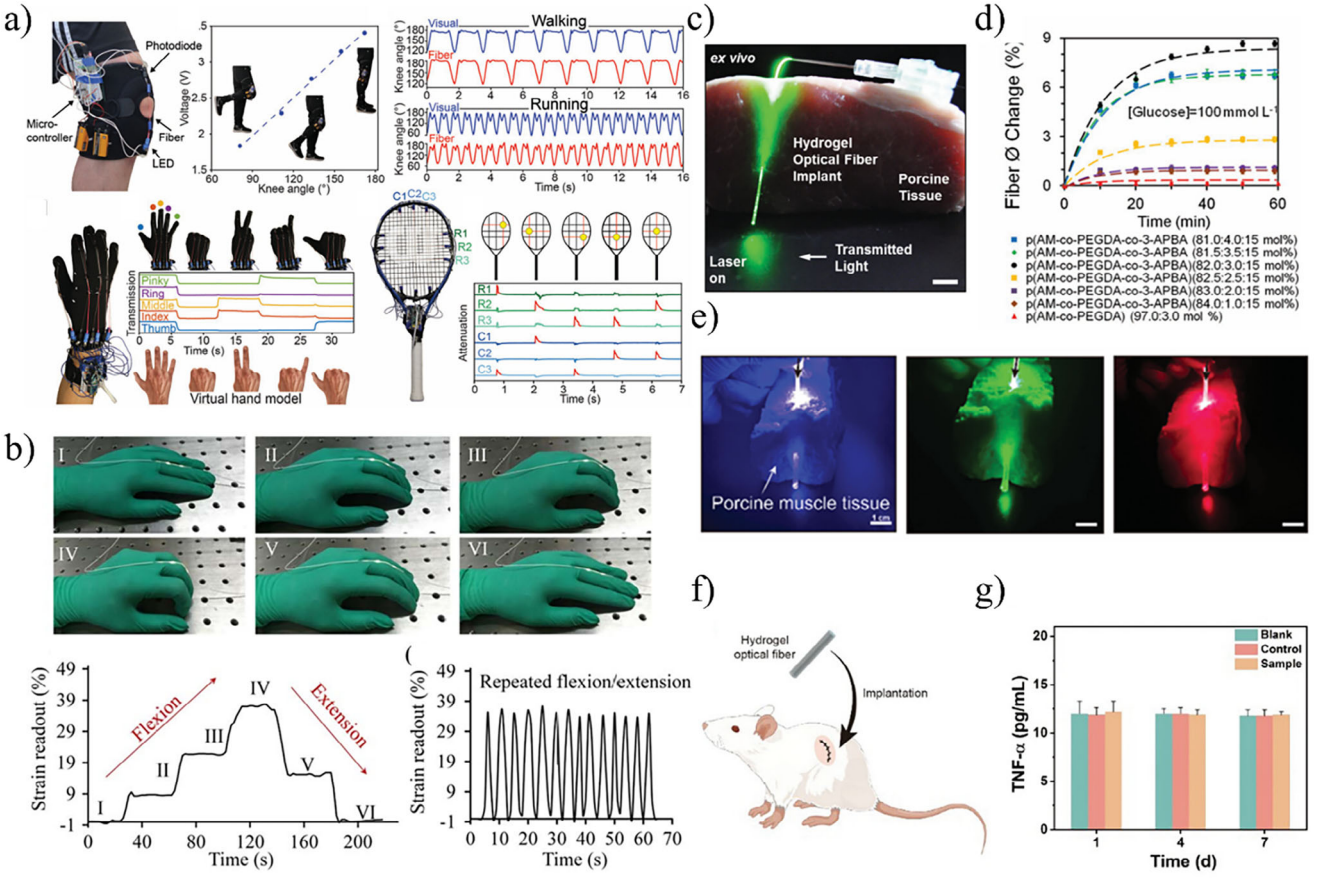

Figure 10. Applications of fiber-optic devices in physical and chemical sensing. a) Examples of optical fiber sensors integrated into everyday objects for activity monitoring. The figure showcases several applications, including a knee brace where the sensor's response is used to measure joint angle, a glove with embedded fibers for real-time hand gesture recognition, and a tennis racket capable of detecting the location of a ball's impact. Reproduced with permission.[207] Copyright 2018, Wiley-VCH. b) A wearable glove instrumented with a strain optic fiber sensor for monitoring finger motion. The figure displays the glove with the integrated sensor, along with corresponding strain readouts for a specific finger posture and for dynamic, repeated flexion and extension movements. Reproduced with permission.[208] Copyright 2017, Optica. c) The implantation of hydrogel optical fibers in porcine tissue. Scale bar = 3 mm. Reproduced with permission.[209] Copyright 2023, Elsevier BV. d) Time-lapse measurements of hydrogel fiber diameter expansion in the presence of glucose, with control experiments fitted to an exponential decay model. Reproduced with permission.[210] Copyright 2017, Wiley-VCH. e) Light transport performance of slippery hydrogel optical fibers in biological tissue. Arrows indicate the direction of light incidence. Scale bar: 1 cm. Reproduced with permission.[211] Copyright 2024, Wiley-VCH. f) Schematic diagram of mouse model for inflammatory response. Reproduced with permission.[211] Copyright 2024, Wiley-VCH. g) Tumor necrosis factor-α (TNF-α) levels from hydrogel optical fiber. Reproduced with permission.[211] Copyright 2024, Wiley-VCH.

hydrogel matrix, a process that can be slow. Furthermore, the hydrogel's physical properties (e.g., swelling/shrinking) are often sensitive to environmental factors like pH and temperature, which can cause non-specific signal drift and cross-sensitivity.

The second approach is surface functionalization, which entails constructing a sensing interface on the fiber surface. G. Zhu et al.[213] sequentially modified the surface of a tapered optical fiber with gold nanoparticles and a specific enzyme to create a localized surface plasmon resonance (LSPR) sensing interface, achieving highly selective detection of ascorbic acid. While this surface-based method offers a much faster response, its primary vulnerability, especially for in vivo applications, is biofouling. Proteins, cells, and other biomacromolecules in complex fluids (like blood) can non-specifically adsorb onto the sensing surface, blocking active sites and rapidly degrading sensor performance and lifespan.

Although these methods have demonstrated feasibility, early sensors often faced challenges, including being limited to single-analyte detection and exhibiting insufficient stability and biocompatibility in complex in vivo environments. To overcome these limitations, subsequent research has primarily focused on the performance optimization and functional expansion of the sensing platform. In terms of enhancing stability and multifunctionality, Zhu et al.[211] proposed an in situ catalytic polymerization method to grow a hydrogel cladding on the fiber surface that possesses both high stability and lubricity (Figure 10e). This design not only significantly improves biocompatibility but also endows the fiber with the potential for photothermal therapy and controlled drug release, extending its capabilities beyond simple sensing. To improve fundamental sensitivity, Liu et al.[209] designed a novel microstructured optical fiber that significantly enhanced the surface plasmon resonance effect, enabling an

ultra-high-sensitivity sensing platform compatible with both gas and liquid analytes. These advancements signify the evolution of fiber-optic biosensing technology from single-molecule detectors to high-performance, multifunctional platforms suitable for complex biological environments. Nonetheless, achieving robust, long-term, and truly multiplexed sensing in complex biological settings remains the central challenge. Future research will likely focus on developing advanced, durable anti-fouling coatings that can resist non-specific adsorption for extended periods in vivo, creating highly multiplexed lab-on-a-fiber platforms that can simultaneously detect dozens of different biomarkers, perhaps using spatially patterned functionalization or novel spectral encoding techniques, and further integrating sensing with therapeutic functions theranostics, moving beyond simple diagnostics to active, on-demand intervention.

8. Optical Fiber-Based Therapeutics

The core functionality of engineered optical fibers lies in their ability to precisely confine the propagation path of photons. This characteristic can be leveraged not only for information acquisition but also for the precise delivery of energy, thereby enabling active intervention in biological processes. In therapeutic and interventional applications, the light emitted from the fiber tip is no longer treated as a probing signal but rather as a form of energy or a control command that acts directly on target tissues to induce specific physical, chemical, or biological effects. For example, photons delivered by the fiber can serve as a heat source to directly ablate tissue, activate photosensitizers to generate cytotoxicity, or act as a switch with high spatiotemporal resolution to activate photosensitive proteins. Centered on this core principle, this section will explore the application of engineered fibers in several representative fields: in optogenetics, for the high-precision modulation of neuronal activity; in photodynamic and photothermal therapies, for targeted energy delivery to deep-seated lesions; and in tissue engineering, for assisting in the fabrication and modulation of functional biological structures or for serving as a carrier for light-assisted drug delivery.

8.1. Optogenetic Neuromodulation

In optogenetic applications, the precise delivery of light pulses to deep brain regions via implantable optical fibers is fundamental to achieving neuronal modulation with high spatiotemporal resolution. However, the extreme stiffness of traditional silica-based optical fibers (Young's modulus ≈70 GPa) creates a significant mechanical mismatch with soft brain tissue (<1 kPa), a factor that limits the application of optogenetic in chronic, long-term studies. The persistent mechanical stress at the implant-tissue interface can trigger chronic inflammation and the formation of glial scars. This not only damages adjacent neurons but can also impede the effective transmission of the optical signal due to an encapsulation effect, ultimately leading to a decline in modulation efficacy over time.

To achieve long-term, stable in-vivo neuromodulation, the key technical challenge lies in overcoming the adverse biological tissue reactions induced by this mechanical mismatch. To this end, researchers have turned to flexible hydrogel optical fibers that are better matched to the mechanical properties of the tissue. For instance, a study by Wang et al.[214] demonstrated that after a four-week implantation of a low-modulus (≈65 kPa) alginate-polyacrylamide hydrogel fiber, glial cells around the implant site were not significantly activated, and the neuron density was comparable to that of normal tissue (**Figure 11**a,b). This provides histological assurance for the effectiveness of long-term optogenetic stimulation. Similarly, PEGDA-based hydrogel optical fibers have also shown minimal tissue reaction and stable light-guiding performance (optical loss of 0.23 dB cm^{-1}), confirming that enhancing flexibility is an effective strategy for improving the biocompatibility of long-term implants[215,216] (Figure 11d–f). Another example is the work of Li et al.,[217] who applied UCNPs to optogenetics to develop a minimally invasive therapy for Parkinson's disease. They delivered 980 nm NIR light via an optical fiber to a brain region injected with UCNPs, which then absorbed the light and emitted 473 nm blue light in situ. This blue light precisely activated photosensitive proteins (ChR2) pre-expressed on neurons, enabling photochemical modulation of neural activity in a deep brain region and effectively improving the motor function of PD mice. This method limits the implantation depth of the fiber to outside the skull, avoiding the damage to deep brain tissue associated with traditional optogenetics and demonstrating great potential as a platform for minimally invasive, optically controlled neuromodulation. Beyond the pursuit of stability for long-term implantation, another class of optogenetic interventions is designed for transient or short-term applications. Here, the core challenge is enabling the interventional tool to be withdrawn with zero impact after its task is completed. Biodegradable optical fibers offer an ideal solution to this need. A study based on poly (L-lactic acid) (PLLA) demonstrated the feasibility of such a transient device[218] (Figure 11c). In its initial phase post-implantation, the fiber could effectively transmit 473 nm laser light to perform its optogenetic stimulation task, but it completely degraded after ≈2 weeks. Histological analysis revealed that by day 60, the number of neurons in the damaged area had recovered to 50% of normal levels, and the glial cell response had gradually subsided. This characteristic of being functionally present on demand and disappearing on schedule opens new pathways for the development of novel, minimally invasive, short-term neuro-interventional therapies.

8.2. Photothermal and Photodynamic Therapies

In the minimally invasive treatment of diseases such as cancer, the core role of the optical fiber is to serve as a highly efficient and precise energy delivery conduit, guiding light from an external source to deep-seated lesions within the body. Based on this functionality, fiber-optic technology has become deeply integrated into two mainstream optical therapeutic modalities: photothermal therapy (PTT) and photodynamic therapy (PDT).

8.2.1. Photothermal Therapy

PTT is a therapeutic method that ablates target cells through a photothermal conversion effect. Its fundamental principle involves the targeted delivery of a photothermal agent (PTA)—such

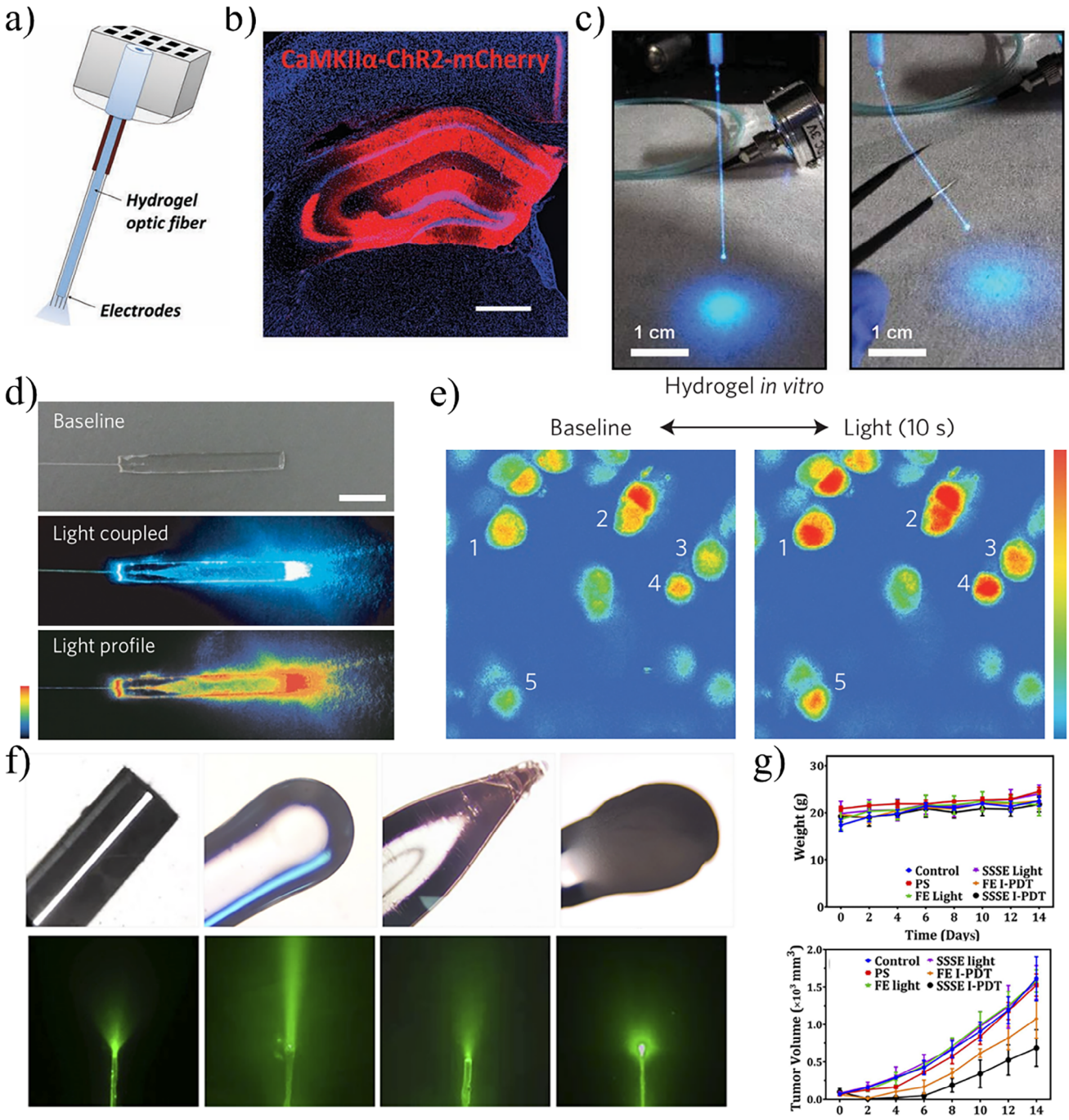

Figure 11. Applications of fiber-optic devices in optogenetics and photodynamic therapy. a) A schematic diagram of a hydrogel optical fiber-coupled electrode array. Reproduced with permission.[214] Copyright 2018, Wiley-VCH. b) Using hydrogel optical fiber-coupled electrode testing expression of CaMKIIα-ChR2-mCherry (red) in hippocampal neurons 4 weeks after injection (bar = 500 μm). Reproduced with permission.[214] Copyright 2018, Wiley-VCH. c) A 5 cm long PLLA fiber coupled to a blue LED (473 nm). Left, no bending; right, bended with a tweezer. Reproduced with permission.[218] Copyright 2017, Wiley-VCH. d) Imaging of light coupling to a hydrogel. Top: hydrogel before light coupling; middle: hydrogel after light coupling; bottom: pseudo-color image of the spatial profile of the scattered light. Reproduced with permission.[215] Copyright 2013, Springer Nature. e) Fluorescence calcium-level imaging of optogenetic cells in the hydrogel optical fiber optical fiber in vitro. Scale bar, 20 mm. Reproduced with permission.[215] Copyright 2013, Springer Nature. f) Four different fiber ends (flat, spherical, conical, and strongly scattering spherical ends from left to right) and distributions of 532 nm laser with different ends. Reproduced with permission.[216] Copyright 2023, Optica. g) Body weight curves and tumor volume curves for different groups of mice post-treatment ($n = 4$) by four different fiber ends. Reproduced with permission.[216] Copyright 2023, Optica.

as gold nanoparticles or graphene, which possess high photothermal conversion efficiency—to a lesion. Subsequently, a laser of a specific wavelength, typically within the near-infrared tissue window, is used to irradiate the area via an optical fiber. The PTA absorbs the light energy and generates localized hyperthermia (>42 °C), thereby inducing irreversible damage and even necrosis in tumor cells.

The introduction of optical fibers has made the precise and minimally invasive photothermal ablation of deep-seated tumors (e.g., in the liver and prostate) possible. In contrast, traditional cancer treatments like surgical resection are generally suited for early-stage or localized tumors but are highly invasive. Radiotherapy and chemotherapy, while effective at killing tumor cells, may also damage surrounding healthy tissue and can be associated with toxic side effects. To further advance the field, researchers are dedicated to developing theranostic (a portmanteau of therapeutics and diagnostics) fiber-optic platforms that integrate diagnostic or sensing functions. For instance, He et al.[219] proposed a fiber-optic probe based on a gold-nanoparticle-modified silver film (AuNPs-AgFM), which can be used not only for the detection of tumor cells but also for performing PTT at the same location. To achieve more intelligent therapies, Jin et al.[220] developed a fiber-optic probe integrated with a graphene/gold nanostar (Gr/AuNS) composite. This probe is capable of first rapidly sensing key indicators of the tumor microenvironment (such as hypoxia) and then using the same fiber to administer PTT, thus enabling precise intervention based on the real-time status of the lesion.

8.2.2. Photodynamic Therapy

PDT is a therapeutic technique that utilizes a photochemical reaction to kill target cells. Its principle relies on three essential elements: a photosensitizer (PS), excitation light of a specific wavelength, and oxygen present in the tissue. During treatment, the photosensitizer is targeted to and enriched in the tumor tissue. Upon irradiation with a specific wavelength of light delivered via an optical fiber, the photosensitizer is elevated to a high-energy excited state. The excited photosensitizer then transfers its energy to surrounding oxygen molecules, generating reactive oxygen species (ROS), primarily the highly cytotoxic singlet oxygen. These ROS can rapidly destroy the biomacromolecules of tumor cells, inducing apoptosis or necrosis.

Because the cytotoxic effect of PDT is strictly confined to the area where light, the photosensitizer, and oxygen coexist, the precise delivery of light is of paramount importance. For tumors in deep or complex locations, such as glioma, optical fibers are the ideal tool for achieving precise illumination. Zhang et al.[221] combined aggregation-induced emission (AIE) photosensitizers with fiber-optic delivery technology. This strategy leverages the characteristic of AIE photosensitizers to be efficiently activated only after they have aggregated within tumor cells, thereby achieving targeting at the chemical level. Simultaneously, a minimally invasive optical fiber is used to deliver the excitation light directly to the core of the lesion, achieving precise energy delivery at the physical level. This dual-precision strategy, combining both chemical and physical targeting, effectively enhances the therapeutic efficacy for deep-seated tumors and significantly reduces collateral damage to surrounding healthy tissue. Similarly, Pang et al.[216] designed and fabricated a biocompatible POF based on PLA with a strong scattering spherical end (SSSE) for interstitial photodynamic therapy (I-PDT). The fiber, prepared by a thermal drawing method, exhibits good flexibility and low transmission/bending loss. Its SSSE structure significantly expands the excitation light field and achieves a uniform light intensity distribution, demonstrating excellent tumor ablation effects in both in vitro and in vivo experiments.

8.3. Tissue Engineering and Drug Delivery

The ability of optical fibers to precisely control the spatiotemporal distribution of light energy gives them a key role in the fields of tissue engineering and drug delivery. This section will explore their application as light conduits for the in-situ crosslinking and structural formation of photosensitive biomaterials during 3D bioprinting, as well as their capacity to enable the on-demand activation of photo-responsive drug release or therapeutic functions from implanted devices.

8.3.1. Bioprinting and Tissue Scaffolding

In the field of tissue engineering, the core role of an optical fiber is to act as a mobile, miniature light source, providing precise photocrosslinking energy for 3D bioprinting based on photosensitive hydrogels. Through the precise control of illumination position, intensity, and duration, the layer-by-layer or freeform fabrication of complex 3D biological scaffolds can be achieved, providing a structural foundation for tissue repair and regeneration.

One strategy is to integrate the optical fiber within the printing head. For instance, Lee et al.[222] embedded a UV optical fiber into a 3D printing nozzle to perform in situ photocrosslinking of the bio-ink (GelMA) as it flowed through the printing channel. This method effectively solved the challenge of maintaining the shape of low-viscosity inks during the printing process and successfully constructed functional muscle tissue with uniaxially aligned cells. To overcome the limitations on structural complexity imposed by the printing nozzle, Cianciosi et al.[12] proposed a fiber-assisted printing technique. They immersed an LED-coupled quartz optical fiber directly into a photosensitive resin bath and, by dynamically adjusting the light spot parameters, achieved the freeform fabrication of self-supporting hydrogels up to 8 mm in thickness, offering a new pathway for building large-scale organ and tissue models with complex internal structures.

In situ 3D bioprinting within a living body represents a more advanced strategy, aiming to directly construct functional tissues in vivo. This approach can circumvent cell damage and environmental discrepancies associated with in vitro culture, promoting the integration of the printed structure with the host and facilitating tissue self-repair within a true physiological microenvironment. Significant progress has been made in this area of research. For example, Urciuolo et al.[223] developed an in vivo 3D bioprinting technique that uses near-infrared two-photon excitation ($\lambda > 850$ nm) for the in-situ crosslinking of photosensitive polymers. Without the need for surgical exposure, this technique can construct complex 3D structures with micron-scale

resolution in deep tissues of living mice, such as the dermis, skeletal muscle, and brain, and has successfully guided the differentiation and vascularization of donor stem cells. To address the challenges of flexibility and accessibility in in vivo printing, Thai et al.[224] developed a flexible in situ 3D bioprinting system (F3DB). The system integrates a soft printing head with high degrees of freedom and a robotic arm, which can enter the body through natural orifices or minimally invasive incisions to perform precise, multi-material, and multi-location printing on the surfaces of deep organs like the colon and heart. Experiments on *ex-vivo* porcine models confirmed that hydrogels printed by the system containing a high density of living cells (L929, 1.4×10^6 cells/mL) exhibited extremely high cell viability and proliferative capacity. Furthermore, the F3DB system also integrates endoscopic surgical functions, demonstrating its significant potential as an all-in-one regenerative medicine tool and opening up new possibilities for in situ tissue repair and regeneration under minimally invasive conditions.

8.3.2. Controlled Drug Delivery

In this application scenario, the role of the optical fiber shifts from that of a direct energy-based therapeutic tool to that of a high-precision external control switch, used to trigger the release of therapeutic molecules on demand at a specific time and location. Its core advantage lies in transforming the drug delivery process from a conventional systemic, passive-diffusion model to a localized, actively controllable one, thereby dramatically enhancing therapeutic efficacy while reducing systemic toxic side effects. The technical approaches to achieving this goal are primarily based on two different photophysical or photochemical mechanisms. The first mechanism is photothermal-controlled release. This strategy involves encapsulating a drug within a temperature-sensitive carrier, such as a thermoresponsive hydrogel or a phase-change material. An optical fiber delivers NIR light to the implanted carrier, where the light energy is absorbed by integrated photothermal converting agents and transformed into localized heat. When the temperature surpasses the material's critical threshold (e.g., the lower critical solution temperature (LCST) of a polymer or the phase transition temperature of a liposome), the carrier undergoes a rapid physical conformational change—such as shrinking, melting, or increasing in permeability—which in turn squeezes out or releases its loaded drug molecules. The advantage of this method is its ability to utilize NIR light, which has good tissue penetration, although its spatial precision is limited by the diffusion range of the heat. For example, Zheng et al.[217] utilized this mechanism to develop an injectable implant for treating vocal fold scarring. In their system, gold nanorods, acting as photothermal agents, were encapsulated within thermosensitive liposomes. Through the precise delivery of 1064 nm NIR laser light via an optical fiber, the gold nanorods absorbed the light energy and generated localized hyperthermia. When the temperature exceeded the liposome's phase transition threshold, its permeability increased instantaneously, triggering the release of the loaded drug, dexamethasone. Here, the optical fiber served not only as a precise energy conduit but also as a sensor, enabling real-time monitoring of the drug release kinetics through fluorescence imaging. Similarly, Peng et al.[225] combined the photothermal effect with gas therapy to construct a self-healing hydrogel for eradicating biofilms and promoting wound healing. In this system, an optical fiber guided an 808 nm laser to excite polydopamine nanoparticles within the hydrogel, generating mild photothermal heat (<50 °C). This localized temperature increases not only directly weakened the bacterial biofilm but, more critically, synergistically triggered the decomposition of a nitric oxide (NO) donor, achieving a dual assault of hyperthermia and gas therapy (**Figure 12**a–c). This study also highlighted the multifunctionality of the optical fiber, which acted as both a trigger and a sensor for precise feedback and control via real-time temperature monitoring, significantly accelerating the healing process of infected wounds in an animal model.

The second mechanism is photochemical-controlled release, which offers higher, molecular-level precision. The core of this approach is to covalently link drug molecules to a carrier backbone or nanoparticle via a photocleavable linker. This chemical bond is stable in the absence of light of a specific wavelength, effectively locking the drug in place. When an optical fiber delivers light of the appropriate wavelength (UV or visible light) to the target site, the photon energy directly breaks this bond, causing the drug molecule to detach from the carrier and regain its activity. To overcome the poor tissue penetration of UV/visible light, more advanced designs employ photon upconversion technology. This involves using NIR light to excite upconversion nanoparticles (UCNPs) within the carrier, causing them to emit high-energy UV/visible photons in situ and thus achieving deep-tissue, low-damage cleavage of the photosensitive linkers. For instance, Zamadar[3] et al. developed a fiber-optic microprobe with a tip-loaded photosensitizer. Upon photoirradiation, singlet oxygen ($^1O_2$), generated in situ, triggers the cleavage of an olefin linker, leading to the release of the photosensitizer. This system not only enables the controlled release of the photosensitizer but also co-delivers cytotoxic $^1O_2$, offering a novel strategy for highly localized, topical administration for the PDT of hypoxic tumors. In another example, Choi et al.[4] designed a nano-delivery platform where the anticancer drug methotrexate (MTX) was released from a PAMAM dendrimer carrier through the cleavage of a UV-light-sensitive o-nitrobenzyl (ONB) linker. The study demonstrated that active and controllable drug release could be triggered by external photo-irradiation, offering a new paradigm for targeted therapy with high spatiotemporal precision. Such light-responsive materials are promising candidates for integration with fiber-optic systems. For example, they could be incorporated as a coating on the fiber tip or as a component in a composite fiber scaffold. By combining these approaches, optical fibers could be engineered with advanced photochemical drug release capabilities, enabling precise, on-demand therapy in deep-seated lesions.

In addition to the release of exogenous drugs, light-controlled strategies can also be extended to regulate the intrinsic functions of cells, enabling the on-demand production of endogenous therapeutic substances. In such designs, the light signals delivered via optical fibers serve as a high-precision control tool, capable of directly activating specific intracellular gene pathways. This activation promotes the engineered cells to synthesize and secrete therapeutic proteins or peptides. This approach transforms engineered cells into cellular drug factories that can be

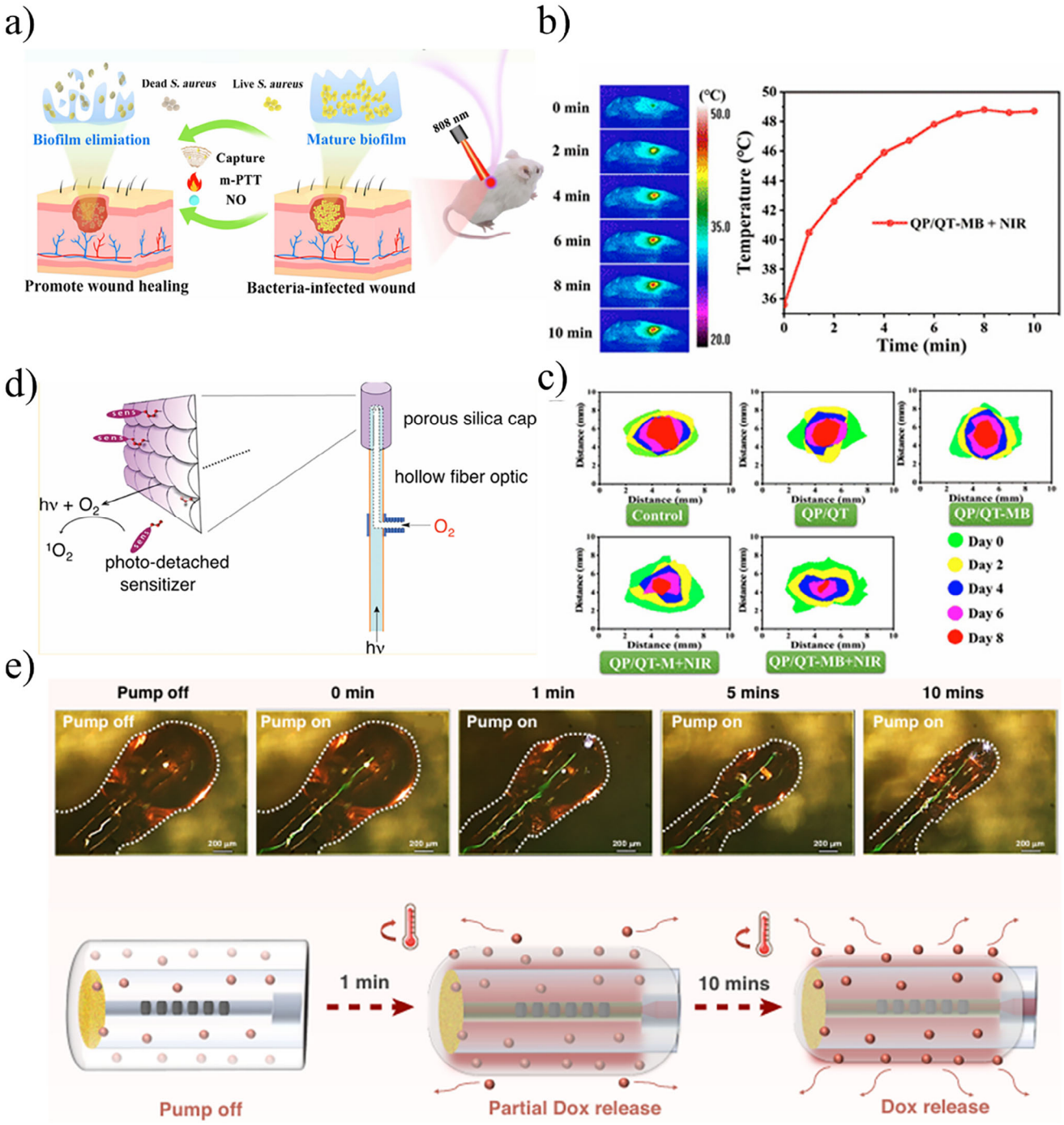

Figure 12. Applications of fiber-optic devices in controlled drug delivery. a) Schematic of a multifunctional hydrogel platform designed for anti-infection and wound regeneration. Reproduced with permission.[225] Copyright 2023, RSC. b) Thermographic images and corresponding temperature curves confirm localized heating at the wound site upon NIR irradiation. Reproduced with permission.[225] Copyright 2023, RSC. c) Quantitative analysis of wound closure over 8 days demonstrates accelerated healing in the NIR-treated group. Reproduced with permission.[225] Copyright 2023, RSC. d) Design concept of a singlet oxygen fiber optic for photochemical release. Light delivered through the fiber generates singlet oxygen ($^1O_2$), which cleaves a photocleavable linker to release a sensitizer molecule. Reproduced with permission.[226] Copyright 2011, ACS. e) Microscopic observation and schematic illustration of photothermally triggered release of the chemotherapy drug doxorubicin (Dox). Reproduced with permission.[27] Copyright 2024, Springer Nature.

remotely controlled by external light signals, thereby establishing a novel in vivo model for on-demand therapeutic drug production. Based on this principle, Akshaya et al.[227] developed an NIR-light-controlled gene expression system based on UCNPs. In this system, they co-encapsulated genetically engineered cells responsive to blue light with UCNPs in a hydrogel. The combination of this strategy with fiber-optic technology shows immense potential. A minimally invasive implanted optical fiber can act as a highly efficient conduit for NIR light (980 nm), delivering the light energy precisely and with low loss to deep-body locations. Upon reaching the target, the highly penetrating NIR light is absorbed by the UCNPs and converted in situ into blue light, which activates the cells, thereby driving the endogenous production and secretion of a therapeutic peptide (GLP-1). This model of fiber-guided, in situ upconversion significantly reduces the invasiveness and photothermal damage to surrounding tissues compared to traditional approaches that require the blue-light fiber tip to be placed in direct proximity to the cells.

The true value of fiber-optic controlled release lies not just in delivery but in modulation. Because the on/off switching and intensity adjustment of a light signal are exceptionally simple, researchers can program an external light source to precisely regulate the drug release profile. For instance, pulsatile delivery can be achieved to mimic the body's physiological rhythms, or the dosage can be dynamically adjusted in response to changes in a patient's condition. Furthermore, by integrating multiple photosensitive linkers responsive to different wavelengths of light onto the same carrier, it is theoretically possible to use a single multi-wavelength-output fiber to independently and sequentially control the release of various drugs, opening up possibilities for complex synergistic treatment regimens. For example, Zhang[27] proposed a highly integrated theranostic fiber-optic probe aimed at achieving synergistic photothermal-chemotherapy for deep-seated tumors. The system ingeniously encapsulates a photothermal sensitizer (rare-earth ions) within the fiber core and loads a chemotherapy drug (doxorubicin) into a thermoresponsive hydrogel coated on the fiber's surface (Figure 11e). When 980 nm laser light is transmitted through the fiber, it not only generates a localized photothermal effect to directly kill tumor cells but also produces heat that triggers a phase change in the hydrogel, enabling the on-demand, precise release of the chemotherapy drug. Moreover, the platform achieves real-time, closed-loop monitoring of drug concentration and local temperature via sensors integrated within the fiber, ensuring the treatment process is precisely controllable. Its unique center-to-periphery drug penetration mechanism and long-term retention effect, similar to that of transarterial chemoembolization (TACE), achieved complete tumor eradication in an animal model after a single treatment. The core advantage of this system is its integration of precise delivery, on-demand release, and in situ monitoring. This lays the foundation for the development of the next generation of intelligent, programmable, implantable drug delivery systems.

9. Summary and Future Outlook

This article has systematically reviewed the research progress of engineered optical fibers in deep-tissue biomedical applications. Whether in in situ imaging, sensing, or precision therapy, engineered fibers have demonstrated immense potential. However, although we have summarized a variety of technical paradigms, each faces its own inherent challenges, and a universal, perfect solution does not yet exist. Therefore, to further enhance the performance of optical fibers to meet complex biomedical demands, relying solely on incremental improvements to existing materials and structures is insufficient. Future breakthroughs are more likely to originate from a paradigm shift in research—moving from a materials-driven approach to an application-oriented inverse design strategy, where novel materials and structures are created based on functional requirements. In light of this, this section will present a structured outlook on the future challenges and opportunities in this field from the key dimensions of performance enhancement, functional expansion, and frontier integration, with the aim of providing insights for the development of the next generation of high-performance biomedical optical fibers.

9.1. Advanced Materials and Structural Engineering

Although the preceding sections have systematically elaborated on various strategies for enhancing the sensing performance of optical fibers by optimizing single-material systems, the intrinsic performance limits of any single material often make it difficult to meet the demands of future intelligent systems for multifunctionality and high-level integration. Consequently, the multicomponent and composite materials strategy is gaining increasing attention as a promising design approach. This method aims to organically integrate multiple functional nanomaterials within a single fiber matrix, leveraging the synergistic effects between materials to achieve performance gains and provide a feasible pathway for breaking through the performance bottlenecks of traditional materials.

In the field of biosensing, this synergistic effect was first demonstrated to have significant potential in enhancing detection sensitivity. For example, Chaudhary et al.[228] functionalized the surface of a polymer optical fiber with polyamide-amine (PAMAM) dendrimers to successfully construct a high-density layer of bioreceptors. This nano-composite interface dramatically enhanced molecular capture efficiency, thereby achieving an ultralow limit of detection (LOD < 10 pg mL^{-1}) for the preeclampsia biomarker PlGF. This work showcases the potential of leveraging the synergy between nanostructures and biomolecules to further push the limits of sensing performance.

Furthermore, this strategy has shown advantages in systematically addressing practical application challenges, such as multiparameter cross-interference. The research by Xia et al.[221] provides a key reference in this regard. They deposited a graphene oxide/polyacrylic acid (GO/PAA) composite coating onto the surface of an excessively tilted fiber grating (ex-TFG). In this design, the GO/PAA coating significantly improved humidity sensitivity and response speed, while the underlying ex-TFG ingeniously provided simultaneous temperature compensation (**Figure 13b**). This design philosophy—using multi-component synergy to both optimize a core performance metric and build in an environmental compensation mechanism—offers a valuable model for the future development of highly stable and reliable sensor devices.

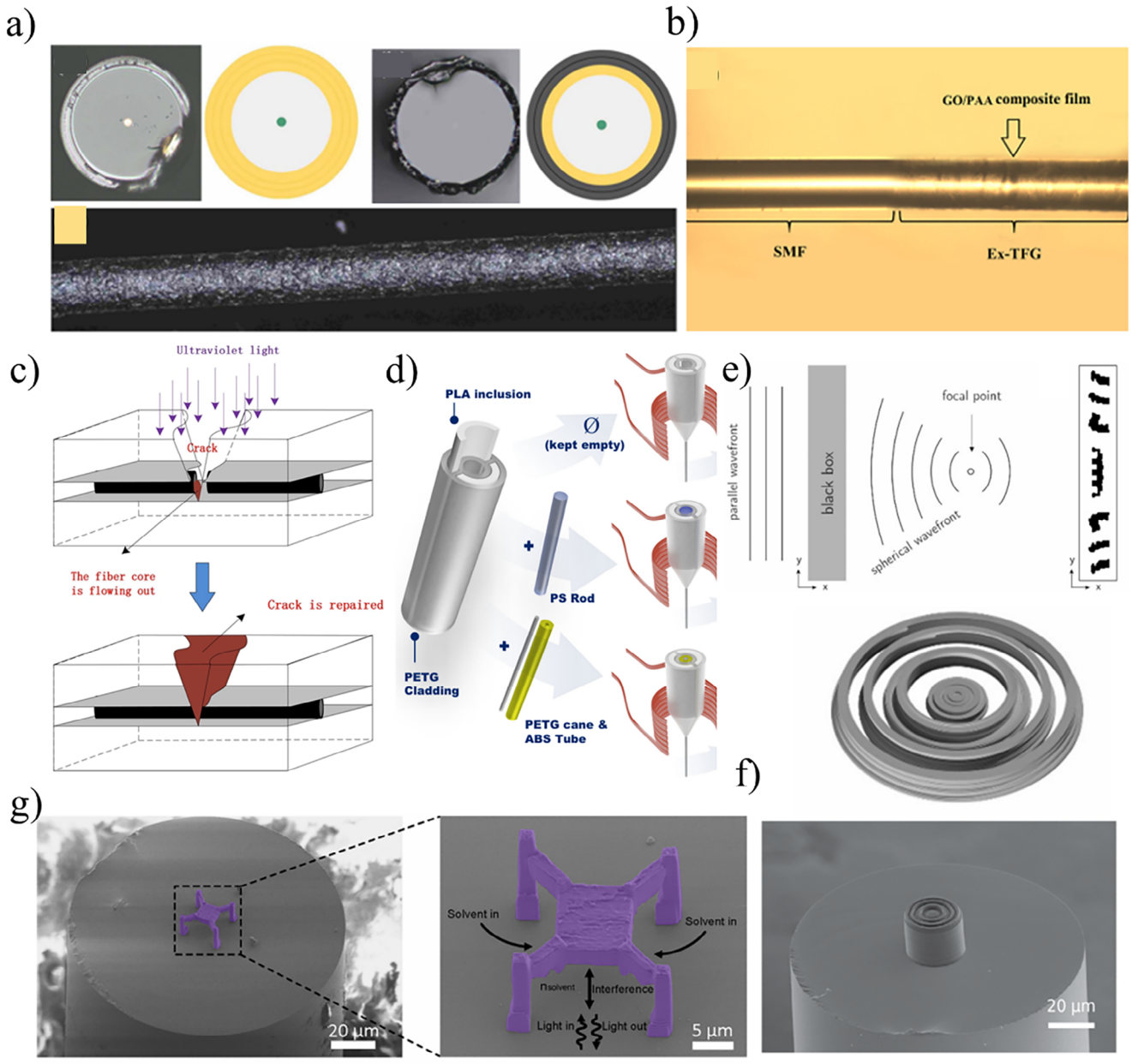

Figure 13. Advanced Materials and Structural Engineering. a) Schematics comparing the cross-sections of a standard polyimide-coated reference fiber with a nanocomposite (NC)-coated fiber, along with a side-view photograph of a drawn 5 wt% rGO/polyimide fiber. Reproduced with permission.[229] Copyright 2024, IEEE. b) Microscope image of a functional film coated with ex-TFG. Reproduced with permission.[230] Copyright 2022, ACS. c) Schematic illustration of the self-healing principle for an integrated fiber optic material. Reproduced with permission.[231] Copyright 2022, Optica). d) 3D model of a polylactic acid (PLA) /polyethylene terephthalate glycol (PETG) frame used for the production of shape-memory fibers in various architectures. Reproduced with permission.[232] Copyright 2023, Springer Nature. e) The inverse design process for a photonic lens, illustrating the problem definition of transforming a plane wave into a spherical wave, the resulting 2D optimized structure, and the final 3D lens generated via rotational symmetry. Reproduced with permission.[233] Copyright 2021, ACS. f) Scanning electron microscopy (SEM) image of a micro-lens fabricated directly on the tip of a SMF. Reproduced with permission.[233] Copyright 2021, ACS. g) A colored SEM image of a fiber-tip refractive index sensor, accompanied by an enlarged schematic that illustrates its working principle. Reproduced with permission.[234] Copyright 2024, ACS.

Moving further, multi-material integration holds the promise of endowing optical fibers with composite functions that unite sensing and actuation. The graphene-polyimide-coated fiber developed by Tow's team[229] is a case in point. This composite coating not only imparts excellent sensing properties to the fiber, but its electrical conductivity also enables localized, precision heating (Figure 13a). This design transforms the fiber from a passive information collector into an active functional executor, greatly

expanding its application prospects in fields such as implantable biomedical sensing, targeted thermotherapy, and directed cell guidance.

While exploring material combination strategies, the conventional trial-and-error approach to material development is facing challenges in efficiency and cost when confronted with complex future functional requirements. In response, function-oriented inverse material exploration is emerging as a new design methodology and attracting widespread academic interest. This strategy leverages computational simulation and artificial intelligence to reverse the research and development workflow—shifting from exploring materials to discover functions, to defining a function, and then designing the material. It provides a new method for the systematic design of smart and active materials with specific advanced properties, such as self-healing and adaptability. For instance, Wang et al.,[235] through inverse design, precisely controlled hydrogen bond density and chain segment mobility at the molecular level to successfully develop a PDES-based self-healing optical fiber. This material achieved the simultaneous self-repair of multiple physical properties and maintained stability across a wide temperature range, demonstrating the possibility of constructing living devices capable of long-term, stable operation in complex biological environments. Following a similar line of reasoning, Shen's team[231] drew inspiration from biological bone repair mechanisms. By using computational simulation to prematch, the optical and mechanical properties of materials and to optimize repair kinetics, they constructed a biomimetic self-healing fiber-optic composite, offering a promising solution to the problem of long-term health monitoring for implantable devices or large-scale structures (Figure 13c).

Inverse design also holds the potential to fundamentally enhance sensing precision by optimizing the intrinsic physical properties of a material. The work of Bahin et al.[236] provides evidence for this. They utilized multi-scale computational simulation to pre-establish a quantitative structure-property relationship between the bending stiffness of a material and its optical loss. This enabled them to precisely screen for the optimal combination of PDMS and PMMA, which significantly improved the sensor's ability to differentiate between pressure and bending signals. This highlights the important role of computational simulation in decoupling complex biomechanical signals to achieve high-fidelity monitoring.

The promise of this methodology also lies in its potential to endow materials with dynamically programmable properties. Strutynski et al.[232] combined a shape-memory PLA with a thermoplastic material (PETG) to fabricate an optical fiber with shape-memory capabilities. This fiber can autonomously return to a pre-set shape upon external stimulation while maintaining efficient light-transmission performance (Figure 13d). This work provides a new direction for the development of adaptive photonic devices and biomedical sensors that can actively adapt to changes in the physiological environment to perform specific tasks.

Parallel to innovations in material composition, another dimension crucial for future development arises from the precise structural engineering of the optical fiber itself at the micro- and nano-scales. By integrating cutting-edge concepts such as metasurfaces, chiral photonics, and topological physics with fiber-optic technology, researchers are actively exploring finer and more flexible ways to manipulate the light field. This endeavor opens up possibilities for achieving new functionalities that are unattainable with conventional optical fibers.

The foundation of this direction lies in advanced micro- and nano-fabrication techniques, which have made it possible to construct complex optical systems directly on the fiber. For instance, Lai et al.[234] proposed a method for the direct laser writing of 3D glass micro-optical structures with sub-wavelength resolution on a fiber facet. By precisely controlling the printing patterns, they successfully integrated functional devices such as refractive index sensors and compact polarization beam splitters (Figure 13g). This technology combines the excellent material stability of glass with the plug-and-play nature of optical fibers, offering new device implementation schemes for fields like fiber-optic sensing, optical MEMS, and quantum photonics.

This approach to structural design is not limited to the fiber's end face but can also be extended deep into its interior to enhance specific light-matter interactions. The work of Dezaki et al.[237] serves as a prime example. They proposed a circular dichroism (CD) sensing method based on a chiral-core fiber. By introducing a chiral material as the fiber core to break mode degeneracy, they leveraged the cutoff frequency differences between various modes to detect the handedness of chiral molecules. By defining a new optical fiber CD parameter (CDw), this method significantly enhances the differential signal response of traditional CD spectroscopy, offering a new path for high-sensitivity chirality detection in the biomedical and pharmaceutical industries.

Pushing this structural design philosophy to an even deeper level is the introduction of concepts from topological physics to achieve robust control over light transmission. Roberts et al.[238] designed a photonic crystal fiber (TopoPCF) that supports topologically protected supermodes. Through a helically arranged multi-core structure, they achieved the topologically protected transmission of visible light over meter-scale distances, meaning the transmission state remains stable even under perturbations such as fiber bending. This research lays a vital experimental foundation for the study and application of topological photonic effects on a scalable fiber platform, particularly for future quantum photonic networks. Building on this, recent studies have begun to further explore how to utilize the unique properties of topological interface modes for more complex light field manipulation. For example, Huang et al.[239] proposed a novel topological photonic crystal fiber based on a honeycomb structure, which introduces a topological difference between the core and cladding by adjusting the position of the air holes. The resulting topological interface modes exhibit a pseudo-spin-momentum locking effect, causing the light field to display a unique helical propagation behavior within the fiber. This work more tightly integrates the concepts of topological photonics with fiber-optic technology, providing new theoretical and design insights for information transmission and light field control using new degrees of freedom, such as orbital angular momentum.

Beyond expanding functional boundaries with new materials and physical concepts, another frontier with significant application value is the fine-grained optimization of the fiber structure for specific scenarios using advanced computational methods. The core idea of this direction is to shift from general-purpose to special-purpose design—that is, to use algorithms like inverse design and artificial intelligence to search for the optimal

solution within a complex design parameter space, thereby pushing the performance of fiber-optic devices to their absolute limits in specific applications.

This strategy has already demonstrated notable success in the functional integration of fiber facets. For example, Hadibrata et al.[233] utilized an inverse design algorithm to propose a metalens that can be 3D-printed directly on a fiber facet. This design breaks free from the geometric constraints of traditional lenses, achieving a numerical aperture as high as 0.85 and a focusing efficiency of 73% at a wavelength of 980 nm. It has been successfully applied in a high-resolution two-photon direct-write lithography system (Figure 13e,f). This work clearly illustrates the immense potential of inverse design in customizing high-performance integrated optical components for specific applications like micro- and nano-fabrication and optical tweezers.

This optimization philosophy is equally applicable to enhancing the core metrics of sensors. Dogan et al.[240] proposed an optimization method that combines artificial neural networks (ANN) and a genetic algorithm (GA) for designing D-shaped fiber SPR refractive index sensors. By integrating finite element simulation data with their AI model, they systematically optimized multiple key geometric parameters, including grating gap, number of gratings, and cladding thickness, ultimately achieving a high sensitivity of 3890 nm/RIU. Compared to traditional parameter-sweep methods, this data-driven optimization approach can more efficiently and comprehensively reveal the complex correlations among multiple parameters, providing a powerful tool for the high-performance design of complex-structure fiber-optic sensors.

Furthermore, the most advanced structural optimization efforts not only pursue optimal performance under ideal conditions but are also beginning to address the problem of uncertainty, which is pervasive in real-world applications. Although the following study does not directly target fiber-optic sensors, its methodology is highly instructive. Wang et al.[241] proposed a reliability-based structural optimization method for fiber-reinforced composite materials. They innovatively embedded reliability analysis into a simultaneous design process for topology optimization and fiber orientation to cope with load uncertainties in practical working conditions. The results showed that structures optimized by this method exhibited higher reliability under uncertain conditions.

In summary, application-oriented structural optimization is becoming a critical link between theoretical design and practical high-performance devices. From using inverse design to customize optical components and leveraging artificial intelligence to optimize sensor parameters, to introducing reliability analysis to handle environmental uncertainties, these computation-driven design methods are ensuring that fiber-optic technology can deliver its best possible performance in a wide array of diverse and demanding application scenarios.

9.2. Integration and System Expansion

A core future direction for intelligent sensing systems lies in moving beyond the limitations of single-parameter measurement and advancing toward multimodal information acquisition on a single probe. By integrating multi-dimensional sensing capabilities—including optical, electrical, chemical, and physical—within a compact fiber-optic structure, it is possible to gain a more comprehensive and precise understanding of complex pathophysiological environments. This, in turn, can enhance diagnostic reliability and open up new therapeutic and interventional functionalities.

One of the immediate advantages of multimodal integration is its ability to solve the pervasive problem of signal cross-sensitivity in sensing processes. The work of Zhou et al.[242] provides a clear example of this. They designed a dual-function SPR biosensor based on a C-shaped optical fiber that, by integrating optical-chemical and temperature sensing capabilities, achieved the simultaneous detection of DNA hybridization and ambient temperature. In this design, two distinct SPR effects were spatially separated and used to respond to refractive index and temperature, respectively, thereby effectively decoupling the interference of temperature variations from the biomolecular detection. This demonstrates the fundamental value of multimodal design in improving signal fidelity and detection reliability.

Building on this foundation, multimodal integration has been further extended to the synchronous monitoring of multiple physical parameters to meet the demands of monitoring in complex or extreme environments. For example, Zheng et al.[10] proposed a stress/temperature dual-modal sensing technique based on a flexible optical fiber. By integrating mechanoluminescence (ML) and upconversion luminescence (UCL) materials onto a single fiber-optic probe, they leveraged the unique responses of each material to different physical quantities to achieve remote and simultaneous monitoring of stress and temperature (**Figure 14d**). This technology has shown application potential in high-temperature, high-pressure, or hazardous environments, proving the effectiveness of the multimodal strategy in acquiring multi-dimensional physical field information. Physiological signal recording, optogenetic stimulation, localized drug delivery, the most forward-looking exploration in this field lies in the deep fusion of multimodal sensing with active functions such as navigation and therapy, transforming the optical fiber from a passive sensor into an active microrobot. The sub-millimeter-scale multifunctional ferromagnetic fiber robots (MFFRs) proposed by Zhang et al.[243] are representative of this direction. Through an advanced thermal drawing process, they integrated ferromagnetic materials, electrodes, optical fibers, and microfluidic channels into a single fiber (Figure 14c). This allows the fiber robot not only to be precisely navigated through complex environments using an external magnetic field but also to simultaneously perform multiple tasks, including electro and endoscopic imaging. This high degree of functional integration—combining navigation-sensing-therapy—provides a highly promising technological platform for future developments in minimally invasive medical fields, such as cardiac intervention and the treatment of deep-brain tumors.

In summary, from resolving signal crosstalk and enabling multi-physics field monitoring to achieving the high-level integration of sense-and-actuate functionalities, multimodal information acquisition has become a key research dimension. Integrating an ever-increasing array of functions onto a single fiber-optic probe is the definitive path toward providing comprehensive, real-time information for complex biological and industrial environments, and it lays the foundation for the development of

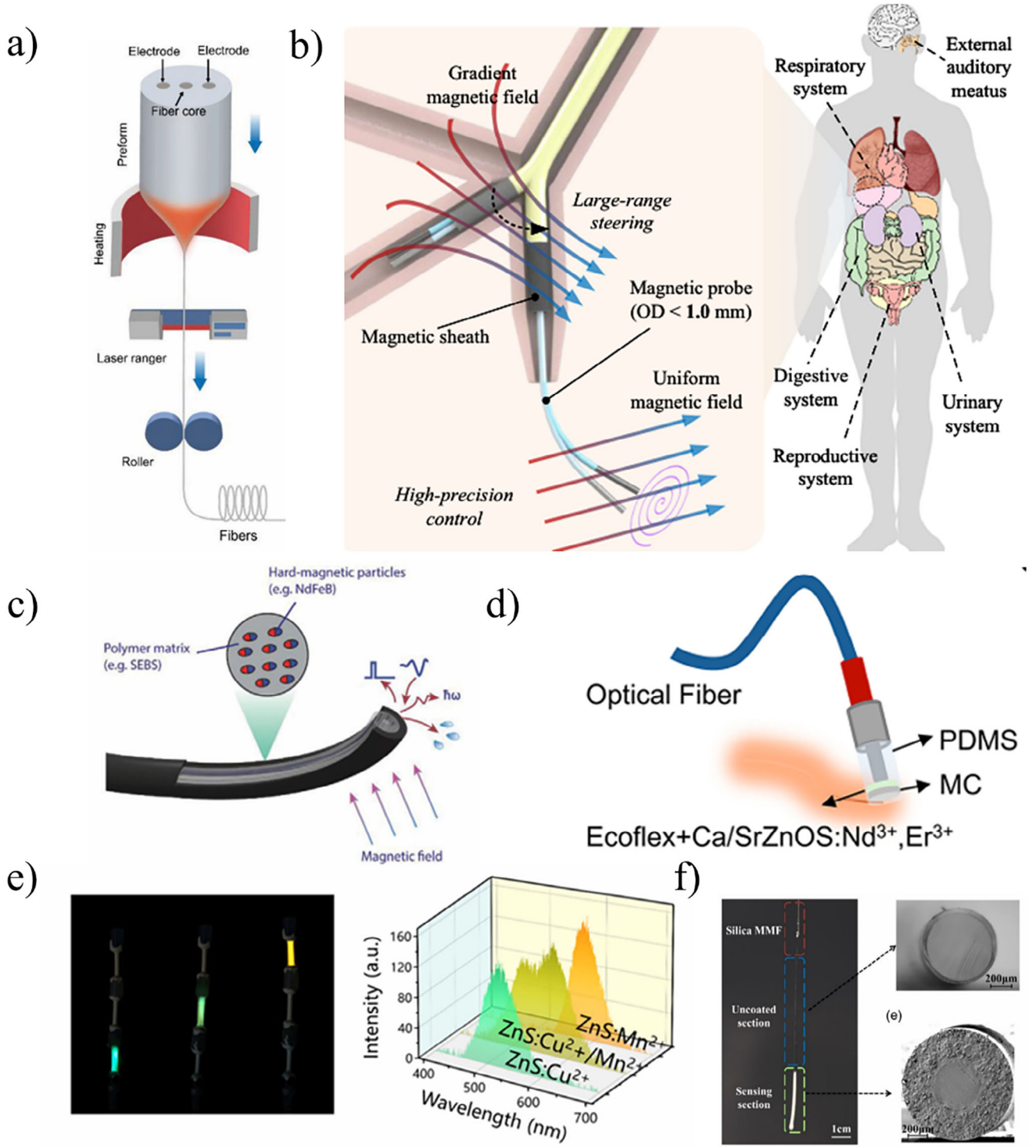

Figure 14. Integration and system expansion. a) A multimodal fiber with integrated platinum (Pt) electrodes, fabricated via thermal drawing. Reproduced with permission.[244] Copyright 2023, Wiley-VCH. b) A submillimeter continuum robot, driven by multi-sectional magnetic fields, that integrates the fiber in narrow anatomical channels for real-time diagnosis and treatment. Reproduced with permission.[245] Copyright 2024, Springer Nature. c) ML emission images with different optical fiber sections stretched. Reproduced with permission. Copyright 2023, Wiley-VCH. d) Propagation loss of the optical fiber measured in the air using the cutback method. Reproduced with permission.[10] Copyright 2025, Wiley-VCH. e) Mechanoluminescence (ML) emission images and corresponding spectra collected from a stretched optical fiber, demonstrating the conversion of mechanical energy into an optical signal. Reproduced with permission.[246] Copyright 2023, Wiley-VCH. f) A plan view and cross-sectional images of the self-powered, stretchable ML optical fiber sensor. Reproduced with permission.[247] Copyright 2021, Wiley-VCH.

the next generation of precision diagnostic and intelligent therapeutic tools.

Building upon the continuous development of materials, structures, and multimodal sensing capabilities, a more transformative frontier lies in the construction of closed-loop systems. This direction is dedicated to the deep integration of real-time sensing, decision-making analysis, and precision intervention functionalities, aiming to achieve an autonomous sense-decide-execute workflow. This represents a critical shift from passive monitoring tools to active theranostic platforms and stands as the core development direction for the future of precision medicine and intelligent interaction.

Neuromodulation is a quintessential field that showcases the potential of closed-loop systems. For instance, Du et al.[244] proposed a closed-loop optogenetic modulation system (CLOMs) based on a multifunctional fiber-optic probe. By integrating optical stimulation and electrophysiological recording functions, the system established a complete sense-decide-intervene paradigm in an epileptic mouse model. Its multimodal probe continuously monitors neural electrical signals in the hippocampus (sensing), combines this with a deep-learning algorithm to rapidly identify seizure precursors (decision-making), and automatically triggers optical stimulation to suppress the abnormal discharge (intervention), achieving an episode suppression rate as high as 86%. This work provides a clear technical framework for the automated, personalized treatment of neurodegenerative diseases (Figure 14a).

The closed-loop concept is equally applicable to precision drug delivery and synergistic therapy. Zhang et al.[27] designed a drug delivery system that integrates a temperature-responsive hydrogel with a built-in fiber-optic sensor. This system can trigger drug release at a tumor site using a localized photothermal effect while simultaneously monitoring the drug release dynamics and local temperature in real-time via the fiber sensor. This real-time feedback mechanism creates a treatment-monitoring closed loop that significantly enhances the efficiency and controllability of targeted drug delivery, achieving complete tumor eradication in a mouse model and offering a precisely controllable, closed-loop therapeutic platform for cancer treatment.

Applying the closed-loop philosophy to anatomically complex in vivo environments, however, places higher demands on the integration and flexibility of the execution platform. To address this, Zhang et al.[245] developed a sub-millimeter-scale fiber-optic continuum robot that integrates imaging, high-precision motion, and multifunctional operational capabilities. The robot achieves high-precision navigation via a magnetic actuation system and utilizes real-time imaging feedback for path planning and target localization (Figure 14b). In ex vivo trials, it successfully navigated to narrow passages such as the terminal bronchioles of the lung and performed various operations, including sampling, drug delivery, and laser ablation. Through the synergy of real-time imaging with precise navigation and intervention, this research lays a critical platform foundation for establishing a closed-loop, theranostic working model in difficult-to-reach areas within the body.

Additionally, the future development of fiber-optic sensing systems, especially for applications involving long-term implantation and imperceptible wearables, is constrained by a critical engineering bottleneck: the reliance on external physical tethers. Therefore, a crucial frontier dimension lies in investigating the integration of miniature energy harvesting and wireless communication technologies into fiber-optic systems, with the goal of constructing untethered or self-powered systems that require no external power sources or data lines.

A straightforward strategy is to harvest mechanical energy from the surrounding environment. Self-powered optical fibers based on mechanoluminescence are a prime example of this direction. For instance, Liang et al.[247] developed a tensile strain sensor based on an elastomeric optical fiber and a ZnS:Cu mechanoluminescent material. In their design, mechanical deformation can be directly converted into an optical signal without the need for any external light source or power supply (Figure 14f). Building on this, Zhou et al.[246] further extended this technique to distributed sensing. By employing multiple mechanoluminescent (ML) materials and combining wavelength- and time-domain demodulation, they achieved the simultaneous identification of both the magnitude and location of strain on a single fiber. These two studies jointly demonstrate the feasibility of using mechanical energy to directly drive an optical signal, offering a highly attractive self-powered solution for wearable devices and implantable strain monitoring (Figure 14e).

Besides harvesting mechanical energy from the environment, another approach is to enable the optoelectronic device itself to directly draw energy from the light signal it is detecting. This concept of light-driven power can be more tightly integrated into the optoelectronic device itself. Yang et al.[248] proposed an all-fiber self-powered photodetector integrated onto a fiber facet. By constructing a graphene/palladium selenide (Graphene/$PdSe_2$) van der Waals heterojunction, they utilized its built-in electric field to achieve a photovoltaic effect, allowing the detector to operate without an external bias voltage. This design enables the device to harvest the energy required for its operation directly from the light signal being detected, offering a new path toward achieving localized, passive operation for node devices in fiber-optic communication and sensing systems.

In summary, whether through the harvesting of ambient mechanical energy or the on-site conversion of energy from light signals, wireless and self-powered technologies are becoming a definitive development trend in the field of fiber-optic sensing. These strategies fundamentally solve the wiring and power supply challenges that have hindered traditional sensing systems in long-term, non-disruptive applications. They lay the foundation for the development of the next generation of fully implantable medical devices, smart textiles, and distributed structural health monitoring networks.

9.3. Bionic Intelligence and Biological Integration

As the structure and functionality of fiber-optic systems become increasingly complex, a frontier dimension that runs through the entire workflow of design, control, and data analysis is emerging: the deep integration of artificial intelligence (AI). AI is evolving from a conventional post-processing tool for data into a core engine capable of participating in system inverse design, real-time dynamic control, and complex signal interpretation. This shift provides a new paradigm for solving high-dimensional, nonlinear problems that are intractable with traditional methods.

First, at the level of data interpretation, AI can efficiently extract valid information from complex sensor signals with low signal-to-noise ratios. For example, Zaidi et al.[249] utilized a bilayer neural network (BNN) to directly process the full-wavelength spectrum from a multimode interference (MMI) sensor. Without the need for traditional feature extraction, they successfully resolved the signal ambiguity that occurs during high-to-low refractive index transitions, achieving a prediction accuracy of 99.7%. Similarly, Li et al.[250] designed a bionic fiber-optic tactile sensor that used a cascaded neural network (BP-ELM) to decouple the coupled signals from multiple fiber Bragg gratings, enabling the simultaneous and precise perception of both tactile position and pressure magnitude. These studies demonstrate that AI can significantly simplify the hardware structure of sensors by shifting complexity to the software level, thereby enhancing the robustness and intelligence of the system.

Second, at the level of system design, AI is subverting the traditional forward design-and-verify model. Mahmoud et al.[251] proposed an inverse design paradigm based on reinforcement learning (RL), where an AI agent autonomously explores a multi-dimensional parameter space. This approach successfully improved the dispersion performance of a photonic crystal fiber by 41.8% and increased the convergence speed by nearly 20-fold compared to conventional algorithms (**Figure 15a**). In the field of computational imaging, the physics-informed neural network (ASNet) proposed by Tang et al.[252] can accurately reconstruct phase information from the speckle pattern output of an optical fiber without requiring large-scale labeled datasets, effectively solving the inverse problem for complex optical systems. These works showcase the powerful capability of AI in automatically and efficiently finding optimal photonic structures and solutions (Figure 15b).

The most transformative potential of AI, however, is manifested in the real-time control of complex systems. Zhang et al.[257] developed an intelligent, controllable, ultrafast fiber laser system based on deep learning and an adaptive optimization algorithm. The system utilizes a recurrent neural network (LSTM) to rapidly establish the complex mapping relationship between the polarization controller and the output spectrum. This enables the system to automatically lock onto the optimal mode-locking state within 1.8 seconds and to quickly recover after mode-locking is lost. This provides an unprecedented level of system stability and autonomy for demanding applications in precision manufacturing and scientific research.

Building on these advances in real-time control, a natural extension lies in the domain of information processing. To cope with the rapidly increasing demand for ultrafast data handling and to overcome the inherent bottlenecks of conventional electronic computing, a highly forward-looking research direction is emerging: leveraging the specific physical structures of optical fibers and photonic devices to perform pre-processing or computation-like operations directly in the optical domain. This approach shifts part of the computational workload from the electronic to the photonic domain, exploiting the intrinsic advantage of light-speed propagation to dramatically reduce processing latency and energy consumption.

This concept is first embodied in the construction of fundamental optical computing units. For instance, Liu et al.[258] designed an all-optical signal processing device based on the integration of a multimode fiber and a phase-change material (GST). They used a specific length of multimode fiber to shape the input light beam into a Bessel-like field. This specific physical structure design can disperse the light energy, which, when combined with the non-linear reflection properties of the GST material, enables up to 19 levels of all-optical memory and matrix-vector multiplication (MVM) operations. The device performs the computation directly within the optical path, with a single-pulse switching time as low as 200 ns, demonstrating its potential for embedding physical-layer computation in high-speed optical communications and photonic neural networks.

Building on this, the concept has been further applied to solve a key challenge in high-speed fiber-optic communications: signal distortion. Lu et al.[253] proposed a high-dimensional fiber-optic communication system based on a reconfigurable silicon photonic processor. By using an integrated optical mesh, the system performs an optical-domain matrix inverse operation on the various spatial and polarization modes that have become mixed in the fiber, thereby completing a real-time descrambling of the signal before it even enters the electronic domain (Figure 15c). Similarly, to address the more complex issue of non-linear distortion, Huang et al.[259] designed a silicon photonic-electronic neural network that uses an array of micro-ring resonators (MRRs) as a tunable weight bank to perform real-time, non-linear compensation on the corrupted signal within the optical domain. These two works collectively point to a core trend: offloading complex signal processing algorithms (such as MIMO decoupling and non-linear equalization) from high-power, high-latency digital signal processors (DSPs) and having them executed instead by specially designed photonic physical structures. This computing with light paradigm can reduce processing energy consumption by over 90%, offering a highly attractive low-latency, high-efficiency solution for short-reach interconnects in data centers and long-haul submarine fiber-optic communications. By pre-embedding computational functions at the photonic hardware level, it is possible to fundamentally enhance the real-time response capabilities of a system, opening up new technological pathways for the development of next-generation ultra-high-speed optical communications, photonic artificial intelligence, and real-time sensing and analysis.

Additionally, the development of future implantable and interactive devices is driving a profound paradigm shift in materials science: a move away from pursuing traditional, passive biocompatibility toward designing active biofunctionality. This new approach aims to develop functionalized materials and devices that are not merely tolerated by the biological system but can become active participants, capable of exchanging information or substances with the physiological environment.

The overarching strategy in this direction is the deep integration of micro- and nano-structured fiber-optic probes with functional materials. As described by Yu et al.,[260] by integrating materials such as gold nanoparticles, graphene oxide, or metal-organic frameworks onto an optical fiber and leveraging physical mechanisms like surface plasmon resonance (SPR), LSPR, and surface-enhanced Raman scattering (SERS), the fiber platform can be transformed from a passive information collector into a tool that actively interacts with its environment. These functionalized platforms can not only achieve high-sensitivity molecular detection

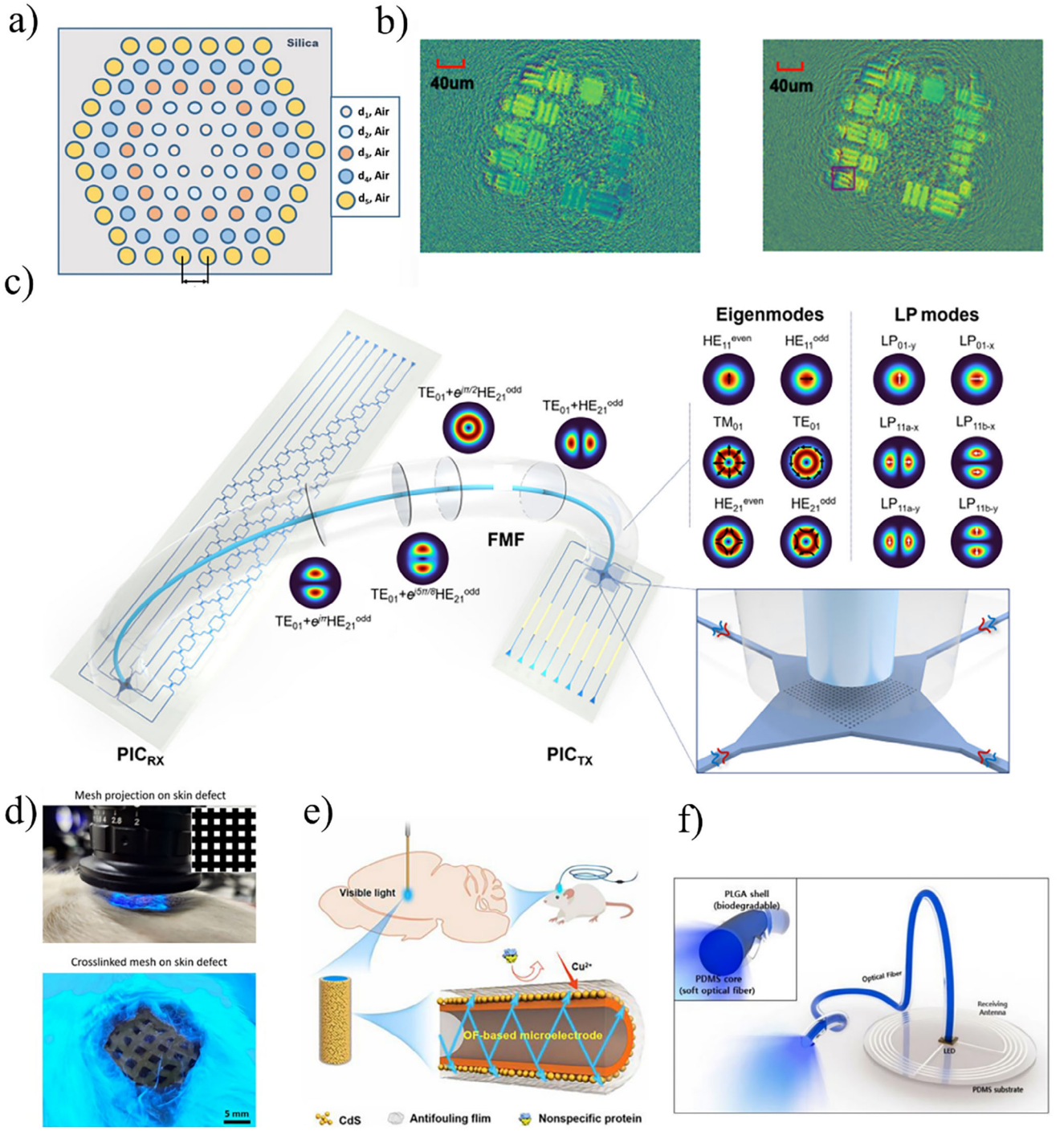

Figure 15. Bionic intelligence and biological integration. a) Schematic of a photonic crystal fiber (PCF) structure, detailing the different air hole diameters (d_1, d_2, d_3, d_4, d_5) and the pitch between adjacent holes. Reproduced with permission.[251] Copyright 2025, Elsevier. b) Experimental demonstration of high-resolution imaging through a fiber using a USAF-1951 target. The image captured via digital holography is computationally refocused to reconstruct a clear image of the target. Reproduced with permission.[252] Copyright 2025, Optica. c) System architecture for high-dimensional optical fiber communication using reconfigurable photonic integrated circuits at the transmitter (PICTX) and receiver (PICRX). The schematic also illustrates how optical signals in different modes can experience mixing during propagation through a circular-core few-mode fiber (FMF). Reproduced with permission.[253] Copyright 2024, Springer Nature. d) An illustration of fiber-assisted in situ bioprinting for wound repair. A pre-defined mesh pattern (inset, top panel) is projected onto a skin defect on a rat model, selectively photocrosslinking a GelMA-based bio-ink at 405 nm. The bottom panel shows the resulting hydrogel scaffold formed directly over the defect site. Reproduced with permission.[254] Copyright 2025, Wiley-VCH. e) Schematic diagram illustrating an in vivo assay performed using a specialized fiber-optic-based micro-electrode (SA-CM/CdS@ZnO/GOFME). Reproduced with permission.[255] Copyright 2023, Elsevier. f) Schematic of a soft, wireless optoelectronic device designed for implantable applications, featuring a biodegradable PLGA shell and a soft Polydimethylsiloxane (PDMS) core optical fiber. Reproduced with permission.[256] Copyright 2019, IEEE.

but also perform targeted interventional tasks, such as photothermal therapy or optogenetic modulation.

This philosophy is clearly reflected in specific device designs. In the realm of active chemical information exchange, Tao et al.[255] developed an implantable photoelectrochemical microelectrode. Its surface, coated with a sodium alginate-cell membrane composite, forms a hydrophilic interface that effectively reduces protein adsorption, achieving a high level of biocompatibility. More importantly, its integrated CdS/ZnO heterojunction, upon photoexcitation, enables photo-electro-chemical signal transduction with the surrounding brain tissue, thereby facilitating the in-situ monitoring of dynamic changes in Cu^{2+} (Figure 15e).

In the area of active biomechanical interaction and multifunctional integration, the hybrid neural probe developed by Park et al.[261] provides another excellent example. By embedding polymer fibers within a hydrogel matrix, they endowed the device with adaptive stiffness. The probe is rigid upon insertion but becomes soft after hydrating in vivo, allowing it to match the mechanical modulus of the brain tissue. This minimizes chronic tissue stress and the associated immune response. This intelligent physical response at the material level, combined with its integrated electrical, optical, and fluidic channels, enables stable, long-term neural signal recording and modulation. It serves as a classic example of enhancing biofunctionality through the active optimization of the physical interface.

Beyond serving as an interface for sensing and interaction, fiber-optic technology is demonstrating its immense potential as an active tool in regenerative medicine. In this emerging dimension, the optical fiber is no longer just a carrier of information but is directly involved in the fabrication of tissue-engineering constructs, guiding cell behavior, and serving as an energy delivery platform to modulate the tissue regeneration process.

A key direction is the use of optical fibers to achieve the precise fabrication of tissue-engineering scaffolds. For example, the fiber-assisted bioprinting (OAB) technique developed by Lee et al.[1] integrates an optical fiber into the printing nozzle, enabling the in situ and uniform photocrosslinking of the bioink. This allows for precise control over the scaffold's mechanical properties and micro-topography, which effectively guides the directed differentiation of stem cells. Building on this, the image-guided fiber system (FaSt-Light) proposed by Chansoria et al.[254] uses a fiber bundle to project customized light patterns into deep tissue, achieving in situ and minimally invasive bio-fabrication directly at the defect site. These two works jointly showcase the value of optical fibers as high-precision manufacturing tools for constructing tissue-engineering scaffolds with complex, biomimetic structures, both in vitro and in situ (Figure 15d).

In addition to its role as a manufacturing tool, an implantable optical fiber can itself serve as a therapeutic platform to directly modulate the regeneration process in vivo. The research by Zuo et al.[262] provides a case in point. They developed an implantable diffusing optical fiber to deliver NIR light directly and precisely to damaged spinal cord tissue. Through the effect of photobiomodulation (PBM), this technique provides a highly efficient means of energy intervention to promote neural repair without causing tissue damage. This study shifts the role of the optical fiber from a scaffold-builder to a functionalized implant, actively guiding and promoting endogenous tissue regeneration through the controllable delivery of energy.

While implantable optical fibers open up new possibilities for directly guiding tissue regeneration, their long-term presence in the body inevitably raises concerns regarding secondary removal surgeries and chronic foreign-body reactions To avoid the trauma and risks associated with secondary surgery for implant removal and to mitigate long-term foreign body reactions, a significant research direction is the development of transient optical devices that can be safely degraded and absorbed in vivo after completing their pre-set tasks. These devices are ingeniously designed in terms of both material selection and structure, aiming to unify functionality with a pre-determined operational lifetime.

For example, starting from the basic materials, Agnieszka et al.[256] fabricated optical fibers with excellent performance from biodegradable poly (D, L-lactide) (PDLLA) using a thermal drawing process. Not only did these fibers achieve the lowest optical loss (0.11 dB cm^{-1}) ever reported for a bioresorbable material, but their degradation rate could also be precisely tuned by adjusting the fiber's dimensions to match the therapeutic window of different clinical scenarios (Figure 15f). In another study, Han et al.[263] cleverly utilized degradation properties to solve an engineering challenge. They developed a composite optical fiber for optogenetics, in which a rigid, degradable outer shell (PLGA) provided sufficient stiffness for insertion. This shell would then completely degrade within a few days post-implantation, leaving only an extremely soft optical fiber (PDMS) inside the brain. This design minimizes long-term mechanical damage and thermal effects. Together, these studies show that biodegradability has evolved from a simple exit strategy into an active design element. Through precise control over material degradation kinetics or by leveraging the degradation process to achieve a dynamic evolution of the device's physical properties, transient optical fibers offer safer and smarter solutions for clinical applications that require short-term, precise light-based interventions, such as photodynamic therapy, post-operative monitoring, and chronic neuromodulation.

9.4. Challenges and Perspectives

Despite the exciting prospects for engineered optical fibers in biomedicine, significant challenges at the levels of fundamental science, engineering, and technology, and clinical translation must be overcome before their full potential can be released for reliable clinical applications.

On the level of fundamental science, a deeper understanding of the interaction mechanisms at the complex interface of biophotonic intelligent systems is still required. When a functional optical fiber is implanted into living tissue, it forms not merely a simple physical contact surface but rather a dynamic and evolving complex system. How does the tissue microenvironment affect the sensing accuracy and optical performance of the fiber over the long term? Conversely, how do the fiber materials and the photonic energy they deliver influence cell behavior, tissue remodeling, and even the immune response? Answering these questions will demand interdisciplinary efforts to establish more sophisticated theoretical models that can predict and guide the

long-term stability and functionality of optical fibers in complex physiological environments, thereby enabling a leap from passive implantation to active adaptation.

The challenges at the engineering and technology level are equally pronounced, with the high-precision, scalable integration of heterogeneous materials and advanced manufacturing techniques remaining key bottlenecks. Traditional fiber drawing techniques are well-suited for materials with matched thermodynamic properties. However, next-generation biomedical fibers require the integration of materials with vastly different properties—such as inorganic glasses, flexible polymers, hydrogels, metal electrodes, and semiconductor nanoparticles—into a single fiber with micron- or even nanometer-scale precision. The core engineering problem that will determine the widespread adoption of this technology is how to achieve the co-drawing or multi-step integration of these dissimilar materials while ensuring structural integrity and functionality, and how to transition from laboratory prototypes to repeatable, low-cost, large-scale production.

Ultimately, the challenges on the path to practical use are concentrated at the clinical translation level. This requires the establishment of standardized evaluation systems, the completion of long-term biosafety validation, and the construction of corresponding ethical and regulatory frameworks. Currently, the performance evaluation methods for different biomedical fiber platforms vary, lacking uniform standards and making direct comparisons difficult. Furthermore, for devices intended for long-term implantation, issues such as their slow degradation processes, potential biotoxicity, and the possibility of inducing chronic inflammation must be systematically validated through large-scale, long-term animal studies and eventually clinical trials. These innovative technologies, particularly those involving neuromodulation and gene editing, must be advanced under the guidance of clear ethical norms and regulatory policies to ensure they can benefit human health safely and compliantly.

Acknowledgements

Y.L., S.Z. and W.L. contributed equally to this work. This work was supported by National Natural Science Foundation of China (Nos. 81930048 and 82330061), Guangdong Science and Technology Commission (No. 2019BT02 × 105), Hong Kong Research Grant Council (Nos. 15125724, 15217721 and C7074-21GF), Shenzhen Science and Technology Innovation Commission (No. JCYJ20220818100202005), and Hong Kong Polytechnic University (Nos. P0039517, P0043485, P0045762, and P0048314).

Conflict of Interest

The authors declare no conflict of interest.

Keywords

biomaterial, biomedical optics, deep tissue, endoscopic imaging, optical fiber

Received: September 1, 2025
Revised: December 22, 2025
Published online: March 5, 2026

[1] Q. Zhang, B. Song, Y. Xu, Y. Yang, J. Ji, W. Cao, J. Lu, J. Ding, H. Cao, B. Chu, J. Hong, H. Wang, Y. He, *Nat. Commun.* **2023**, *14*, 2331. https://doi.org/10.1038/s41467-023-37827-9.
[2] W. Wang, Y. Pan, Y. Shui, T. Hasan, I. M. Lei, S. G. S. Ka, T. Savin, S. Velasco-Bosom, Y. Cao, S. B. P. McLaren, Y. Cao, F. Xiong, G. G. Malliaras, Y. Y. S. Huang, *Nat. Electron.* **2024**, *7*, 586. https://doi.org/10.1038/s41928-024-01174-4.
[3] H. Bai, S. Li, J. Barreiros, Y. Tu, C. R. Pollock, R. F. Shepherd, *Science* **2020**, *370*, 848. https://doi.org/10.1126/science.aba5504.
[4] N. Gupta, H. Cheung, S. Payra, G. Loke, J. Li, Y. Zhao, L. Balachander, E. Son, V. Li, S. Kravitz, S. Lohawala, J. Joannopoulos, Y. Fink, *Nature* **2025**, *639*, 79. https://doi.org/10.1038/s41586-024-08568-6.
[5] W. Yang, S. Lin, W. Gong, R. Lin, C. Jiang, X. Yang, Y. Hu, J. Wang, X. Xiao, K. Li, Y. Li, Q. Zhang, J. S. Ho, Y. Liu, C. Hou, H. Wang, *Science* **2024**, *384*, 74.
[6] A. Sahasrabudhe, L. E. Rupprecht, S. Orguc, T. Khudiyev, T. Tanaka, J. Sands, W. Zhu, A. Tabet, M. Manthey, H. Allen, G. Loke, M. J. Antonini, D. Rosenfeld, J. Park, I. C. Garwood, W. Yan, F. Niroui, Y. Fink, A. Chandrakasan, D. V. Bohorquez, P. Anikeeva, *Nat. Biotechnol.* **2024**, *42*, 892. https://doi.org/10.1038/s41587-023-01833-5.
[7] Z. Wang, Z. Wang, D. Li, C. Yang, Q. Zhang, M. Chen, H. Gao, L. Wei, *Nature* **2024**, *626*, 72. https://doi.org/10.1038/s41586-023-06946-0.
[8] X. Liu, S. Rao, W. Chen, K. Felix, J. Ni, A. Sahasrabudhe, S. Lin, Q. Wang, Y. Liu, Z. He, J. Xu, S. Huang, E. Hong, T. Yau, P. Anikeeva, X. Zhao, *Nat. Methods* **2023**, *20*, 1802. https://doi.org/10.1038/s41592-023-02020-9.
[9] Y. Liang, W. Fu, Q. Li, X. Chen, H. Sun, L. Wang, L. Jin, W. Huang, B. O. Guan, *Nat. Commun.* **2022**, *13*, 7604. https://doi.org/10.1038/s41467-022-35259-5.
[10] P. Zheng, Y. Xiao, P. Xiong, S. Su, A. Yang, X. Wang, S. Xu, P. Shao, Z. Zhou, S. Wu, E. Song, J. Gan, D. Chen, *Adv. Funct. Mater.* **2025**, *35*.
[11] H. Liu, Y. He, J. Luo, N. Li, T. Wang, E. Song, Q. Guo, Z. Ma, Z. Yang, J. Gan, Z. Yang, *Adv. Mater.* **2025**, *37*, 05776. https://doi.org/10.1002/adma.202505776.
[12] A. Cianciosi, M. Pfeiffle, P. Wohlfahrt, S. Nurnberger, T. Jungst, *Adv. Sci. (Weinh)* **2024**, *11*, 2403049.
[13] J. Yao, Z. Yu, Y. Gao, B. Wang, Z. Wang, T. Zhong, B. Pan, H. Li, H. Hui, W. Zheng, Q. Zhan, P. Lai, *Nano Lett.* **2025**, *25*, 5485. https://doi.org/10.1021/acs.nanolett.5c01030.
[14] Y. Liu, P. Lai, C. Ma, X. Xu, A. A. Grabar, L. V. Wang, *Nat. Commun.* **2015**, *6*, 5904. https://doi.org/10.1038/ncomms6904.
[15] P. Lai, L. Wang, J. W. Tay, L. V. Wang, *Nat. Photonics* **2015**, *9*, 126. https://doi.org/10.1038/nphoton.2014.322.
[16] R. Li, D. Fu, X. Yuan, G. Niu, Y. Fan, J. Shi, Y. Yang, J. Ye, J. Han, Y. Kang, X. Ji, *Small* **2024**, *20*, 2404741. https://doi.org/10.1002/smll.202404741.
[17] S. Haziza, R. Chrapkiewicz, Y. Zhang, V. Kruzhilin, J. Li, J. Li, G. Delamare, R. Swanson, G. Buzsaki, M. Kannan, G. Vasan, M. Z. Lin, H. Zeng, T. L. Daigle, M. J. Schnitzer, *Cell* **2025**, *188*, 4401.e31. https://doi.org/10.1016/j.cell.2025.06.028.
[18] W. Li, Z. Lu, Y. Zhang, L. Zhu, J. Zhang, Y. Zhang, M. Wu, X. Zhou, J. Xiong, *Adv. Funct. Mater.* **2025**, *35*, 2423596. https://doi.org/10.1002/adfm.202423596.
[19] A. Orth, M. Ploschner, E. R. Wilson, I. S. Maksymov, B. C. Gibson, *Sci. Adv.* **2019**, *5*, aav1555. https://doi.org/10.1126/sciadv.aav1555.
[20] W. Li, W. Liu, Y. Deng, Y. Chen, H. Yang, Q. Chen, J. Zheng, H. Xiao, Z. Chen, Z. Pan, P. Ma, Z. Wang, L. Si, S. Xu, J. Chen, *Light Sci Appl* **2025**, *14*, 271. https://doi.org/10.1038/s41377-025-01956-1.
[21] A. Shanker, J. E. Froch, S. Mukherjee, M. Zhelyeznyakov, S. L. Brunton, E. J. Seibel, A. Majumdar, *Light Sci Appl* **2024**, *13*, 305. https://doi.org/10.1038/s41377-024-01587-y.

[22] R. Wang, R. Wang, C. Dou, S. Yang, R. Gnanasambandam, A. Wang, Z. J. Kong, *Nat. Commun.* **2024**, *15*, 7568. https://doi.org/10.1038/s41467-024-51235-7.
[23] T. A. La, O. Ulgen, R. Shnaiderman, V. Ntziachristos, *Nat. Commun.* **2024**, *15*, 7521. https://doi.org/10.1038/s41467-024-51497-1.
[24] J. Pan, Q. Wang, S. Gao, Z. Zhang, Y. Xie, L. Yu, L. Zhang, *Opto-Electronic Advances* **2023**, *6*, 230076. https://doi.org/10.29026/oea.2023.230076.
[25] *Opto-Electronic Advances* **2025**, *8*, 250026. https://doi.org/10.29026/oea.2025.250026.
[26] B. Kiraly, D. Balazsfi, I. Horvath, N. Solari, K. Sviatko, K. Lengyel, E. Birtalan, M. Babos, G. Bagamery, D. Mathe, K. Szigeti, B. Hangya, *Nat. Commun.* **2020**, *11*, 4686. https://doi.org/10.1038/s41467-020-18472-y.
[27] Y. Zhang, J. Zheng, F. Jin, J. Xiao, N. Lan, Z. Xu, X. Yue, Z. Li, C. Li, D. Cao, Y. Wang, W. Zhong, Y. Ran, B. O. Guan, *Light Sci Appl* **2024**, *13*, 228. https://doi.org/10.1038/s41377-024-01586-z.
[28] X. Hu, J. Zhao, J. E. Antonio-Lopez, R. A. Correa, A. Schulzgen, *Light Sci Appl* **2023**, *12*, 125. https://doi.org/10.1038/s41377-023-01183-6.
[29] J. T. Li, B. Chang, J. T. Du, T. Tan, Y. Geng, H. Zhou, Y. P. Liang, H. Zhang, G. F. Yan, L. M. Ma, Z. L. Ran, Z. N. Wang, B. C. Yao, Y. J. Rao, *Sci. Adv.* **2024**, *10*, adf8666. https://doi.org/10.1126/sciadv.adf8666.
[30] R. Jha, P. Mishra, S. Kumar, *Biosens. Bioelectron.* **2024**, *254*, 116232. https://doi.org/10.1016/j.bios.2024.116232.
[31] H. Qiu, Y. Yao, Y. Dong, J. Tian, *Biosens. Bioelectron.* **2024**, *255*, 116265. https://doi.org/10.1016/j.bios.2024.116265.
[32] B. Cao, Y. Huang, L. Chen, W. Jia, D. Li, Y. Jiang, *Biosens. Bioelectron.* **2024**, *259*, 116378. https://doi.org/10.1016/j.bios.2024.116378.
[33] H. Cao, T. Čižmár, S. Turtaev, T. Tyc, S. Rotter, *Adv. Opt. Photonics* **2023**, *15*, 524. https://doi.org/10.1364/AOP.484298.
[34] D. Sheng, Y. Chang, Z. Han, Y. Liu, H. Tian, *Opt. Express* **2025**, *33*, 30686. https://doi.org/10.1364/OE.568157.
[35] P. Xu, B. Cui, Y. Bu, H. Wang, X. Guo, P. Wang, Y. R. Shen, L. Tong, *Science* **2021**, *373*, 187. https://doi.org/10.1126/science.abh3754.
[36] H. Yu, X. Liu, Y. Zhang, J. Shen, X. Liu, S. Liu, X. Wang, B. Sun, H. Du, L. Xu, B. Zou, J. Ding, Q. Xu, L. Zhang, B. Wang, *Sci Robot* **2025**, *10*, adt0720. https://doi.org/10.1126/scirobotics.adt0720.
[37] S. H. Yun, S. J. J. Kwok, *Nat. Biomed. Eng.* **2017**, *1*, 0008. https://doi.org/10.1038/s41551-016-0008.
[38] V. Ntziachristos, *Nat. Methods* **2010**, *7*, 603. https://doi.org/10.1038/nmeth.1483.
[39] R. Horstmeyer, H. Ruan, C. Yang, *Nat. Photonics* **2015**, *9*, 563. https://doi.org/10.1038/nphoton.2015.140.
[40] S. Zheng, W. Li, W. Pang, T. Zhong, P. Lai, *Advanced Photonics* **2024**, *6*, 060504. https://doi.org/10.1117/1.AP.6.6.060504.
[41] J. Zhu, X. Liu, Z. Liu, Y. Deng, J. Xu, K. Liu, R. Zhang, X. Meng, P. Fei, T. Yu, D. Zhu, *Nat. Commun.* **2024**, *15*, 8303. https://doi.org/10.1038/s41467-024-52560-7.
[42] S. Nizamoglu, M. C. Gather, M. Humar, M. Choi, S. Kim, K. S. Kim, S. K. Hahn, G. Scarcelli, M. Randolph, R. W. Redmond, S. H. Yun, *Nat. Commun.* **2016**, *7*, 10374. https://doi.org/10.1038/ncomms10374.
[43] Y. Hu, P. Minzioni, J. Hui, S. H. Yun, A. K. Yetisen, *Adv. Opt. Mater.* **2024**, *12*, 2400478. https://doi.org/10.1002/adom.202400478.
[44] L. Tingye, *Proc. IEEE* **1980**, *68*, 1175. https://doi.org/10.1109/PROC.1980.11825.
[45] F. Pisano, M. Pisanello, S. J. Lee, J. Lee, E. Maglie, A. Balena, L. Sileo, B. Spagnolo, M. Bianco, M. Hyun, M. De Vittorio, B. L. Sabatini, F. Pisanello, *Nat. Methods* **2019**, *16*, 1185. https://doi.org/10.1038/s41592-019-0581-x.
[46] M. Lin, H. Hu, S. Zhou, S. Xu, *Nat. Rev. Mater.* **2022**, *7*, 850. https://doi.org/10.1038/s41578-022-00427-y.
[47] S. Wang, B. Li, F. Zhang, *ACS Cent. Sci.* **2020**, *6*, 1302.
[48] W. T. Huang, V. Rajendran, M. H. Chan, M. Hsiao, H. Chang, R. S. Liu, *Adv. Opt. Mater.* **2022**, *11*, 2202061. https://doi.org/10.1002/adom.202202061.
[49] S. Jiang, D. C. Patel, J. Kim, S. Yang, W. A. Mills, 3rd, Y. Zhang, K. Wang, Z. Feng, S. Vijayan, W. Cai, A. Wang, Y. Guo, I. F. Kimbrough, H. Sontheimer, X. Jia, *Nat. Commun.* **2020**, *11*, 6115. https://doi.org/10.1038/s41467-020-19946-9.
[50] K. C. Kao, G. A. Hockham, *PROC. IEE* **1966**, *113*, 1151.
[51] A. C. Peacock, U. J. Gibson, J. Ballato, *Adv. Phys.: X* **2016**, *1*, 114.
[52] M. S. A. Gandhi, S. Chu, K. Senthilnathan, P. R. Babu, K. Nakkeeran, Q. Li, *Appl. Sci.* **2019**, *9*, 949.
[53] P. Vaiano, B. Carotenuto, M. Pisco, A. Ricciardi, G. Quero, M. Consales, A. Crescitelli, E. Esposito, A. Cusano, *Laser Photonics Rev.* **2016**, *10*, 922. https://doi.org/10.1002/lpor.201600111.
[54] K. Schuster, S. Unger, C. Aichele, F. Lindner, S. Grimm, D. Litzkendorf, J. Kobelke, J. Bierlich, K. Wondraczek, H. Bartelt, *Adv. Opt. Technol.* **2014**, *3*, 447.
[55] J. G. Fujimoto, *Nat. Biotechnol.* **2003**, *21*, 1361. https://doi.org/10.1038/nbt892.
[56] S. Yoon, M. Kim, M. Jang, Y. Choi, W. Choi, S. Kang, W. Choi, *Nat. Rev. Phys.* **2020**, *2*, 141. https://doi.org/10.1038/s42254-019-0143-2.
[57] S. Turtaev, I. T. Leite, T. Altwegg-Boussac, J. M. P. Pakan, N. L. Rochefort, T. Cizmar, *Light Sci Appl* **2018**, *7*, 92. https://doi.org/10.1038/s41377-018-0094-x.
[58] Y. Wang, Y. Zhou, L. Qi, Y. Zhang, *Adv. Funct. Mater.* **2025**.
[59] E. Pshenay-Severin, H. Bae, K. Reichwald, G. Matz, J. Bierlich, J. Kobelke, A. Lorenz, A. Schwuchow, T. Meyer-Zedler, M. Schmitt, B. Messerschmidt, J. Popp, *Light Sci Appl* **2021**, *10*, 207. https://doi.org/10.1038/s41377-021-00648-w.
[60] B. A. Flusberg, E. D. Cocker, W. Piyawattanametha, J. C. Jung, E. L. M. Cheung, M. J. Schnitzer, *Nat. Methods* **2005**, *2*, 941. https://doi.org/10.1038/nmeth820.
[61] K. Sui, M. Meneghetti, R. W. Berg, C. Markos, *Opt. Express* **2023**, *31*, 21563. https://doi.org/10.1364/OE.493602.
[62] H. Ma, A. K. Y. Jen, L. R. Dalton, *Adv. Mater.* **2002**, *14*, 1339.
[63] Kenry, Y. D., B. Liu, *Adv. Mater.* **2018**, *30*, 1802394. https://doi.org/10.1002/adma.201802394.
[64] E. L. Schmidt, Z. Ou, E. Ximendes, H. Cui, C. H. C. Keck, D. Jaque, G. Hong, *Nature Reviews Methods Primers* **2024**, *4*. https://doi.org/10.1038/s43586-024-00301-x.
[65] D. Huang, E. A. Swanson, C. P. Lin, J. S. Schuman, W. G. Stinson, W. Chang, M. R. Hee, T. Flotte, K. Gregory, C. A. Puliafito, et al., *Science* **1991**, *254*, 1178.
[66] K. Mondal, *Optical and Quantum Electronics* **2024**, *56*, 1726. https://doi.org/10.1007/s11082-024-07616-9.
[67] Y. Du, S. Turtaev, I. T. Leite, A. Lorenz, J. Kobelke, K. Wondraczek, T. Čižmár, *Light: Advanced Manufacturing* **2022**, *3*, 29.
[68] T. Zhong, Z. Qiu, Y. Wu, J. Guo, H. Li, Z. Yu, S. Cheng, Y. Zhou, J. Zhu, J. Tian, L. Sun, P. Lai, *Adv. Photonics Res.* **2021**, *3*, 2100231. https://doi.org/10.1002/adpr.202100231.
[69] S. K. Turitsyn, J. E. Prilepsky, S. T. Le, S. Wahls, L. L. Frumin, M. Kamalian, S. A. Derevyanko, *Optica* **2017**, *4*, 307. https://doi.org/10.1364/OPTICA.4.000307.
[70] G. P. Agrawal, *J. Opt. Soc. Am. B* **2011**, *28*, 12.
[71] P. J. Winzer, D. T. Neilson, A. R. Chraplyvy, *Opt. Express* **2018**, *26*, 24190. https://doi.org/10.1364/OE.26.024190.
[72] M. E. Lines, *Science* **1984**, *226*, 663. https://doi.org/10.1126/science.226.4675.663.
[73] Y. Koike, K. Koike, *J. Polym. Sci., Part B: Polym. Phys.* **2010**, *49*, 2. https://doi.org/10.1002/polb.22170.
[74] I. S. Martins, H. F. Silva, E. N. Lazareva, N. V. Chernomyrdin, K. I. Zaytsev, L. M. Oliveira, V. V. Tuchin, *Biomed. Opt. Express* **2023**, *14*, 249.

[75] M. Woerdemann, C. Alpmann, M. Esseling, C. Denz, *Laser Photonics Rev.* **2013**, *7*, 839. https://doi.org/10.1002/lpor.201200058.
[76] R. Nazempour, Q. Zhang, R. Fu, X. Sheng, *Materials (Basel)* **2018**, *11*, 1283.
[77] N. Jiang, R. Ahmed, A. A. Rifat, J. Guo, Y. Yin, Y. Montelongo, H. Butt, A. K. Yetisen, *Adv. Opt. Mater.* **2017**, *6*, 1701118. https://doi.org/10.1002/adom.201701118.
[78] D. Shan, C. Zhang, S. Kalaba, N. Mehta, G. B. Kim, Z. Liu, J. Yang, *Biomaterials* **2017**, *143*, 142. https://doi.org/10.1016/j.biomaterials.2017.08.003.
[79] M.-j. Yin, B. Gu, Q.-F. An, C. Yang, Y. L. Guan, K.-T. Yong, *Coord. Chem. Rev.* **2018**, *376*, 348. https://doi.org/10.1016/j.ccr.2018.08.001.
[80] W. M. Saeed, P. J. O'Brien, J. Yoshino, A. R. Restelli, A. J. Traynham, N. M. Fried, *Lasers Surg. Med.* **2023**, *55*, 886. https://doi.org/10.1002/lsm.23740.
[81] V. Andresen, S. Alexander, W. M. Heupel, M. Hirschberg, R. M. Hoffman, P. Friedl, *Curr. Opin. Biotechnol.* **2009**, *20*, 54. https://doi.org/10.1016/j.copbio.2009.02.008.
[82] J. Petrovic, F. Lange, D. Hohlfeld, *J. Neural Eng.* **2023**, *20*, 036007. https://doi.org/10.1088/1741-2552/accecf.
[83] R. Nazempour, B. Zhang, Z. Ye, L. Yin, X. Lv, X. Sheng, *Adv. Fiber Mater.* **2021**, *4*, 24. https://doi.org/10.1007/s42765-021-00092-w.
[84] J. Xiao, J. Jiang, J. Zhang, Y. Wang, B. Wang, *Opt. Express* **2022**, *30*, 35014. https://doi.org/10.1364/OE.469550.
[85] J. Feng, Printed Soft Optical Waveguides for Delivering Light into Deep Tissue **2020**.
[86] Y. Wang, S. Dai, *PhotoniX* **2021**, *2*, 9. https://doi.org/10.1186/s43074-021-00031-3.
[87] J. Guo, X. Liu, N. Jiang, A. K. Yetisen, H. Yuk, C. Yang, A. Khademhosseini, X. Zhao, S. H. Yun, *Adv. Mater.* **2016**, *28*, 10244.
[88] S. Shabahang, S. Kim, S. H. Yun, *Adv. Funct. Mater.* **2018**, *28*, 1706635. https://doi.org/10.1002/adfm.201706635.
[89] S. Reis-Dennis, *Monash Bioeth Rev* **2020**, *38*, 83.
[90] A. Gierej, T. Geernaert, S. Van Vlierberghe, P. Dubruel, H. Thienpont, F. Berghmans, *Materials (Basel)* **2021**, *14*, 1972.
[91] M. Klimczak, B. Siwicki, A. Heidt, R. Buczyński, *Photonics Res.* **2017**, *5*, 710. https://doi.org/10.1364/PRJ.5.000710.
[92] M. Calcerrada, C. García-Ruiz, M. González-Herráez, *Laser Photonics Rev.* **2015**, *9*, 604. https://doi.org/10.1002/lpor.201500045.
[93] M. Chemnitz, S. Junaid, M. A. Schmidt, *Laser Photonics Rev.* **2023**, *17*. https://doi.org/10.1002/lpor.202300126.
[94] Y. Ohishi, *Opt. Mater. Express* **2022**, *12*, 3990. https://doi.org/10.1364/OME.462792.
[95] J. Du, Q. Ma, B. Wang, L. Sun, L. Liu, *iScience* **2023**, *26*, 106796.
[96] W. Li, J. Liu, J. Wei, Z. Yang, C. Ren, B. Li, *Adv. Funct. Mater.* **2023**, *33*, 2213485.
[97] G. K. Park, S. H. Kim, K. Kim, P. Das, B. G. Kim, S. Kashiwagi, H. S. Choi, N. S. Hwang, *Theranostics* **2019**, *9*, 4255. https://doi.org/10.7150/thno.35606.
[98] G. Chen, Z. Yang, H. Pan, J. Zhang, Y. Guo, Z. Zhou, J. Zheng, Z. Zhang, R. Cao, K. Hou, M. Zhu, *Chem. Rev.* **2025**, *125*, 5991.
[99] T. Ermatov, J. S. Skibina, V. V. Tuchin, D. A. Gorin, *Materials (Basel)* **2020**, *13*, 921.
[100] Y. Xiong, F. Xu, *Advanced Photonics* **2020**, *2*, 064001. https://doi.org/10.1117/1.AP.2.6.064001.
[101] Y. Meng, Y. Chen, L. Lu, Y. Ding, A. Cusano, J. A. Fan, Q. Hu, K. Wang, Z. Xie, Z. Liu, Y. Yang, Q. Liu, M. Gong, Q. Xiao, S. Sun, M. Zhang, X. Yuan, X. Ni, *Light Sci Appl* **2021**, *10*, 235.
[102] K. Beaudette, N. Godbout, C. Boudoux, *J. Lightwave Technol.* **2019**, *37*, 5674. https://doi.org/10.1109/JLT.2019.2929926.
[103] J. C. Knight, T. A. Birks, P. S. J. Russell, D. M. Atkin, *Opt. Lett.* **1996**, *21*, 1547. https://doi.org/10.1364/OL.21.001547.
[104] D. K. W. Lam, B. K. Garside, *Appl. Opt.* **1981**, *20*, 440. https://doi.org/10.1364/AO.20.000440.
[105] M. Kirshenbaum, E. Seibel, *SPIE digital library* **2011**.
[106] A. M. Smith, *Appl. Opt.* **1978**, *17*, 52. https://doi.org/10.1364/AO.17.000052.
[107] Y. Liu, P. Yu, Y. Wu, Z. Wang, Y. Li, J. Liang, P. Lai, L. Gong, *Appl. Phys. Lett.* **2023**, *122*, 063701. https://doi.org/10.1063/5.0132123.
[108] R. Fan, L. Li, Y. Zheng, *Opt. Laser Technol.* **2024**, *175*, 110732. https://doi.org/10.1016/j.optlastec.2024.110732.
[109] J. Li, S. C. Warren-Smith, R. A. McLaughlin, H. Ebendorff-Heidepriem, *Biomed. Opt. Express* **2024**, *15*, 2392. https://doi.org/10.1364/BOE.517920.
[110] S. A. Vasquez-Lopez, R. Turcotte, V. Koren, M. Ploschner, Z. Padamsey, M. J. Booth, T. Cizmar, N. J. Emptage, *Light Sci Appl* **2018**, *7*, 110. https://doi.org/10.1038/s41377-018-0111-0.
[111] S. Ohayon, A. Caravaca-Aguirre, R. Piestun, J. J. DiCarlo, *Biomed. Opt. Express* **2018**, *9*, 1492. https://doi.org/10.1364/BOE.9.001492.
[112] M. S. Pochechuev, I. V. Fedotov, G. N. Martynov, M. A. Solotenkov, O. I. Ivashkina, O. S. Rogozhnikova, A. B. Fedotov, K. V. Anokhin, A. M. Zheltikov, *J Biophotonics* **2022**, *15*, 202200025. https://doi.org/10.1002/jbio.202200025.
[113] X. Zhuo, Y. Han, Y. Bian, A. Xu, H. Shen, *Adv. Opt. Mater.* **2023**, *12*, 2301613. https://doi.org/10.1002/adom.202301613.
[114] J. D. Shephard, A. Urich, R. M. Carter, P. Jaworski, R. R. J. Maier, W. Belardi, F. Yu, W. J. Wadsworth, J. C. Knight, D. P. Hand, *Front. Phys.* **2015**, *3*. https://doi.org/10.3389/fphy.2015.00024.
[115] D. Septier, G. Brévalle-Wasilewski, E. Lefebvre, N. G. Kumar, Y. J. Wang, A. Kaszas, H. Rigneault, A. Kudlinski, *IEEE J. Sel. Top. Quantum Electron.* **2024**, *30*, 6. https://doi.org/10.1109/JSTQE.2024.3411821.
[116] K. Zolnacz, R. Stephan, J. Dremel, K. Hausmann, M. Ließmann, M. Steinke, J. Czarske, R. Kuschmierz, *Light: Advanced Manufacturing* **2024**, *5*, 580.
[117] K. Charan, B. Li, M. Wang, C. P. Lin, C. Xu, *Biomed. Opt. Express* **2018**, *9*, 2304. https://doi.org/10.1364/BOE.9.002304.
[118] A. Perperidis, K. Dhaliwal, S. McLaughlin, T. Vercauteren, *Medical Image Analysis* **2020**, *62*, 101620. https://doi.org/10.1016/j.media.2019.101620.
[119] P. Roldán-Varona, C. A. Ross, L. Rodríguez-Cobo, J. M. López-Higuera, E. Gaughan, K. Dhaliwal, M. G. Tanner, R. R. Thomson, H. E. Parker, *APL Photonics* **2023**, *8*.
[120] J. Lich, T. Glosemeyer, J. Czarske, R. Kuschmierz, *Light: Advanced Manufacturing* **2024**, *5*.
[121] T. Z. N. Sokkar, W. A. Ramadan, M. A. Shams El-Din, H. H. Wahba, S. S. Aboleneen, *Optics and Lasers in Engineering* **2014**, *53*, 133. https://doi.org/10.1016/j.optlaseng.2013.09.002.
[122] N. Roy, S. DasMahapatra, M. Tiwari, *Materials Today: Proceedings* **2023**, *79*, 204.
[123] R. Olshansky, D. B. Keck, *Appl. Opt.* **1976**, *15*, 483. https://doi.org/10.1364/AO.15.000483.
[124] L. Jacomme, *Appl. Opt.* **1975**, *14*, 2578. https://doi.org/10.1364/AO.14.002578.
[125] H. Yoda, P. Polynkin, M. Mansuripur, *J. Lightwave Technol.* **2006**, *24*, 1350. https://doi.org/10.1109/JLT.2005.863337.
[126] T. S. Saini, T. H. Tuan, T. Suzuki, Y. Ohishi, *Sci. Rep.* **2020**, *10*, 2236. https://doi.org/10.1038/s41598-020-59288-6.
[127] G. S. D. Gordon, R. Mouthaan, T. D. Wilkinson, S. E. Bohndiek, *J. Lightwave Technol.* **2019**, *37*, 5733. https://doi.org/10.1109/JLT.2019.2932901.
[128] H. S. Yazdi, T. D. O'Sullivan, A. Leproux, B. Hill, A. Durkin, S. Telep, J. Lam, S. S. Yazdi, A. M. Police, R. M. Carroll, F. J. Combs, T. Stromberg, A. G. Yodh, B. J. Tromberg, *J. Biomed. Opt.* **2017**, *22*, 045003. https://doi.org/10.1117/1.JBO.22.4.045003.

[129] D. Marcuse, *J. Opt. Soc. Am.* **1978**, *68*, 103. https://doi.org/10.1364/JOSA.68.000103.
[130] J. Lægsgaard, *J. Opt. Soc. Am. B* **2017**, *34*, 2266. https://doi.org/10.1364/JOSAB.34.002266.
[131] S. Sivankutty, E. R. Andresen, R. Cossart, G. Bouwmans, S. Monneret, H. Rigneault, *Opt. Express* **2016**, *24*, 825. https://doi.org/10.1364/OE.24.000825.
[132] X. Hu, Z. Duan, Y. Yang, Y. Tan, R. Zhou, J. Xiao, J. Zeng, J. Wang, *Opt. Express* **2023**, *31*, 20616. https://doi.org/10.1364/OE.485664.
[133] S. Silva, P. Roriz, O. Frazão, *Photonics* **2014**, *1*, 516. https://doi.org/10.3390/photonics1040516.
[134] G. Keiser, F. Xiong, Y. Cui, P. P. Shum, *J. Biomed. Opt.* **2014**, *19*, 080902. https://doi.org/10.1117/1.JBO.19.8.080902.
[135] G. Chen, G. Wang, X. Tan, K. Hou, Q. Meng, P. Zhao, S. Wang, J. Zhang, Z. Zhou, T. Chen, Y. Cheng, B. S. Hsiao, E. Reichmanis, M. Zhu, *Natl. Sci. Rev.* **2021**, *8*, nwaa209. https://doi.org/10.1093/nsr/nwaa209.
[136] Y. Ma, Y. Chu, S. Lyu, Y. He, Y. Wang, *Adv. Mater. Technol.* **2021**, *7*. https://doi.org/10.1002/admt.202101464.
[137] A. V. V. Nampoothiri, A. M. Jones, C. Fourcade-Dutin, C. Mao, N. Dadashzadeh, B. Baumgart, Y. Y. Wang, M. Alharbi, T. Bradley, N. Campbell, F. Benabid, B. R. Washburn, K. L. Corwin, W. Rudolph, *Optical Materials Express* **2012**, *2*, 948.
[138] W. Ding, Y.-Y. Wang, S.-F. Gao, M.-L. Wang, P. Wang, *IEEE J. Sel. Top. Quantum Electron.* **2020**, *26*, 4. https://doi.org/10.1109/JSTQE.2019.2957445.
[139] J. Li, H. Yan, H. Dang, F. Meng, *Opt. Laser Technol.* **2021**, *135*, 106658. https://doi.org/10.1016/j.optlastec.2020.106658.
[140] D. Septier, D. Labat, A. Pastre, R. Bernard, G. Brévalle-Wasilewski, H. Rigneault, G. Bouwmans, A. Kudlinski, *J. Lightwave Technol.* **2023**, *41*, 4792. https://doi.org/10.1109/JLT.2023.3242875.
[141] C. Zhang, K. Sui, M. Meneghetti, J. E. Antonio-Lopez, M. K. Dasa, R. W. Berg, R. Amezcua-Correa, Y. Wang, C. Markos, *Neurophotonics* **2024**, *11*, 045012. https://doi.org/10.1117/1.NPh.11.4.045012.
[142] Z. Lyu, L. V. Amitonova, *Opt. Express* **2024**, *32*, 37098. https://doi.org/10.1364/OE.535374.
[143] X. Zhang, H. Wang, T. Yuan, L. Yuan, *Sensors (Basel)* **2024**, *24*, 4532. https://doi.org/10.3390/s24144532.
[144] Z. Zhao, M. Tang, C. Lu, *Opto-Electronic Advances* **2020**, *3*, 19002401. https://doi.org/10.29026/oea.2020.190024.
[145] A. Steinkopff, C. Aleshire, A. Klenke, C. Jauregui, J. Limpert, *Opt. Express* **2023**, *31*, 28564. https://doi.org/10.1364/OE.498460.
[146] Y. Yao, Z. Zhao, M. Tang, *Sensors (Basel)* **2023**, *23*, 3436. https://doi.org/10.3390/s23073436.
[147] T. Wang, J. Dremel, S. Richter, W. Polanski, O. Uckermann, I. Eyupoglu, J. W. Czarske, R. Kuschmierz, *Neurophotonics* **2024**, *11*, S11505. https://doi.org/10.1117/1.NPh.11.S1.S11505.
[148] 程. C. Shengfu, 仲. Zhong Tianting, 胡. M. Woo Chi, 李. Li Haoran, 赖. L. Puxiang, *Laser & Optoelectronics Progress 61* **2024**.
[149] Z. Zhao, H. Fu, L. Ling, P. Westerhoff, *Acc. Chem. Res.* **2025**, *58*, 1596. https://doi.org/10.1021/acs.accounts.5c00022.
[150] H. Li, Z. Yu, T. Zhong, P. Lai, *J. Biomed. Opt.* **2024**, *29*, S11512.
[151] Z. Yu, H. Li, T. Zhong, J.-H. Park, S. Cheng, C. M. Woo, Q. Zhao, J. Yao, Y. Zhou, X. Huang, W. Pang, H. Yoon, Y. Shen, H. Liu, Y. Zheng, Y. Park, L. V. Wang, P. Lai, *The Innovation* **2022**, *3*, 100292.
[152] S. Yue, M. N. Slipchenko, J. X. Cheng, *Laser Photon Rev* **2011**, *5*, 496. https://doi.org/10.1002/lpor.201000027.
[153] S. Zhang, L. Liu, S. Ren, Z. Li, Y. Zhao, Z. Yang, R. Hu, J. Qu, *Opto-Electronic Advances* **2020**, *3*, 200003. https://doi.org/10.29026/oea.2020.200003.
[154] B. Dong, C. Sun, H. F. Zhang, *IEEE Trans. Biomed. Eng.* **2017**, *64*, 4. https://doi.org/10.1109/TBME.2016.2605451.
[155] W. Ke, N. G. Horton, K. Charan, C. Xu, *IEEE J. Sel. Top. Quantum Electron.* **2014**, *20*, 50.
[156] V. Crosignani, A. Dvornikov, J. S. Aguilar, C. Stringari, R. Edwards, W. W. Mantulin, E. Gratton, *J. Biomed. Opt.* **2012**, *17*, 116023. https://doi.org/10.1117/1.JBO.17.11.116023.
[157] C. Shu, W. Zheng, Z. Wang, C. Yu, Z. Huang, *Opt. Lett.* **2021**, *46*, 5197. https://doi.org/10.1364/OL.438713.
[158] Z. Qin, P. Lai, M. Sun, *Photoacoustics* **2024**, *40*, 100651. https://doi.org/10.1016/j.pacs.2024.100651.
[159] Y. Zhang, Y. Wang, P. Lai, L. Wang, *IEEE Trans Med Imaging* **2022**, *41*, 727. https://doi.org/10.1109/TMI.2021.3122240.
[160] B. Sun, J. Y. Teo, J. Wu, Y. Zhang, *Acc. Chem. Res.* **2023**, *56*, 1143. https://doi.org/10.1021/acs.accounts.2c00699.
[161] H. Li, Z. Yu, T. Zhong, S. Cheng, P. Lai, *Advanced Photonics* **2023**, *5*, 020502. https://doi.org/10.1117/1.AP.5.2.020502.
[162] E. Ciaramella, *J. Lightwave Technol.* **2012**, *30*, 572. https://doi.org/10.1109/JLT.2011.2177492.
[163] K. C. Li, L. L. Huang, J. H. Liang, M. C. Chan, *Biomed. Opt. Express* **2016**, *7*, 4803. https://doi.org/10.1364/BOE.7.004803.
[164] D. Kobat, M. E. Durst, N. Nishimura, A. W. Wong, C. B. Schaffer, C. Xu, *Opt. Express* **2009**, *17*, 13354. https://doi.org/10.1364/OE.17.013354.
[165] Z. Yu, H. Li, P. Lai, *Applied Sciences* **2017**, *7*, 1320.
[166] H. Xu, Z. Chen, Y. Wu, C. Hou, J. Ma, B.-O. Guan, *Photonics Res.* **2024**, *12*, 2996. https://doi.org/10.1364/PRJ.534972.
[167] T. Zhao, T. T. Pham, C. Baker, M. T. Ma, S. Ourselin, T. Vercauteren, E. Zhang, P. C. Beard, W. Xia, *Biomed. Opt. Express* **2022**, *13*, 4414. https://doi.org/10.1364/BOE.463057.
[168] T. D. Yang, K. Park, H. J. Kim, N. R. Im, B. Kim, T. Kim, S. Seo, J. S. Lee, B. M. Kim, Y. Choi, S. K. Baek, *Biomed Opt Express* **2017**, *8*, 3482.
[169] Z. Wen, Z. Dong, Q. Deng, C. Pang, C. F. Kaminski, X. Xu, H. Yan, L. Wang, S. Liu, J. Tang, W. Chen, X. Liu, Q. Yang, *Nat. Photonics* **2023**, *17*, 679. https://doi.org/10.1038/s41566-023-01240-x.
[170] S. Cheng, T. Zhong, C. M. Woo, Q. Zhao, H. Hui, P. Lai, *Opt. Express* **2022**, *30*, 32565. https://doi.org/10.1364/OE.462275.
[171] Z. Liu, L. Wang, Y. Meng, T. He, S. He, Y. Yang, L. Wang, J. Tian, D. Li, P. Yan, M. Gong, Q. Liu, Q. Xiao, *Nat. Commun.* **2022**, *13*, 1433. https://doi.org/10.1038/s41467-022-29178-8.
[172] A. C. Stier, W. Goth, A. Hurley, T. Brown, X. Feng, Y. Zhang, F. Lopes, K. R. Sebastian, P. Ren, M. C. Fox, J. S. Reichenberg, M. K. Markey, J. W. Tunnell, *J. Biomed. Opt.* **2021**, *26*, 096007. https://doi.org/10.1117/1.JBO.26.9.096007.
[173] S. Cheng, Computationally Assisted Deep-Tissue Optical Imaging And Patterned Light Delivery **2024**.
[174] Z. Cheng, C. Li, A. Khadria, Y. Zhang, L. V. Wang, *Nat. Photonics* **2023**, *17*, 299. https://doi.org/10.1038/s41566-022-01142-4.
[175] J. E. Fröch, S. Colburn, D. J. Brady, F. Heide, A. Veeraraghavan, A. Majumdar, *Optica* **2025**, *12*, 774.
[176] S. N. Khonina, N. L. Kazanskiy, A. R. Efimov, A. V. Nikonorov, I. V. Oseledets, R. V. Skidanov, M. A. Butt, *iScience* **2024**, *27*, 110270.
[177] H. Yu, Z. Huang, S. Lamon, B. Wang, H. Ding, J. Lin, Q. Wang, H. Luan, M. Gu, Q. Zhang, *Nat. Photonics* **2025**, *19*, 486. https://doi.org/10.1038/s41566-025-01621-4.
[178] J. E. Fröch, L. Huang, Q. A. A. Tanguy, S. Colburn, A. Zhan, A. Ravagli, E. J. Seibel, K. F. Böhringer, A. Majumdar, *eLight* **2023**, *3*, 13.
[179] Y. Liu, Q.-Y. Yu, Z.-M. Chen, H.-Y. Qiu, R. Chen, S.-J. Jiang, X.-T. He, F.-L. Zhao, J.-W. Dong, *Photonics Research* **2021**, *9*, 106.
[180] X. Zhang, J. Gao, Y. Gan, C. Song, D. Zhang, S. Zhuang, S. Han, P. Lai, H. Liu, *PhotoniX* **2023**, *4*, 10.
[181] L. Tian, B. Hunt, M. A. L. Bell, J. Yi, J. T. Smith, M. Ochoa, X. Intes, N. J. Durr, *Lasers Surg. Med.* **2021**, *53*, 748. https://doi.org/10.1002/lsm.23414.
[182] M. Chisanga, J. F. Masson, *Annu Rev Anal Chem (Palo Alto Calif)* **2024**, *17*, 313.

[183] M. Badar, M. Haris, A. Fatima, *Computer Science Review* **2020**, *35*, 100203. https://doi.org/10.1016/j.cosrev.2019.100203.
[184] S. McAleer, A. Fast, Y. Xue, M. J. Seiler, W. C. Tang, M. Balu, P. Baldi, A. W. Browne, *Transl Vis Sci Technol* **2021**, *10*, 30. https://doi.org/10.1167/tvst.10.12.30.
[185] X. Zhang, M. Tan, M. Nabil, R. Shukla, S. Vasavada, S. Anandasabapathy, M. A. Anastasio, E. Petrova, *J. Biomed. Opt.* **2024**, *29*, 046001. https://doi.org/10.1117/1.JBO.29.4.046001.
[186] W. Liu, Z. Zhang, G. Yan, *J. Lightwave Technol.* **2024**, *42*, 6153. https://doi.org/10.1109/JLT.2024.3403694.
[187] Z. Dong, G. Liu, G. Ni, J. Jerwick, L. Duan, C. Zhou, *J Biophotonics* **2020**, *13*, 201960135. https://doi.org/10.1002/jbio.201960135.
[188] A. Venketeswaran, N. Lalam, J. Wuenschell, P. R. Ohodnicki, M. Badar, K. P. Chen, P. Lu, Y. Duan, B. Chorpening, M. Buric, *Advanced Intelligent Systems* **2021**, *4*, 2100067. https://doi.org/10.1002/aisy.202100067.
[189] D. Cheng, P. Wan, X. Zou, C. Kan, *Opt. Laser Technol.* **2025**, *189*, 113176. https://doi.org/10.1016/j.optlastec.2025.113176.
[190] M. Xiang, F. Liu, J. Liu, X. Dong, Q. Liu and X. Shao, Computational optical imaging: challenges, opportunities, new trends, and emerging applications. Front. Imaging. **2024** *3*, 1336829, https://doi.org/10.3389/fimag.2024.1336829.
[191] S. Farahi, D. Ziegler, I. N. Papadopoulos, D. Psaltis, C. Moser, *Opt. Express* **2013**, *21*, 22504. https://doi.org/10.1364/OE.21.022504.
[192] A. Abid, S. Mittal, C. Boutopoulos, *J. Biomed. Opt.* **2019**, *25*, 3. https://doi.org/10.1117/1.JBO.25.3.032006.
[193] T. Wu, Y. Huang, Y. Liu, J. Wang, Y. Shi, X. Gu, H. Shen, C. He, Y. Lu, *Optics and Lasers in Engineering* **2022**, *154*, 107043. https://doi.org/10.1016/j.optlaseng.2022.107043.
[194] M. Chen, J. Wang, W. Tan, Y. Feng, G. Zheng, *J Biophotonics* **2021**, *14*, 202000239. https://doi.org/10.1002/jbio.202000239.
[195] S. Lee, C. Lee, R. Verkade, G. W. Cheon, J. U. Kang, *Optical Engineering* **2019**, *58*, 2. https://doi.org/10.1117/1.OE.58.2.026116.
[196] A. Tanskanen, J. Malone, C. MacAulay, P. Lane, *Opt. Express* **2023**, *31*, 44224. https://doi.org/10.1364/OE.504854.
[197] Y. Li, S. Moon, Y. Jiang, S. Qiu, Z. Chen, *Sci. Rep.* **2022**, *12*, 6831. https://doi.org/10.1038/s41598-022-10709-8.
[198] J. Qiu, Y. Shen, Z. Shangguan, W. Bao, S. Yang, P. Li, Z. Ding, *Opt. Commun.* **2018**, *413*, 276. https://doi.org/10.1016/j.optcom.2017.12.048.
[199] A. L. Buenconsejo, G. Hohert, M. Manning, E. Abouei, R. Tingley, I. Janzen, J. McAlpine, D. Miller, A. Lee, P. Lane, C. MacAulay, *J. Biomed. Opt.* **2019**, *25*, 3. https://doi.org/10.1117/1.JBO.25.3.032005.
[200] L. Bijoch, U. Wlodkowska, R. Kasztelanic, M. Pawlowska, D. Pysz, L. Kaczmarek, R. Lapkiewicz, R. Buczynski, R. Czajkowski, *ACS Appl. Mater. Interfaces* **2023**, *15*, 12831. https://doi.org/10.1021/acsami.2c22985.
[201] L. Wang, Y. Zhao, B. Zheng, Y. Huo, Y. Fan, D. Ma, Y. Gu, P. Wang, *Sci. Adv.* **2023**, *9*,. https://doi.org/10.1126/sciadv.adg8600.
[202] T.-S. Chang, S. Feng, G. Li, H. Li, X. Wu, S. Jaiswal, G. Xu, H. Jiang, E.-Y. K. Choi, K. R. Oldham, T. D. Wang, *Biosens. Bioelectron.* **2025**, *288*, 117757. https://doi.org/10.1016/j.bios.2025.117757.
[203] G. Li, Z. Guo, S.-L. Chen, *IEEE Sens. J.* **2019**, *19*, 909. https://doi.org/10.1109/JSEN.2018.2878801.
[204] J. Wang, S. Chen, R. Zhang, K. Lin, T. Wang, W. Liu, A. Zhang, *Opt. Lett.* **2023**, *48*, 4885. https://doi.org/10.1364/OL.495912.
[205] S. Harmsen, S. Rogalla, R. Huang, M. Spaliviero, V. Neuschmelting, Y. Hayakawa, Y. Lee, Y. Tailor, R. Toledo-Crow, J. W. Kang, J. M. Samii, H. Karabeber, R. M. Davis, J. R. White, M. van de Rijn, S. S. Gambhir, C. H. Contag, T. C. Wang, M. F. Kircher, *ACS Nano* **2019**, *13*, 1354.
[206] T. Wang, J. Jiang, K. Liu, S. Wang, P. Niu, Y. Liu, T. Liu, *PhotoniX* **2022**, *3*, 11. https://doi.org/10.1186/s43074-022-00058-0.
[207] A. Leber, B. Cholst, J. Sandt, N. Vogel, M. Kolle, *Adv. Funct. Mater.* **2018**, *29*, 1802629.
[208] J. Guo, M. Niu, C. Yang, *Optica* **2017**, *4*, 1285. https://doi.org/10.1364/OPTICA.4.001285.
[209] W. Liu, C. Liu, J. Wang, J. Lv, Y. Lv, L. Yang, N. An, Z. Yi, Q. Liu, C. Hu, P. K. Chu, *Results in Physics* **2023**, *47*, 106365. https://doi.org/10.1016/j.rinp.2023.106365.
[210] A. K. Yetisen, N. Jiang, A. Fallahi, Y. Montelongo, G. U. Ruiz-Esparza, A. Tamayol, Y. S. Zhang, I. Mahmood, S. A. Yang, K. S. Kim, H. Butt, A. Khademhosseini, S. H. Yun, *Adv. Mater.* **2017**, *29*, 1606380. https://doi.org/10.1002/adma.201606380.
[211] B. Zhu, D. Liu, J. Wu, C. Meng, X. Yang, Y. Wang, X. Jia, P. Jiang, X. Wang, *Advanced Functional Materials* **2024**, *34*, 2309795.
[212] D. Wang, B. Sheng, L. Peng, Y. Huang, Z. Ni, *Polymers (Basel)* **2019**, *11*, 1433. https://doi.org/10.3390/polym11091433.
[213] G. Zhu, L. Singh, Y. Wang, R. Singh, B. Zhang, F. Liu, B. K. Kaushik, S. Kumar, *Photonic Sensors* **2020**, *11*, 418. https://doi.org/10.1007/s13320-020-0605-2.
[214] L. Wang, C. Zhong, D. Ke, F. Ye, J. Tu, L. Wang, Y. Lu, *Adv. Opt. Mater.* **2018**, *6*, 1800427. https://doi.org/10.1002/adom.201800427.
[215] M. Choi, J. W. Choi, S. Kim, S. Nizamoglu, S. K. Hahn, S. H. Yun, *Nat. Photonics* **2013**, *7*, 987. https://doi.org/10.1038/nphoton.2013.278.
[216] W. Pang, Z. Xiao, X. Wei, B. Gu, *Opt. Lett.* **2023**, *48*, 3849. https://doi.org/10.1364/OL.497596.
[217] X. Li, X. Wang, T. Zhou, J. Yu, H. Xiang, C. Zhang, S. K. Sun, R. Liu, *Biomaterials* **2026**, *324*, 123509.
[218] R. Fu, W. Luo, R. Nazempour, D. Tan, H. Ding, K. Zhang, L. Yin, J. Guan, X. Sheng, *Adv. Opt. Mater.* **2017**, *6*, 1700941. https://doi.org/10.1002/adom.201700941.
[219] F. He, Z. Luo, Z. Wen, H. Huangfu, Y. Feng, X. Qi, Y. Duan, *Optik* **2022**, *271*, 170227. https://doi.org/10.1016/j.ijleo.2022.170227.
[220] F. Jin, H. Wang, Q. Ye, Z. Li, Y. Zhang, B.-O. Guan, Y. Ran, *Chin. Opt. Lett.* **2025**, *23*, 051701. https://doi.org/10.3788/COL202523.051701.
[221] W. Zhang, M. Kang, X. Li, Y. Pan, Z. Li, Y. Zhang, C. Liao, G. Xu, Z. Zhang, B. Z. Tang, Z. Xu, D. Wang, *Adv. Mater.* **2024**, *36*, 2410142. https://doi.org/10.1002/adma.202410142.
[222] J. Lee, H. Lee, E. J. Jin, D. Ryu, G. H. Kim, *NPJ Regen Med* **2023**, *8*, 18. https://doi.org/10.1038/s41536-023-00292-5.
[223] A. Urciuolo, I. Poli, L. Brandolino, P. Raffa, V. Scattolini, C. Laterza, G. G. Giobbe, E. Zambaiti, G. Selmin, M. Magnussen, L. Brigo, P. De Coppi, S. Salmaso, M. Giomo, N. Elvassore, *Nat Biomed Eng* **2020**, *4*, 901.
[224] M. T. Thai, P. T. Phan, H. A. Tran, C. C. Nguyen, T. T. Hoang, J. Davies, J. Rnjak-Kovacina, H. P. Phan, N. H. Lovell, T. N. Do, *Adv Sci (Weinh)* **2023**, *10*, 2205656.
[225] W. Peng, L. Li, Y. Zhang, H. Su, X. Jiang, H. Liu, X. Huang, L. Zhou, X. C. Shen, C. Liu, *J. Mater. Chem. B* **2023**, *12*, 158. https://doi.org/10.1039/D3TB02040A.
[226] M. Zamadar, G. Ghosh, A. Mahendran, M. Minnis, B. I. Kruft, A. Ghogare, D. Aebisher, A. Greer, *J. Am. Chem. Soc.* **2011**, *133*, 7882. https://doi.org/10.1021/ja200840p.
[227] A. Bansal, J. Zhang, Q. Lu, Q. Mei, Y. Zhang, *Biomater. Sci.* **2023**, *11*, 2046. https://doi.org/10.1039/D2BM01890J.
[228] R. K. Chaudhary, N. Madaboosi, J. Satija, B. Nandagopal, R. Srinivasan, V. V. R. Sai, *Biosens. Bioelectron.* **2024**, *257*, 116312. https://doi.org/10.1016/j.bios.2024.116312.
[229] K. H. Tow, S. Alomari, J. M. B. Pereira, T. Neves, Å. Claesson, *J. Lightwave Technol.* **2024**, *42*, 6457. https://doi.org/10.1109/JLT.2024.3405891.
[230] B. Xia, B. Liu, N. Wang, C. Liao, G. Long, C. Zhao, Z. Liao, D. Lyu, *ACS Appl. Mater. Interfaces* **2022**, *14*, 41379. https://doi.org/10.1021/acsami.2c08228.

[231] L. B. Shen, Y. X. Jiang, L. P. Tian, M. Q. Chen, *Opt. Mater. Express* **2022**, *12*, 3060. https://doi.org/10.1364/OME.464316.
[232] C. Strutynski, M. Evrard, F. Desevedavy, G. Gadret, J. C. Jules, C. H. Brachais, B. Kibler, *F. Nat. Commun.* **2023**, *14*, 6561. https://doi.org/10.1038/s41467-023-42355-7.
[233] W. Hadibrata, H. Wei, S. Krishnaswamy, K. Aydin, *Nano Lett.* **2021**, *21*, 2422. https://doi.org/10.1021/acs.nanolett.0c04463.
[234] L. L. Lai, P. H. Huang, G. Stemme, F. Niklaus, K. B. Gylfason, *ACS Nano* **2024**, *18*, 10788. https://doi.org/10.1021/acsnano.3c11030.
[235] X. Wang, G. Chen, K. Zhang, R. Li, Z. Jiang, H. Zhou, J. Gan, M. He, *Chem. Mater.* **2023**, *35*, 1345. https://doi.org/10.1021/acs.chemmater.2c03396.
[236] L. Bahin, M. Tourlonias, M.-A. Bueno, K. Sharma, R. M. Rossi, *Sens. Actuators, A* **2023**, *350*, 114117. https://doi.org/10.1016/j.sna.2022.114117.
[237] S. K. Dezaki, A. N. Askarpour, A. Abdipour, *Opt. Express* **2021**, *29*, 23096. https://doi.org/10.1364/OE.426239.
[238] N. Roberts, G. Baardinket, J Nunn, P. J. Mosley and A. Souslov, Topological supermodes in photonic crystal fiber.Sci.Adv **2022** *8*, eadd3522, https://doi.org/10.1126/sciadv.add3522.
[239] H. Huang, Z. Y. Ning, T. Kariyado, T. Amemiya, X. Hu, *Opt Express* **2023**, *31*, 27006.
[240] Y. Dogan, R. Katirci, İ. Erdogan, E. Yartasi, *Opt. Commun.* **2023**, *534*, 129332. https://doi.org/10.1016/j.optcom.2023.129332.
[241] X. Wang, Z. Meng, B. Yang, C. Cheng, K. Long, J. Li, *Compos. Struct.* **2022**, *291*, 115537. https://doi.org/10.1016/j.compstruct.2022.115537.
[242] X. Zhou, Y. Hui, Z. Chen, Y. Yang, F. Wang, Y. Zhang, Y. Zhao, S. C. Warren-Smith, L. V. Nguyen, X. Li, *Opt. Laser Technol.* **2024**, *177*, 111187. https://doi.org/10.1016/j.optlastec.2024.111187.
[243] Y. Zhang, X. Wu, R. A. Vadlamani, Y. Lim, J. Kim, K. David, E. Gilbert, Y. Li, R. Wang, S. Jiang, A. Wang, H. Sontheimer, D. F. English, S. Emori, R. V. Davalos, S. Poelzing, X. Jia, *Adv Healthc Mater* **2023**, *12*, 2300964.
[244] M. Du, J. Zheng, Y. Huang, X. Wang, Y. Qi, J. Qiu, L. Huang, C. Ren, Z. Yu, S. Zhou, *Adv. Opt. Mater.* **2023**, *12*, 2302044. https://doi.org/10.1002/adom.202302044.
[245] T. Zhang, G. Li, H. Ren, L. Yang, X. Yang, R. Tan, Y. Tang, D. Guo, H. Zhao, W. Shang, Y. Shen, *Nat Commun* **2024**, *15*, 10874.
[246] H. Zhou, X. Wang, Y. He, H. Liang, M. Chen, H. Liu, A. Qasem, P. Xiong, D. Peng, J. Gan, Z. Yang, *Advanced Intelligent Systems* **2023**, *5*, 2300113.
[247] H. Liang, Y. He, M. Chen, L. Jiang, Z. Zhang, X. Heng, L. Yang, Y. Hao, X. Wei, J. Gan, Z. Yang, *Advanced Intelligent Systems* **2021**, *3*, 2100035.
[248] H. Yang, Y. Xiao, K. Zhang, Z. Chen, J. Pan, L. Zhuo, Y. Zhong, H. Zheng, W. Zhu, J. Yu, Z. Chen, *Opt. Express* **2021**, *29*, 15631. https://doi.org/10.1364/OE.425777.
[249] N. F. Adilla Zaidi, M. Y. Mohd Noor, N. N. Huda Saris, M. R. Salim, S. Ambran, A. Azizan, R. K. Raja Ibrahim, F. Ahmad, N. A. Daud, N. Ali, N. M. Nawawi, I. Yulianti, G.-D. Peng, *Optical Fiber Technology* **2025**, *90*, 104113. https://doi.org/10.1016/j.yofte.2024.104113.
[250] T. Li, Y. Su, H. Zheng, F. Chen, X. Li, Y. Tan, Z. Zhou, *Advanced Intelligent Systems* **2023**, *5*, 2200460. https://doi.org/10.1002/aisy.202200460.
[251] M. G. Mahmoud, M. F. O. Hameed, S. S. A. Obayya, *Opt. Laser Technol.* **2025**, *189*, 112981. https://doi.org/10.1016/j.optlastec.2025.112981.
[252] Y. Tang, B. Zhao, X. Ye, J. Sun, X. Li, *Opt. Express* **2025**, *33*, 10951. https://doi.org/10.1364/OE.551221.
[253] K. Lu, Z. Chen, H. Chen, W. Zhou, Z. Zhang, H. K. Tsang, Y. Tong, *Nat. Commun.* **2024**, *15*, 3515. https://doi.org/10.1038/s41467-024-47907-z.
[254] P. Chansoria, M. Winkelbauer, S. Zhang, J. Janiak, H. Liu, D. Boev, A. Morandi, R. Grange, M. Zenobi-Wong, *Adv. Mater.* **2025**, *37*, 2419350. https://doi.org/10.1002/adma.202419350.
[255] L. Tao, Y. Kong, Y. Xiang, Y. Cao, X. Ye, Z. Liu, *Chin. Chem. Lett.* **2023**, *34*, 107481. https://doi.org/10.1016/j.cclet.2022.04.079.
[256] A. Gierej, F. Berghmans, M. Vagenende, A. Filipkowski, B. Siwicki, R. Buczynski, H. Thienpont, S. V. Vlierberghe, T. Geernaert, P. Dubruel, *Poly(D,L-Lactic Acid) J. Lightwave Technol.* **2019**, *37*, 1916. https://doi.org/10.1109/JLT.2019.2895220.
[257] C. Zhang, P. Xiang, W. Zhu, C. Chen, X. Liu, *Infrared Phys. Technol.* **2024**, *142*, 105572. https://doi.org/10.1016/j.infrared.2024.105572.
[258] Z. Liu, S. Cheng, Y. Li, X. Li, J. Sun, W. Jin, Y. Zhang, Y. Qin, Y. Zhang, X. Yang, A. Lotnyk, L. Yuan, *ACS Photonics* **2023**, *10*, 3531.
[259] C. Huang, S. Fujisawa, T. F. de Lima, A. N. Tait, E. C. Blow, Y. Tian, S. Bilodeau, A. Jha, F. Yaman, H.-T. Peng, H. G. Batshon, B. J. Shastri, Y. Inada, T. Wang, P. R. Prucnal, *Nat. Electron.* **2021**, *4*, 837. https://doi.org/10.1038/s41928-021-00661-2.
[260] X. Yu, S. Zhang, M. Olivo, N. Li, *Photonics Res.* **2020**, *8*, 1703. https://doi.org/10.1364/PRJ.387076.
[261] S. Park, H. Yuk, R. Zhao, Y. S. Yim, E. W. Woldeghebriel, J. Kang, A. Canales, Y. Fink, G. B. Choi, X. Zhao, P. Anikeeva, *Nat. Commun.* **2021**, *12*, 3435. https://doi.org/10.1038/s41467-021-23802-9.
[262] X. Zuo, Z. Liang, J. Zhang, S. Wang, Q. Zheng, Y. Ma, P. Li, T. Ding, X. Hu, Z. Wang, *Lasers Med Sci* **2022**, *37*, 259. https://doi.org/10.1007/s10103-020-03231-8.
[263] S. Han, G. Shin, *Coatings* **2020**, *10*, 1153. https://doi.org/10.3390/coatings10121153.

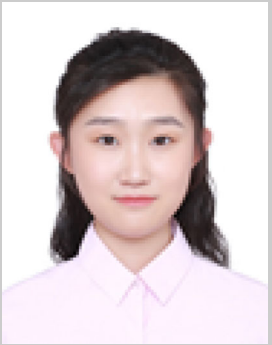

Yuzhen Li received the B.E. degree in Communication Engineering from Minzu University of China and the M.S. degree in Electronic Information from Tsinghua University. She is currently pursuing the Ph.D. degree in the Department of Biomedical Engineering at The Hong Kong Polytechnic University. Her research interests include 3D additive manufacturing, MEMS and biomedical optics. She has published papers in IEEE Sensor Journals and IEEE CISP-BMEI, contributing to flexible sensors and wearable devices.

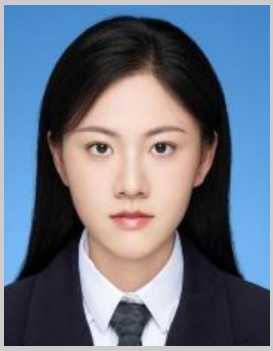

Siyang Zheng is a Ph.D. candidate in the Department of Biomedical Engineering at the Hong Kong Polytechnic University. Her research focuses on flexible sensors and non-invasive wearable medical devices for biomedical applications.

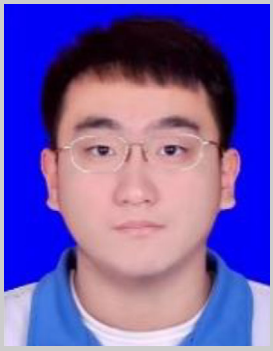

Wenzhao Li Ph.D. from the Department of Biomedical Engineering, The Hong Kong Polytechnic University. His research focuses on optical devices and materials, flexible electronics, etc. He has designed various integrated devices with functions such as optical response, tissue regeneration, and physiological parameter monitoring. He has published 9 articles as first or co-first author in journals including The Innovation, Advanced Science, and Advanced Photonics. He has received awards such as the Wiley China Open Science High Contribution Author Award.

Kai Chen is a Ph.D. student at The Hong Kong Polytechnic University. His research focuses on optical computing, computational holography, and optical neural networks, with particular emphasis on developing high-speed, energy-efficient optical systems for next-generation artificial intelligence. His work bridges photonics and computer science, leveraging light to overcome the limitations of traditional electronic computing. He has published papers in Optics Letters and Optics Express, contributing to advanced holographic techniques and optical information processing.

Tianting Zhong received his Ph.D. degree in Biomedical Engineering from The Hong Kong Polytechnic University. He is currently a Postdoctoral Fellow in the Department of Electrical and Electronic Engineering at The University of Hong Kong. His research concentrates on multidisciplinary explorations of high-resolution optical imaging in deep tissue, including optical wavefront shaping, photoacoustic imaging, fiber-optic endoscopy, and transmission matrix reconstruction algorithms. He holds 5 granted or pending Chinese/U.S. patents and has published over 20 papers in peer-reviewed journals such as Advanced Science, Advanced Photonics, The Innovation, and Photonics Research.

Chi Man Woo is a postdoctoral fellow in the Department of Biomedical Engineering at The Hong Kong Polytechnic University, where she also earned her Ph.D. Her research focuses on utilizing optical wavefront shaping to overcome light scattering, enabling high-resolution fluorescence and photoacoustic imaging deep within biological tissues.

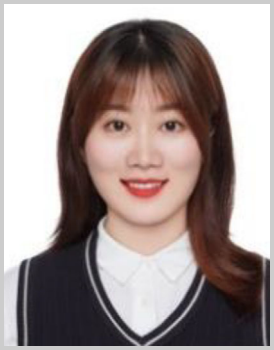

Weiran Pang is a Postdoctoral Fellow at The Hong Kong Polytechnic University (PolyU), where she also completed her Ph.D. Her research focuses on advancing photoacoustic imaging technologies, including tomography and microscopy, for translational biomedical applications. She has published in leading journals such as Laser & Photonics Reviews and serves as a peer reviewer for several prestigious journals in the field.

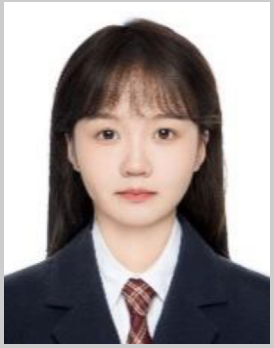

Chuqi Yuan is currently pursuing her Ph.D. degree in the Department of Biomedical Engineering at The Hong Kong Polytechnic University, working under the supervision of Prof. Puxiang Lai. Her primary research interests lie in the fields of photoacoustic imaging, photoacoustic sensing, and advanced biomedical imaging techniques. She has authored and co-authored several papers in international journals such as Biosensors and Bioelectronics, Talanta, and iScience.

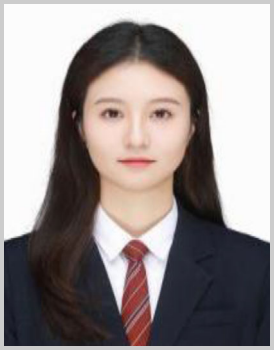

Xiaozhou Xiao is a Ph.D. student in the Department of Biomedical Engineering at The Hong Kong Polytechnic University. She received her bachelor's and master's degrees in Biomedical Engineering from Central South University. Her research focuses on photoacoustic microscopy and fluorescence imaging techniques, particularly their application in deep-tissue imaging to advance the understanding of biological structures and functions.

Xianguang Yang is an Associate Professor at the Institute of Nanophotonics, Jinan University. He received his B.S. and direct Ph.D. degrees from Sun Yat-sen University in 2012 and 2016, respectively. His research focuses on low-dimensional optoelectronic materials (e.g., quantum dots, nanowires) and their applications in micro-scale devices for photonic integration. He has published over 20 first/corresponding-author papers in leading journals, including Nano Letters, Applied Physics Reviews, and ACS Photonics. His work has been widely cited and highlighted by prominent researchers and international academic media.

Long Jin is a Professor at the Institute of Photonics Technology, Jinan University, where he specializes in fiber-optic devices for sensing and imaging. He has authored over 90 SCI papers, with his pioneering research on fiber-optic photoacoustic imaging gaining significant international recognition, including a highlight in Optics & Photonics News. He is a recipient of the Guangdong "Special Support Program" for Young Talents and has won multiple prestigious awards, including the Best Paper Award at the OFS conference.

Xiang Qian received his B. Eng and Ph.D. degrees from the Department of Biomedical Engineering, Tsinghua University, China in 2002 and 2009, respectively. He then conducted Postdoctoral research work in the Tsinghua-Shenzhen International Graduate School and joined the faculty team as a lecturer in 2012. From 2017, he became an associate professor of instrument science and technology. His research interests mainly focus on the key problem of modularized microfluidics, flexible sensors and actuators, and data processing methods for on-site instruments. He has published over 50 technical journal and conference papers, including Advanced Functional Materials, Soft Robotics, Biosensors and Bioelectronics, Analytical Chemistry, etc.

Qiyao Tan is a Research Assistant Professor in the Department of Biomedical Engineering at The Hong Kong Polytechnic University, where he also earned his Ph.D. in 2021. His research focuses on sports biomechanics, muscle physiology, and brain function evaluation using both experimental and computational methods. He has published over 20 SCI papers, holds 4 innovation patents, and has received several academic honors, including best paper and presentation awards at major biomedical engineering conferences.

Changyuan YU received his Ph.D. in Electrical Engineering from University of Southern California, USA in 2005. He then joined National University of Singapore in 12/2005, where he served as the founding leader of Photonic System Research Group in Department of Electrical and Computer Engineering and a joint senior scientist with A*STAR Institute for Infocomm Research. In 12/2015, he joined Hong Kong Polytechnic University, where he is now the Chair Professor of Photonic Information System in Department of Electrical and Electronic Engineering. His research focuses on photonic devices, optical communication/sensing systems, and biomedical instruments. He is an Optica/OSA fellow.

Liwei Liu is a Professor and the Executive Vice-President of the College of Physics and Optoelectronics Engineering at Shenzhen University. She is a recipient of the National Science Fund for Distinguished Young Scholars. Her research focuses on nonlinear optics, the manipulation of vector light fields, and their applications in biomedical microscopy. She has published over 80 papers in journals including Light: Science & Applications, Advanced Science, and Optics Letters. She serves as the chair-designate of the Biomedical Photonics Branch of the CSBME and a young editor-inchief for Chinese Journal of Lasers.

Junle Qu is a Chair Professor and the Director of the Medical Photonics Innovation Institute at Shenzhen University. He is a Fellow of SPIE, Optica, CSOE, and COS. His research focuses on multimodal nonlinear optical imaging, super - resolution microscopy, and light - induced therapy. He has published over 600 papers in journals including Nature Photonics, Nature Methods, Nature Communications, PNAS, Nano Letters, and Advanced Materials. He holds 100+ patents and serves as the Executive Editor - in - Chief for Photonix Life.

Puxiang Lai is currently an Associate Professor at Department of Biomedical Engineering at The Hong Kong Polytechnic University. His research centers around deep-tissue optical focusing, imaging, stimulation, and treatment. Current research projects include, but are not limited to, wavefront shaping, photoacoustic imaging, neuron stimulation, computational optics, and artificial intelligence. His research has fueled more than 130 top journal publications, such as Nature Photonics, Nature Communications, Science Advances, and The Innovation. He has been recognized as a Highly Cited Researcher and ranked among the World's Top 2% Scientists by Stanford University and the 2016-2017 Hong Kong RGC Early Career Award.